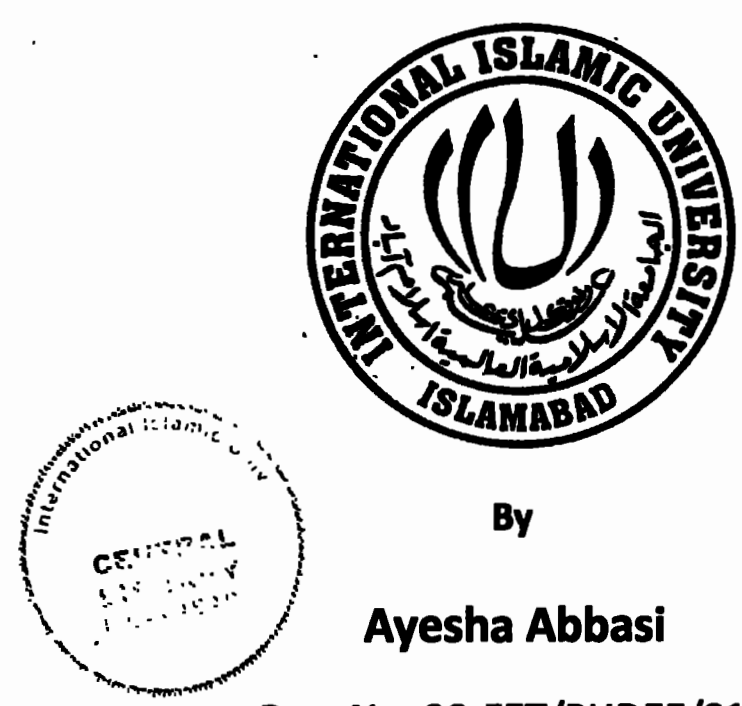
Demand Response based Energy Management System for Stability and Reliability Enhancement of Microgrids



Reg. No. 90-FET/PHDEE/S15

A dissertation submitted to I.I.U. in partial fulfillment of the requirements for the degree of

DOCTOR OF PHILOSOPHY

Department of Electrical Engineering
Faculty of Engineering and Technology
INTERNATIONAL ISLAMIC UNIVERSITY
ISLAMABAD
2023

PhD 621.312 AYD W W TH-26032

Microgrids
Demand Response (Energy)
Energy Management
Power Systems
Power Systems
Power system stability

Copyright © 2019 by Ayesha Abbasi

¢

All rights reserved. No part of the material protected by this copyright notice may be reproduced or utilized in any form or by any means, electronic or mechanical, including photocopying, recording or by any information storage and retrieval system, without the permission from the author.

DEDICATED TO

To my two rocks, my parents.

To my lifelong teacher, Dr. Taj Afsar.

To my lifelong school, Rahimia Institute of Quranic Sciences.

CERTIFICATE OF APPROVAL

Title of Thesis: Demand Response based Energy Management System for Stability and

Reliability Enhancement of Microgrids

Name of Student: Ayesha Abbasi

Registration No: 90-FET/PhDEE/S15

Accepted by the Department of Electrical and Computer Engineering, Faculty of Engineering and Technology, International Islamic University (IIU), Islamabad, in partial fulfillment of the requirements for the Doctor of Philosophy degree in Electronic Engineering.

Viva voce committee:

Dr. Adnan Umar (Supervisor)

Assistant Professor DECE, FET IIU Islamabad

Prof. Dr. Muhammad Amir (Internal)

Professor DECE, FET, IIU Islamabad

Dr. Noaman Ahmad Khan (External-I)

Associate Professor, CASE, Islamabad

Dr. Hammad Umer. (External-II)

Associate Professor, CUI, Islamabad

Dr. Shahid Ikram (Chairman, DEE)

Assistant Professor DECE, FET, IIU Islamabad

Prof. Dr. Nadeem Ahmad Sheikh (Dean, FET)

Professor DME, FET, IIU Islamabad

Abstract

Load shifting and utility grid power peak shaving are two mechanisms that are critical in forming stable and resilient microgrids (MGs). Both the mechanisms have some limitations which this study aims to address. Firstly, the existing cognitive strategies of power scheduling in the research literature mainly focus on a small sample dataset. So, the strategies produce unsatisfactory results when applied to large population. Even when utilizing larger datasets, the static clustering based techniques fail to produce significant improvement. Secondly, the existing peak shaving algorithms have limitations of fixed demand and feed in limits. Power systems with dynamic demand and feed in limits cannot produce significant improvements in community-based networks as they are based on non-dynamic optimization techniques.

The proposed design uses a large population dataset and achieves efficient load scheduling using a dynamic clustered home energy management system (DCHEMS) utilizing time overlap criteria for consumer communities. DCHEMS forms clusters of devices, consumer defined constraints and particle swarm optimization (PSO) to attain optimized power demands. Modified inclined block rate and real-time electricity price (RTP) strategies are deployed to serve the purpose of minimizing electrical costs. A large population sample, of 1000 residential users, from different classes of society were tested. The results validate the proposed DCHEMS showing higher efficiency in comparison to the non-dynamic clustered optimization method. Peak to average ratio (PAR) shows an improvement of 21% while cost is reduced by 4% for the proposed DCHEMS. There is an improvement of 19% in variance to mean ratio.

The study explores dynamic clustering based optimal peak shaving management schemes in community-based MG system. In this study, a two-stage control technique is proposed for establishing the inputs needed for rule-based peak shaving management. It involves both dynamic

demand and day-to-day feed-in limits to estimate battery charge/discharge schedules for the upcoming day. Limited utility grid demand and feed-in powers correspond to the day's demand and feed-in limits. For minimizing peak grid energy consumed from the utility grid, the ideal inputs necessary for suggested rule-based peak shaving management are derived using the PSO algorithm. The suggested optimal peak shaving control scheme is compared quantitatively and qualitatively with previous work. MATLAB is used to test the proposed management method for the different photovoltaic (PV) power and load demand patterns. An improvement of nearly 15% is achieved for peak shaving in different cases.

The main contributions of this work include: 1) Proposes a novel idea of load scheduling using dynamic device clustering scheme for the development of optimized load profiles for controllable devices, applicable to a MG community comprising of societal classes, 2) Proposes the optimal peak shaving control strategy based on two stage efficient distributed resource utilization scheme, involving PV and battery energy storage (BES) power sources in the MG community that reduces utility grid demand.

List of Publications

- [1]. Abbasi, A.; Sultan, S.; Aziz, A.; Khan, Khan, A. U.; Khalid, H.A.; and Guerrero, J. M.; 2021, "A Novel Dynamic Appliance Clustering Scheme in a Community Home Energy Management System for Improved Stability and Resiliency of Microgrids", IEEE Access, vol. 9, pp. 142276-142288, 2021.
- [2]. Abbasi, A.; Khalid, H. A.; Rehman, H.; Khan, A. U.; "A Novel Dynamic Load Scheduling and Peak Shaving Control Scheme in a Community Home Energy Management System based Microgrids", IEEE Access, 2023.
- [3]. Abbasi, A.; Qureshi, I, M., Khalid, H.A, "An Overview of control strategies with emphasis on demand response for stability and reliability enhancement of Microgrids", 4th International conference on Power Generation Systems and Renewable Energy Technologies (PGSRET), 2018,
- [4]. Fida M., Abbasi, A.; Azam M., khan I., "General Overview of Using High Voltage Direct Current (HVDC) Transmission in Pakistan for Maximum Efficiency and Performance" 2nd International conference on Power Generation Systems and Renewable Energy Technologies (PGSRET), 2015,
- [5]. Akif F., Malik A. N., Qureshi, I, M., Abbasi, A., "Transmit and receive antenna selection-based resource allocation for self-backhaul 5G massive MIMO hetnets". Int. Arab J. Inf. Technol. 18(6): 755-766, 2021.

The research work presented in this dissertation is based on the first three publications.

Acknowledgements

I thank Allah Almighty, for giving me the strength, resources, health and focus 19 complete this milestone.

I am truly grateful to my late supervisor, Dr. Ijaz Mansoor Qureshi, who helped me immensely on the subject throughout. I pray to Allah to bless him with a place in Jannat-ul-Firdous. Ameen.

I am also very grateful to my supervisor Dr. Adnan Umar, who helped me and guided me throughout this journey. And amidst all this journey, I would like to add a special note of gratitude to my mentor and teacher Professor Dr. Taj Afsar, who supported, encouraged and motivated me in the toughest of times, never letting me lose hope, for teaching me lifelong lessons. Due to his support, confidence in me and his selfless efforts, I am where I am today.

This accomplishment would not have been possible without the presence of Group Captain (R) Fida Muhammad in my life. He was my guidance and motivation behind joining this research area of power and controls. I have always admired his teaching methods and aspired to be a teacher like him.

)

I offer my sincere thanks to the Chairperson Dr. Shahid Ikram and Dean of the department Dr. Nadeem Ahmad Sheikh for their kind cooperation, Dr. Hassan Abdullah from Nust and Dr. Adnan Aziz from Isra University for helping me shape my ideas and making this work publishable.

I extend my sincerest gratitude to my sister, Dr. Hafsa Abbasi who has always been an inspiration and been the one to pave paths for me. Also, a note of acknowledgement for our mutual friend, Rabia Malik, who helped me polish this document.

(Ayesha Abbasi)

٠,

Table of Contents

Acknowledgements	vii
Table of Contents	i
Abbreviations and Symbols	xv
Introduction	1
1.1. Background	1
1.2. Problem Definition	5
1.3. Objectives	5
1.3.1. Design Objectives	6
1.3.2. Implementation Objectives	7
1.4. Contributions	10
1.5. Thesis Outline	11
Literature Review	13
2.1. Energy Management	13
2.1.1. Load Scheduling	14
2.1.2. Peak Clipping	14
2.1.3. Strategic Conservation	14
2.1.4. Valley Filling	
2.1.5. Strategic Load Growth	
2.1.6. Flexible Load Shape	
2.2. Load Scheduling Techniques: Objectives and Limitations	
2.2.1. Deductions	
2.2.2. Propositions	
2.3. Peak Load Shaving: Objectives and Limitations	
2.3.1. Deductions	
2.3.2. Propositions	
Demand Response Based Load Scheduling in Residential Energy Management System	
3.1. The Usage Pattern for Home CDs	
3.2. Inclined block rate Pricing Scheme	
3.3. Summary	

Dynam	ic Cl	ustered Community Home Energy Management System	31
4.1.	Pro	pposed System Model and Formulated Problem	32
4.1	.1.	Objective of Proposed Approach	33
4.1	.2.	Selected pricing scheme and modified inclined block rate	36
4.2.	Pro	posed PSO Based EMS for Energy Consumption	38
4.2	.1.	Particle Swarm Optimization (PSO)	38
4.2	.2.	Formulation of DCHEMS	41
4.3.	Re	sults of Simulations	47
4.4.	Su	mmary	52
A Study	on i	Renewable Integration on Clustered Community HEMS	53
5.1.		delling and Simulation Method Development for the Analysis of Power Co	_
		ential Community Microgrid System	
5.2.		sign Specifications	
5.3.		crorid Layout	
5.4.		ntrol Scheme	
5.6.		nulation Results	
5.6	•	Case-I	
5.6		Case-II.	
	_	timal BES Scheduling for Peak Shaving and PV Utilization	
5.7		Challenges in BES Technology	
5.7		Control Strategy	
5.7	.3.	Simulation Results	67
5.8.	Sur	mmary	73
Optimal	Pea	k Shaving\Clipping using Dynamic Feed in and Demand limits	76
6.1. S	yste	m Illustration	76
6.2. B	ES (Operating Modes	77
6.3. D	eten	mination of Optimal Inputs	80
6.3	.1. D	emand Limit	80
6.3	.2. T	he Energy Required for Charging BES for a Day	82
6.3	.3. P	V Energy Available to Charge BES Over 24 Hours	82
6.3	4. U	tility Grid Energy Available for Charging BES Over 24 Hours	83
6.3	.5. U	tility Grid Energy Coefficient for Charging the BES	84
6.3	.6. M	lodification of Demand Limit	84

)

)

6.3.7. Feed-in Limit	85
6.4. Control Strategy for Rule-Based Peak Shaving	87
6.5. Determination of Optimal Inputs	89
6.6. Simulation Results	92
6.6.1. Case 1: 5% PV Penetration for Hot and Cloudy Day	93
6.6.2. Case 2: 5% PV penetration for Cold day	95
6.6.3. Case 3: 15% PV penetration for Hot and Cloudy day	96
6.6.4. Case 4: 15% PV penetration for Cold Day	97
6.7. Summary	99
Dynamic HEMS based Optimal Peak Shaving Control in a Microgrid	101
7.1. System Illustration	101
7.1.1. Load Demand	103
7.1.2. Distributed Energy Resources (DERs)	105
7.2. Stage 1- Dynamic HEMs Based Control Scheme	106
7.3. Stage 2 - Optimal Peak Shaving Control Scheme	107
7.4. Simulation Results	109
Deferences	120

)

List of Figures

Fig. 1- 1 Block diagram of the proposed system model for efficient home energy management system .	7
Fig. 2- 1 Strategies for efficient demand-side energy management	16
Fig. 3- 1 Architecture of residential energy management [66]	25
Fig. 3- 2 Parameter constraints of Devices	27
Fig. 3-3 The relationship of devices parameters shown in an example	
Fig. 3- 4 Comparison of load scheduling techniques, (a) Load scheduling with RTP (b) Load scheduling	
with RTP combined with inclined block rate [66].	_
Fig. 3- 5 Generation of power peaks in device's cluster shown as an Example.	
Fig. 4- 1 Community based HEMS framework	32
Fig. 4- 2 Devices with non-homogeneous loads, for all four classes, with power rating in kWh	34
Fig. 4-3 The range illustration of STDO for home devices 'a': (a) device starting right at STDO and (b)
device starting at the latest possible time	36
Fig. 4- 4 RTP on 9th July 2015	38
Fig. 4- 5 Flow chart for PSO	40
Fig. 4- 6 DCHEMS parameters for clustering.	44
Fig. 4- 7 Flow diagram of DCHEMS scheme	46
Fig. 4- 8 Power consumption pattern at 45th day.	49
Fig. 4-9 Simulated Results with PSO over a period of 90 days: (a) Cost of electricity, (b) Peak to avera	ıge
ratio and (c) VMR ratio of power consumption pattern	_
Fig. 5- 1 Illustration of MG layout with BES and PV supply	54
Fig. 5- 2 Flow diagram for MG Control strategy	
Fig. 5-3 Used solar Irradiance for the PV power. (a) Normal irradiance—Sunny plus cloudy day state;	(b)
Low irradiance—Cold day state	
Fig. 5- 4 Electricity load profile used for higher class home users	59
Fig. 5- 5 Electricity response for simulated MG case I	60
Fig. 5- 6 Charging and discharging states of BES for case I	60
Fig. 5- 7 Electricity response for simulated MG case II	61
Fig. 5- 8 Charging and discharging states of BES for case II	62
Fig. 5-9 Flow diagram for peak shaving MG control strategy	64
Fig. 5- 10 Description of Palere and Ppeak	66
Fig. 5- 11 Electricity profile used load for a total of 1000 residential consumers	67
Fig. 5- 12 BES scheduling and PV utilization results for 5% PV penetration	69
Fig. 5- 13 BES scheduling and PV utilization results for 10% PV penetration	71
Fig. 5- 14 BES scheduling and PV utilization results for 15% PV penetration. The figure shown in (a) a	ınd
(b) is the electricity response in the simulated MG for 15% PV penetration, left: cold day, right: hot day	/ .
(c) and (d) Pb and SoC of Energy storage system, L: cold day, R: hot day. (e) and (f) Excess power sen	
back to the source, L: cold day, R: hot day	73

Fig. 6-1 Residential system with PV source, BES, and controllable devices (CDs) as load77
Fig. 6-2 Operating TSs of modes of BES: t_{dis-c} when $P_L(t) > P_{dl}$ && $P_{pv}(t) \le P_L(t) - P_{dl}$; t_{c1} when
$P_L(t) \le P_{dl}$; and t_{c2} when $P_L(t) > P_{dl}$ && $P_{pv}(t) > P_L(t) - P_{dl}$
Fig. 6-3 Input's coordination needed for rule based management control method [57]79
Fig. 6- 4 Particle swarm optimization for finding optimal dischargeable energy of BES91
Fig. 6-5 Flow diagram for optimal rule-based peak shaving control [57]
Fig. 6-6 Case-1. (a) Profiles for PV power supply and load consumption. (b) Schedules of BES
charge/discharge. (c) BES state of charge. (d) Utility grid power94
Fig. 6-7 Case-2. (a) Profiles for PV power supply and load consumption. (b) Schedules of BES
charge/discharge. (c) BES state of charge. (d) Utility grid power95
Fig. 6-8 Case-3. (a) Profiles for PV power supply and load consumption. (b) Schedules of BES
charge/discharge. (c) BES state of charge. (d) Utility grid power97
Fig. 6- 9 Case-4. (a) Profiles for PV power supply and load consumption. (b) Schedules of BES
charge/discharge. (c) BES state of charge. (d) Utility grid power98
Fig. 7- 1(a) Community based Dynamics-HEMS framework (b) BES and PV considered as distributed
energy resources within community MG
Fig. 7- 2 Dynamic-HEMS based peak reduction of load demand for a) Summers day condition b) Winters
day condition107
Fig. 7-3 Operating TSs of modes of BES: t_{dis-c} when $P_L(t) > P_{dl}$ && $P_{pv}(t) \le P_L(t) - P_{dl}$; t_{c1} when
$P_L(t) \le P_{dl}$; t_{c2} when $P_L(t) > P_{dl}$ && $P_{pv}(t) > P_L(t) - P_{dl}$ and t_{c3} when $P_L(t) < P_{dl}$ && $P_{pv}(t) = 0$
Fig. 7- 4 Proposed two stage HEMS optimal peak shaving control flow diagram109
Fig. 7- 5 Dynamic-HEMS Case-1. (a) Profiles for PV power supply and load consumption. (b) Schedules
of BES charge/discharge. (c) BES state of charge. (d) Utility grid power111
Fig. 7- 6 Dynamic-HEMS Case-2. (a) Profiles for PV power supply and load consumption. (b) Schedules
of BES charge/discharge. (c) BES state of charge. (d) Utility grid power113
Fig. 7-7 Dynamic-HEMS Case-3. (a) Profiles for PV power supply and load consumption. (b) Schedules
of BES charge/discharge. (c) BES state of charge. (d) Utility grid power114
Fig. 7-8 Dynamic-HEMS Case-4. (a) Profiles for PV power supply and load consumption. (b) Schedules
of BES charge/discharge. (c) BES state of charge. (d) Utility grid power116
Fig. 7-9 Without-HEMS Case-1. (a) Profiles for PV power supply and load consumption. (b) Schedules of
BES charge/discharge. (c) BES state of charge. (d) Utility grid power117
Fig. 7- 10 Without-HEMS Case-2. (a) Profiles for PV power supply and load consumption. (b) Schedules
of BES charge/discharge. (c) BES state of charge. (d) Utility grid power119
Fig. 7-11 Without-HEMS Case-3. (a) Profiles for PV power supply and load consumption. (b) Schedules
of BES charge/discharge. (c) BES state of charge. (d) Utility grid power120
Fig. 7-12 Without-HEMS Case-4. (a) Profiles for PV power supply and load consumption. (b) Schedules
of BES charge/discharge, (c) BES state of charge. (d) Utility grid power122

)

List of Tables

Table 2. 1 Summarizes a few studies on heuristic computation strategies	19
Table 2. 2 Qualitative comparison of suggested technique with the previous work	23
Table 4- 1 Characteristic parameters used for CDs [24]	42
Table 4- 2 Results summary	51
Table 6- 1 Utility grid power	88
Table 6- 2 System parameters [57]	90
Table 6-3 Optimal inputs of management algorithm with application to four cases	93
Table 6- 4 Comparison of percentage of peak shaving (PPS) for different cases	99
Table 7- 1 Typical usage parameters for CDs in summers and winters	104
Table 7-2 Optimal inputs of management algorithm with application to four cases [57]	110
Table 7-3 Quantitative comparison of suggested technique with the previous work	124
Table 7- 4 Qualitative comparison of suggested technique with the previous work	124

Abbreviations and Symbols

:

Abbreviations

BES Battery energy storage

CD Controllable device

DCHEMS Dynamic clustered community-based home energy management system

DR Demand response

DSEM Demand side energy management

ETDO Ending time of device operation

HEMS Home energy management system

MG Microgrid

NCD Non-controllable device

PAR Peak to average ratio

PCR Percentage of cost reduction

PPS Percentage peak shaving

PSO Particle swarm optimization

PUGP Peak utility grid power

PV Photovoltaic

RTP Real time electricity pricing

SoC BES State of charge

STDO Starting time of device operation

TLDO Time length of device operation

TS Time slot

1

VMR Variance to mean ratio

Symbols

)

)

 A_{ν} Set of controllable devices for k^{th} house.

 α_{a_k} TLDO for device a of house k. β_{a_k} ETDO for device a of house k.

C_g Coefficient of grid energy to charge the battery.

Eb-dis-g
Eb-rated
Energy to be dispatched by BES (kWh).

Rated energy capacity of BES (kWh).

Battery charging required energy (kWh).

E_{DV-C}, E_{g-c} Grid and available PV energy to charge BES (kWh).

 E_{g-pk} Peak energy drawn from the grid (kWh).

 E_{g-d} Grid Energy demand of (kWh). $E_{*b-dis-c}$ Dispatchable BES energy (kWh). l_{ak} TLDO for device a of house k.

p_{cc} Power consumption pattern for community cluster.

p_{scd} Power consumption scheduling vector.

p_c Power consumption of community being optimized.

 p_{ak} Power consumption scheduling vector for device a of house k.

 P_{dl} , P_{fl} Demand and feed-in limitation of the day (kW).

 P_g , E_g Grid energy (kWh) and power (kW). P_L , P_b , P_{pv} , Load demand, BES and PV powers (kW).

P Power Consumption Scheduling matrix (dimension 800*144).

P_{d-10}, P_{f-10} Operating demand and feed-in limitation (kW).

 P_{d-l1} , P_{d-l2} Initial demand limits (kW). P_{f-l1} , P_{f-l2} Initial feed-in limits (kW).

P_{b-c}, P_{b-dis-c} BES charge/discharge power (kW).

 P_{pv-c} , P_{g-c} Available PV and grid powers to charge BES (kW). P_{d-pk} , P_{pv-ins} Peak load demand and installed PV power (kW).

 $P_{b-\psi-mx}$ BES maximum charging power (kW). $P_{b-dis-\psi-mx}$ BES maximum discharging power (kW). $rtp_{pc}(\tau)$ Electricity price in real time for p_c . SoC_{i} , SoC_{f} SoC at the start and end of the day.

tdis-c, tc1, tc2 Discharging mode and charging mode 1,2 time slots.

 t_{ak} Activation time start for device a of house k

 τ Time slot.

Chapter 1

Introduction

Forming stable and resilient microgrids (MGs) have become a necessity of the present times. This work is an endeavor to suggest a solution for the limitations of the two critical areas of MG energy management; load shifting and peak shaving mechanisms. A dynamic clustered home energy management system for a residential community that guarantees efficiency in load shifting for small to the large datasets is proposed. Also, dynamic optimal peak shaving schemes with application to community-based HEMS have been explored.

This chapter presents a background study regarding the impact of load shifting and peak shaving mechanisms in MGs. It highlights the limitations of the existing load shifting and peak shaving techniques. It also discusses the contributions of this work in the field of energy management systems. It presents the methodology adopted to design the system. Lastly, it summarizes the organization of this thesis.

1.1. Background

The per capita power consumption is rapidly increasing worldwide. The electric utility companies are facing immense challenges in fulfilling the ever-rising consumer demands. As per the energy information administration (EIA), till 2025, there are 40% chances of an increase in electricity demand in the residential power sector, and a 25% increase in the commercial sector. Moreover, EIA reports that the electricity demand is expected to increase by 50% during the time span from 2018 till 2050 [1].

The traditional power grid is unable to meet and manage the increasing electricity demands and challenges. To fulfill these rising demands, the trend of utilizing locally generated power has gained popularity in the power sector. Energy is generated by exploiting non-conventional renewable energy resources, such as photovoltaic (PV), microturbines, fuel cells, wind energy, etc. The concept of distributed power generation is a flexible solution for green energy developments in future [2].

Microgrid (MG) is an emerging concept in smart grids that enhances the effectiveness and resiliency of power systems by allowing smart control of consumer's power consumption while integrating distributed generation resources [3]. The MG ensures closer proximity between generation and demand-side as it involves flexible and intelligent control schemes. The transition from passive, centralized, and unidirectional networks to active, distributed and bidirectional networks has emphasized future technologies towards more intelligent, flexible, and efficient entities. MGs consisting of comparatively smaller-sized clusters of distributed generation units and loads can work independently as single entities. They can work in parallel to the utility grid without affecting the upstream network integrity [4]. MGs have huge potential to improve the reliability and stability of the system. MGs allow autonomous operations with dynamic control of both the power generation and consumer sides. They offer a large number of benefits for the utility grid as well as the consumers. For the utility grid, MGs behave as aggregated individuals which do not risk the grid reliability and security and follow grid regulations. For the end-user, MGs offer benefits of continuous and reliable power supply, reduction in transmission losses, and economic arbitrage support [5,6].

)

)

A home energy management system (HEMS) warrants the steadiness and consistency of MGs [7]. It is commonly referred to as the technique attributing to the use of home devices by

demand for electricity in the domestic sector. [8]. It works by allowing variations in the demand curve according to each profile of a user. The variation occurs due to the partaking of a user in the electric power market. The whole process makes use of intelligent data analytics that are located in the software running the database. The data analytics help save the user's profile at various points of consumption. More specifically, an advanced metering infrastructure (AMI) or smart meter serves as a connecting junction between the electrical grid and devices to enable the power supply. HEMS prioritizes this load consumption that concerns cost and energy [9].

Today, the integration of HEMS in an MG is an essential part of smart grid control as domestic consumers substantially contribute to the total electricity consumption. Also, there is a need to improve the existing conservative HEMS techniques to shrink the peak to the average power demand of smart grids. This would fulfill the increasing energy demand and overcome power deficit conditions in underdeveloped countries [10]. The grid generates a controlling signal known as demand response (DR) that reflects altered electricity prices during peak hours. HEMS responds to DR while maintaining a balance between power generation and electricity consumption across the entire grid. It reshapes the power usage pattern by rescheduling load on the consumer end (demand-side management).

)

)

Demand-side energy management (DSEM) using device scheduling is one of the possible solutions for peak power demands in HEMS [11]. Using DSM however, demand can be maintained only till a certain level before it starts hindering system operation and becomes a source of consumers' discomfort. As a result, storage systems provide the possibility of further modifying demand profiles. With correct energy management tactics, an MG has a dual benefit for the power system. Firstly, it can act as a single controllable energy asset to deliver grid-friendly power

responses and various grid services. Secondly, it can also coordinate with distributed energy resources to provide a reliable and steady energy supply for local loads [12]. MG, powered by renewable energy resources, is becoming an important component of the electrical distribution system to meet sustainability metrics of commercial as well as residential facilities [13].

Various robustness problems arise because of the non-dispatchable and intermittent properties of renewable energy resources. Due to stochasticity and behavioral intermittency, fluctuations may occur in the generated output. This may cause disturbances in the constant power supply. Therefore, energy storage integration is perceived to be an efficient buffer to compensate for power mismatch and improve MG reliability and dynamic stability [14,15]. Energy storage systems include batteries, supercapacitors, flywheels, etc. These devices have been extensively used to provide renewable energy resources and play an economic role in DR. Energy storage can also exchange bidirectional power with the utility grid to provide auxiliary services to the end-users, providing them financial relief [16].

)

į

Among the energy storage, battery energy storage (BES) is an effective solution as it absorbs and stores the excess power coming from renewable energy resources and later provides it to MG consumers [18]. BES can increase the local consumption of MG system by reducing the energy demand of the utility grid with the help of increased PV power utilization [17]–[20]. Numerous services can be offered by grid-tied BES such as load shifting, peak clipping, improvements in power quality, and involvement of spinning reserve [21].

Utility grid power peak shaving is an essential application that helps both grid operators as well as end-users. It can ease electric utility companies by maintaining balance in supply and demand which in turn improves load factor and economic stability of utility grid. It can also improve the system efficiency and power reliability of the MG. The utility grid is also improved [22].

Similarly, peak shaving is helpful in reducing consumers' electricity bills by shifting peak demand from a high-price period to a low-price period [23]. Moreover, it offers improved power quality and reliability for end-users.

1.2. Problem Definition

The cognitive strategies of power scheduling in the literature mainly focus on a small population sample size while the results for the large population still need to be investigated. Even the use of large sets has not produced significant improvement due to the use of static clustering techniques [24]. There is a need to explore a dynamic clustered home energy management system for a residential community that eradicates the limitation of underperformance for large population sets.

The existing techniques for peak shaving in the literature are generally based on fixed demand and feed in limits and provide non-optimal solutions for peak shaving. Even those existing in the literature do not propose dynamic HEMS-based optimization and are applied on small data set. There is a need to explore dynamic optimal peak shaving schemes with application to community-based HEMS.

1.3. Objectives

)

The study aims to achieve the following objectives:

i. To suggest an efficient DR-based energy management system that can lead to the stable and reliable operation of MGs as the existing static clustering schemes underperform while managing complex and irregular issues that may arise in the MGs.

- ii. To develop an algorithm by exploiting particle swarm optimization (PSO), dynamic problems, device clustering schemes in the communities of an MG. Not only would the dynamic HEMS peak reduction scheme lead to a more reliable and stable MG system, it will also be applicable for a large number of consumers.
- iii. To analyze and compare the proposed method qualitatively and quantitatively with the existing non-optimized and static clustering techniques. The assessment parameters to utilize are percentage cost reduction (PCR), percentage PAR reduction (PPARR), power usage profile's variance to mean ratio (VMR), percentage peak shaving (PPS), and peak utility grid power (PUGP).

1.3.1. Design Objectives

The proposed system was to be designed as a novel two-phase HEMS optimization strategy, which can be summarized as follows:

i. Phase 1: Load Scheduling

)

This phase would deal with the application of a dynamic clustered community home energy management system (DHEMS) scheme to the residential community. It would focus on residential power scheduling targeting electricity cost reduction for consumers and load profile PAR curtailment for a relatively large consumer population with non-homogeneous loads.

ii. Phase 2: Peak Shaving

The second phase would propose a dynamic rule-based peak shaving management method for the photovoltaic (PV) systems and battery energy storage (BES) systems that are connected to the grid. It would focus on effective utilization of distributed energy resources with significant improvement in utility grid peak power shaving.

The cognitive architecture for the design under consideration is shown in Fig. 1-1. Phase 1 would propose a novel idea of load scheduling with the help of a dynamic device clustering scheme for the development of optimized load profiles for controllable devices. The proposed scheme would be applied to an MG community with various classes of society involved. The second phase would present the optimal peak shaving control strategy by involving PV and BES power sources in the MG community. A novel two-stage efficient distributed resource utilization scheme would be proposed which would offer significant reduction in utility grid demand with the help of optimized peak shaving.

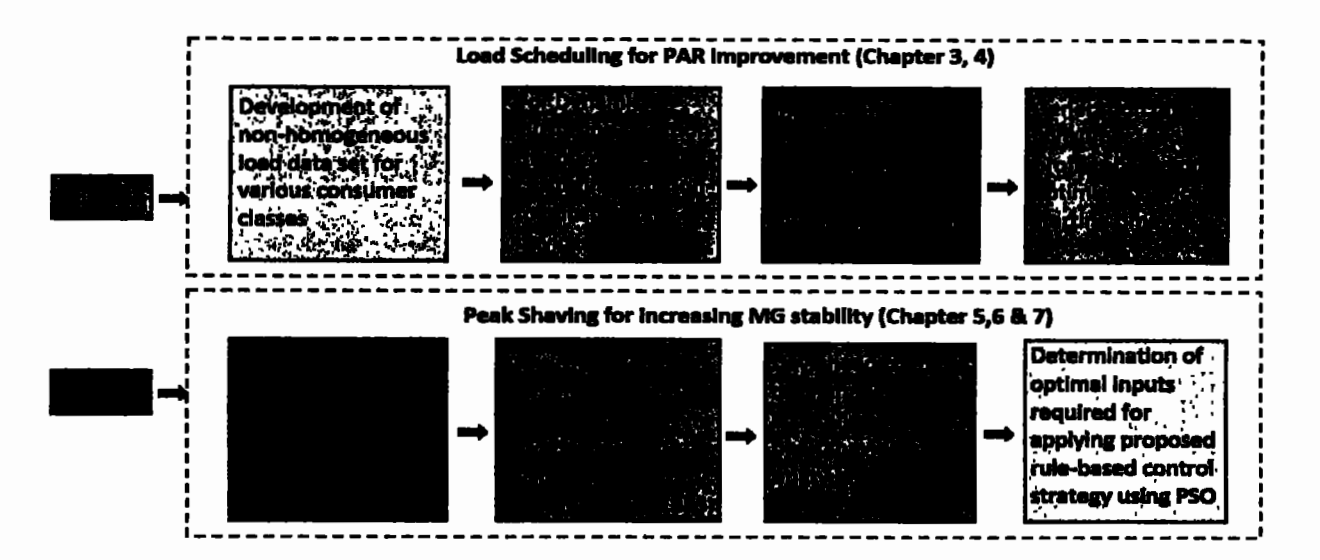


Fig. 1- 1 Block diagram of the proposed system model for efficient home energy management system

1.3.2. Implementation Objectives

The major aspects of the system to be implemented are as follows;

i. Generation of Load Profiles

- A large data set of 1000 dwellings for the period of three months would be considered.
 This would include input comprising of consumers' preference data related to the controllable devices' operations.
- The non-homogeneous consumer residential load profiles would be developed to represent dissimilar properties of consumer devices and distinctive user preferences from various classes of communities.
- To make the model meaningful, realistic and practical, four classes of consumers would be used i.e., lower, middle, upper-middle and higher class.
- Different load profiles for winters and summers along with distinct user preferences in response to the change of seasons would be utilized in the peak shaving algorithm.

ii. Efficient Load Shifting Model

)

- A model of dynamic clustered home energy management (DCHEMS) for MGs communities would be proposed that overcomes underperformance of static clustering schemes.
- The suggested load scheduling model would reduce PAR and consumer electricity costs for a large population.
- A DR-based load scheduling technique for smart devices that incorporates user preferences would be implemented.
- Consumers from different classes would be grouped into various communities with their devices assembled as clusters.
- PSO would be applied on each cluster for determining and allocating optimum starting time to the devices.

- The incorporation of modified inclined block rate in the fitness function of PSO avoids undesired power peaks in the load profiles.
- The tailoring of overlapping time slots (TSs) with inclined block rate would be done
 as it significantly improves PAR.
- Quantitative and qualitative analysis would also be presented against the existing literature.
- A comparison of results with non-dynamic clustering techniques proposed by Aziz
 et. al. and others would be presented [24].

iii. Optimal Peak Shaving Model:

)

- An optimized rule-based peak shaving management method for the PV and BES systems that are linked to the grid-connected MG would be suggested.
- The proposed technique would determine the dynamic demand as well as feed-in restrictions based on the predicted load demand and PV power profiles for the upcoming day.
- The technique would estimate the charge/discharge schedules of the BES for the upcoming day.
- The regulations would be written in such a manner that peak utility grid demands
 and feed-in power correspond to only the day's demand and feed-in limits. And
 while doing so it would ensure that by the end of the day, the battery's state-ofcharge (SoC) is the same as it was at the beginning of the day.
- To minimize peak energy pulled from the utility grid, PSO technique would be used to calculate the optimal inputs needed for implementing the appropriate rule-based management strategy.

- MATLAB software would be used to test the proposed management method for different PV power and load demand patterns.
- The quantitative and qualitative comparison with the existing work would also be presented.
- Finally, a two-stage control technique would be proposed for establishing the inputs
 needed for rule-based peak shaving management. It would involve both dynamic
 demand and day-to-day feed-in limits. The pre-processing stage of dynamic HEMS
 would assist the algorithm in improving PPS for the peak shaving control strategy.
- Detailed analysis of dynamic and non-dynamic schemes implementation would be presented for a community of 40 dwellings with various classes.
- Different load profiles for summer and winter day conditions along with high and low PV penetration would be discussed.
- The performance characteristics of the proposed schemes as compared to the reference schemes would be presented in quantitative and qualitative manner.
- The results would be analyzed with the help of quality assessment parameters e.g.,
 PCR, PPARR, VMR, and PPS.
- The data of real-time electricity prices would be taken from Ameren Illinois Power
 Company (2015) for the duration of 11th April 2015 to 9th July 2015.
- Solar irradiance values would be taken from ESMAP Tier1 Meteorological Station
 NUST university, H-12, Islamabad.

1.4. Contributions

)

The proposed methods will add the following benefits to the existing HEMS schemes;

- i. Overcome the underperformance of static clustering-based load scheduling schemes.
- ii. Significant reduction in consumer load profile PAR and cost of electricity.
- iii. Wide data set implementation on non-homogeneous consumer load profiles by using large data set of 1000 dwellings for three months.
- iv. Efficient utilization of distributed energy resources in community-based grid-connected
 MG.
- v. Optimized peak shaving management schemes with dynamic demand and day-to-day feedin limits.
- vi. A rule-based control algorithm taking flexible day-to-day management into account.
- vii. Minimized peak grid energy consumption from the utility grid.

1.5. Thesis Outline

)

The thesis is organized as follows.

- Chapter 2 presents the literature review of the proposed study. The research gaps in the
 existing literature are highlighted citing a number of papers. A table is also presented to
 highlight the limitations and objectives of existing models and techniques.
- Chapter 3 presents the proposed model of a dynamic clustered home energy management system for communities. The final objective of the proposed approach is highlighted by presenting home electric devices usage patterns and the inclined block rate pricing schemes.

- Chapter 4 discusses the modification in inclined block rate incorporated with the pricing scheme. The use of PSO to target energy consumption management is also detailed. The chapter ends with the simulation results presented in comparison to the reference techniques.
- Chapter 5 presents a study on renewable integration with clustered community HEMS. It
 discusses the scheme for distributed resource energy management and how it manages the
 shortcomings of the management systems. It highlights the drawbacks of fixed demand and
 feed in limits and the requirement of day-to-day management of BES state of charge (SoC).
- Chapter 6 presents an optimal rule-based peak shaving control algorithm using the dynamic feed-in and demand limits. It presents simulations, and rules for charging/discharging.
- Chapter 7 presents the proposed dynamic HEMS-based optimal peak shaving control in an MG system. It presents the load profiles based on appliances' usage preferences for winters and summers. It highlights the percentage improvement in results when using the rule-based peak shaving algorithm.

)

 Chapter 8 presents conclusive remarks regarding the proposed study along with some further research directions in the similar domain of study.

Chapter 2

)

Literature Review

This chapter reviews the literature related to the proposed study. The research gaps pertaining to load scheduling and peak load shaving are highlighted. The objectives and limitations of existing models and techniques have also been summarized.

2.1. Energy Management

There has been a dramatic increase in demand due to continued economic and population growth. As per a survey conducted by U.S. EIA, there are chances of a 48% increase in energy demand between 2012 and 2040 [25]. The growing demand cannot be fulfilled by the already shrinking fossil fuel supplies. Furthermore, this growing energy demand has become a challenge for electric utility companies and a threat to the sustainability of the environment.

The two possible methods to control these rising energy demands are (i) demand-side energy management (DSEM), and (ii) generation-side energy management (GSEM). DSEM deals with an increase in generation units' capacity to fulfill the rising electricity demand. Contrarily, GSEM aims to create awareness among the consumers for effective utilization and active participation in DR-based programs. The main target of these DSEM programs is to maintain a balance between generation and demand aiming to enhance power grid reliability and stability.

The traditional power systems expatiate in turning on peak power plants to meet the peak electricity demand. Contrastingly, DSEM strategies encourage consumers to the reduction of energy consumption actively during peak hours. The details of the DSEM strategies are presented as follows.

2.1.1. Load Scheduling

Load scheduling is defined as shifting load from elevated price to less price time slots. This strategy does not affect the total energy consumption as it remains the same before and after load shifting. The customers are offered benefits of price and incentive-based programs for encouraging them to get their loads scheduled to non-peak hours from peak hours.

2.1.2. Peak Clipping

Peak clipping or peak shaving believes in reducing the energy demand during high price time slots. This can enhance power grid stability by reducing consumption and generation. The distributed alternative energy resources may also be used to shave the peaks that reduce the burden on the electric utility companies and the power grid.

2.1.3. Strategic Conservation

Strategic conservation is a technique utilized by electric utility companies to modify the shape of the load curve based on incentives targeted for end-users. The reduction in energy consumption and consequent reduction sales of energy is represented by modification in the shape of load curve shape. The cost effectiveness of the deployed electric utility companies compensate for the deliberate and naturally occurring changes in energy consumption as well in the shape of the load curve. Improved device efficiency and weatherization can be taken as examples of strategic conservation.

2.1.4. Valley Filling

A classical energy management mechanism of building loads during off-peak periods to smooth out the overall load curve is termed valley filling. It is suitable for time slots when the incremental cost is lesser as compared to the average electricity price. The addition of load to the off-peak periods also decrements the cost of electricity for consumers. One of the ways of employing valley filling is to utilize ESS or plug-in hybrid electric vehicles (PHEV).

2.1.5. Strategic Load Growth

The strategic load growth can be defined as the change in the shape of load curve beyond valley filling. Consumer incentive-based approach is used in electric utility companies for load curve shaping as a result of increased consumption. A major factor for increased load is inclusion of emerging electric technologies such as industrial heating, automation and electric vehicles which is collectively referred to as electrification. These emerging technologies promise to reduce dependence on fossil fuels while improving overall productivity.

2.1.6. Flexible Load Shape

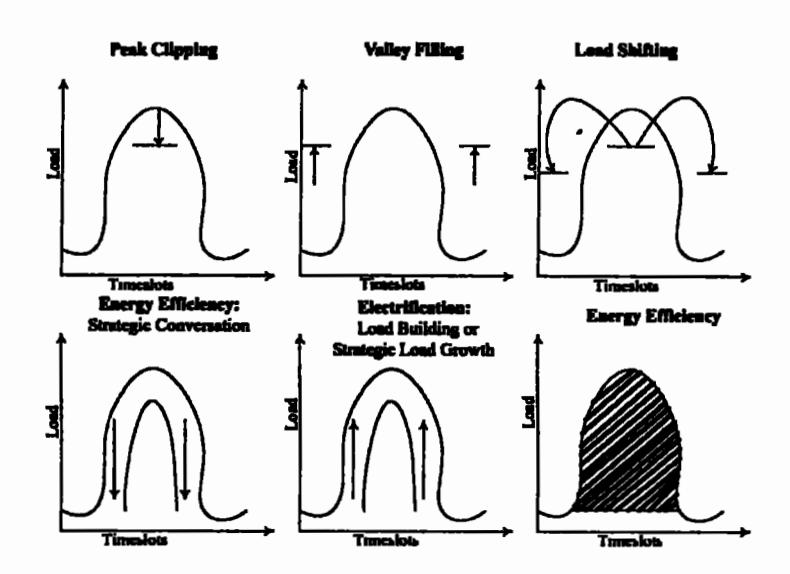
)

Flexible load shape deals with planning constraints and offers reliability improvement of power grid systems. The electric utility companies can comfortably plan the loads once the load behaviors are forecasted. Flexible loads can be acquired when the users are encouraged and motivated to participate in the incentive-based programs. The flexible load like interruptible load, curtailable load, time flexible load, and power flexible load participates in energy management to ensure reliability.

The overall DSEM strategies are depicted in Fig. 2-1 [26], [27]. This work focuses on energy management via the second approach, i.e., DR programs. It explores the first two schemes i.e., load shifting and peak shaving with application to residential consumers termed as HEMS.

2.2. Load Scheduling Techniques: Objectives and Limitations

The DR process generally comprises three pricing schemes; time of use pricing, critical peak pricing, and real-time electricity pricing (RTP). Time of use pricing and critical peak pricing enable electricity price calculation in advance. The price calculation process can be performed quarterly in both the schemes. Due to hourly updates in the price, flexibility in RTP can mirror load profiles or the generation costs.



)

Fig. 2-1 Strategies for efficient demand-side energy management

But using RTP for consumer's electricity cost reduction may increase PAR during low price time slots. This is because the peak values in power consumption pattern will move to low electricity price slots [28]. Hu et al. have proposed a DR-based energy consumption scheduling scheme [29]. Price reduction is achieved but the customer's comfort is compromised with chances of peak load emergence in low price hours. Du et al. suggest an electricity reduction-based optimization model [30] that combines the two schemes of RTP and inclined block rate. Despite achieving significant improvement in cost reduction, the scheme only operates for limited time span of one day or one-

month. Also, the sample data set is small i.e., one household. Imran et al. propose a heuristic computation-based load scheduling mechanism. The main objective of the proposed approach is to improve PAR, minimize electricity bills, reduce carbon emissions, and increase user comfort [31]. But the simulations are presented for a small data set of a single house for a day only.

Many studies addressing various energy parameters have been conducted. The parameters studied include the daily energy cost, allowable home temperature ranges, energy usage, peak hours' energy usage, and consumer's comfort [32-34]. The effects and analysis of usage plans such as fixed pricing, time-of-use pricing and real-time pricing have also been studied. To meet energy demand in real time, Homod et al. proposed the Takagi-Sugeno fuzzy based method. This energy based operational model was developed for HVAC systems that used distributed energy resources, non-controllable appliances (NCDs) and BES systems. Clustering used by output variables made different groups of temperature average data for the entire year. The method was optimized for HVAC systems but it did not consider rest of the commonly used residential loads [35]. The authors have suggested performance improvements for HVAC systems [36]. Recent studies show the application of cluster-based optimization strategies at the MG level [37,38]. Yet they fail to consider consumer's preferences at appliance level. Also, the algorithms have limitations in handling a large dataset with variations in the types of communities.

)

Some proposed models use game theory [39] and fuzzy logic-based models [40] to solve energy management problems of residential buildings. But these models are based on a very small data set of a day, a limited number of houses, and appliances that do not depict practical scenarios. Waseem et al. uses Grey Wolf and Crow Search Optimization (GWCSO) algorithm to reduce PAR and EC [41]. But the proposed technique considers only the HVAC loads for scheduling which limits the scope of GWCSO algorithm. Kim suggests a heuristic computation-based binary

backtracking search algorithm to optimize the energy usage of controllable devices. In comparison with particle swarm optimization (PSO), the algorithm shows higher energy efficiency. But it does not consider EC and PAR [42].

Dong reformulated the economic dispatch problem using data-driven energy management [43]. The model used an optimal algorithm at 30 minutes sampling time and did not consider PAR in the proposed algorithm. Javaid et al. and Hafeez et al. proposed heuristic algorithm-based optimization models for household load scheduling to reduce overall electricity bill and PAR [44-46]. But the models performed well for only small data sizes. The performance lowered as the size of the data increased. The models suggested no mechanism to handle large data. Hafeez et al. proposed an optimization scheme exploiting mixed-integer linear programming (MILP), binary backtracking search algorithm (BBSA), and artificial neural network (ANN) [47]. Although the objective of electricity bill reduction and PAR alleviation was attained but at the cost of increased system's complexity and execution time.

)

Jiang proposes an approach based on genetic algorithms to improve EC and PAR under step tariffs in a power system [48]. The simulation results shown depict a very small data set of three houses. Hussain suggests a genetic harmony-based search scheme to analyze the single-user and the multi-user but with a small population size of 30 [49]. A one-hour sampling time was used. The small data set cannot properly reflect the real-time operation of the appliances. The sampling time used is one hour that cannot reflect proper real time operation of the appliances. Paudyal suggests a load profile's peak reduction using a linear model [50]. But model uses a population of only 25 houses. Aziz et al. presents a power scheduling methodology for a large population [24]. However, the technique is based on the assumption of homogeneous consumption. This means that all

appliances in the entire population have the same properties and belong to a similar class of consumers.

2.2.1. Deductions

)

The literature review suggests that the majority of power scheduling strategies focus on a small population sample size, thus leaving the investigation of their behavior under a larger population size unexplored. So, the algorithm's behavior towards a larger population size does not get investigated. The review suggests a need for clustered community-based home energy management system for large population that is dynamically clustered. For a big population set, such a system would affect performance. Table 2.1. summarizes a few studies on heuristic computation strategies.

Table 2. 1 Summary of a few studies on heuristic computation strategies

Energy Management Models	Techniques	Objectives	Limitations
Efficient residential Load scheduling	GA, MILP	PAR and energy expenses reduction.	Simulations represent a small data set i.e., one house
		Reduction of CO2 emissions.	and of one day.
		Reduce discomfort level of consumers.	
Bi-level optimization model	MILP, IABC algorithm	Increase MG cluster profits.	MG clusters are made via static clustering approach.
		Lower MG operation risks.	User preferences are not incorporated at device level strategies.
HEMs based on fuzzy controller	RTP, inclined block rate, and time of use pricing	Electricity cost, PAR, and energy usage reduction in a reasonable amount of time.	Simulation represents results for a day.
			Model operable for small devices number.

Energy Management Models	Techniques	Objectives	Limitations
Innovative home devices scheduling framework	GWCSO	Reduction in electric bills and an increase in PAR.	Tested only for HVAC loads.
Heuristic based HEMs	Heuristic optimization algorithm	To reduce PAR and electricity expenses.	Considers only homogeneous loads.
			Tested on one house only.
Use of game theory for residential load scheduling	Time of use pricing based on game theory	To reduce PAR and electricity expenses.	Only three homes considered.
Domestic Power scheduling based on time	SCHEMS	To reduce PAR, VMR and electricity expenses.	Homogeneous loads and void of consumer classification.
			Static clustering scheme applied.

2.2.2. Propositions

)

The proposed HEMS aims to improve a larger population's performance as well. The suggested load scheduling approach reduces the load profile's PAR and consumer electricity cost. Consumers of various socioeconomic strata from communities and their devices are grouped into clusters. To each cluster, PSO is applied, and the devices are given the best possible start time. The fitness component of PSO additionally includes a modified inclined block rate to eliminate undesirable peaks during any time slot. When the overlapping time periods of devices are adjusted with inclined block rate, PAR is decreased. The suggested system's results are compared to those of Aziz et al.'s static clustering techniques. To make the model meaningful, realistic and practical, it uses a large data set of 1000 houses for three months. It implements a demand response-based strategy based on consumers' preferences for load scheduling of controllable appliances. Also, it considers the various types of consumable appliances that are commonly used in households.

2.3. Peak Load Shaving: Objectives and Limitations

)

Despite having a large number of advantages, peak reduction of consumer load profiles using load scheduling has a limitation due to certain constraints provided by the consumer as per their comfort. Hence, the researchers have to look for some other solutions for enhancing the reliability and stability of MGs. Peak load shaving can also be one of the promising solutions for creating a balance between electricity supply and power demand. For the optimal peak shaving control strategy, the participation of distributed energy resources is essential in the MG system. Generally, PV and BES are used as DERs. Due to a number of voltage drop and rise issues due to the charging and discharging of BES, the problem of integrating the BES to the MG has been a current research topic in the recent past.

BES charge/discharge schedules are controlled using a variety of methodologies, including genetic and rule-based algorithms, dynamic programming, and so on [51]—[53]. Rule-based methods execute instructions by employing an initial set of data and rules based on if-then statements [54]. In comparison to other approaches, these algorithms have straightforward implementation and development. In [55] and [56], rule-based techniques are contrasted to optimization techniques. They have also compared the rule-based methodologies with optimization techniques. Rampelli et. al. presents an effective rule-based strategy. The evolutionary algorithm [57] is used for the determination of ideal inputs for the suggested rule-based peak shaving management. All of these strategies are demonstrated to ignore the DSM stage before using rule-based peak shaving techniques. To overcome this shortcoming, in the suggested method, the dataset is subjected to a PSO method in load scheduling of home users'-controlled devices prior to the application of the peak shaving algorithm.

For peak shaving, the demand limit (feed-in limit) is the maximum amount of power that can be extracted from (injected into) the electrical grid. Flexible daily management with a BES means keeping the end-of-day SoC the same as it was at the start. A battery controller is discussed to set demand limit in [58]–[60] for peak demand shaving. The feed-in limitation, however, is not discussed. [61] considers flexible daily management as well as operative PV energy consumption for peak demand shaving applications. The demand ceiling, on the other hand, is set. In [62], only the dynamic feed-in restriction is taken into account for peak demand shaving, ignoring the demand limit. In [63], peak demand shaving utilizing BES optimum scheduling with a restriction on the dynamic demand is explored. The feed-in limit is not discussed. In [57], both load demand and feed-in powers are discussed while preserving flexible daily management.

2.3.1. Deductions

The literature review suggests that a peak shaving algorithm be explored with application to a community-based architecture with a large number of households and/or resources. In the existing literature, the optimal rule-based methods fail to provide dynamicity in the heuristic computation-based schemes applied. Additionally, the existing schemes in literature haven't incorporated weather-based fluctuations in consumer behavior whilst incorporating user preferences. The literature review suggests that load scheduling and peak shaving be applied in a more practical scenario with change in consumer preferences with weather conditions. A few papers from optimal power flow management are briefly summarized as given in Table 2.2. As it is obvious from the table that most of the proposed schemes offer fixed demand and feed in limitations.

Table 2. 2 Qualitative comparison of suggested technique with the previous work

	Demand Limit	Feed in limit	Daily management
[58-60]	Fixed	Not considered	Not considered
[61]	Fixed	Not considered	Flexible
[62]	Not considered	Dynamic	Not considered
[63]	Not considered	Not considered	Not considered
[64]	Fixed	Not considered	Not considered
[65]	Fixed	Not considered	Not considered

2.3.2. Propositions

Based on the above highlighted limitations of load scheduling and peak shaving in energy management system, a two-stage dynamic clustered community-based home energy management system (DCHEMS) is proposed and applied to the residential. A pre-processing stage focuses on load scheduling algorithm with application to a community architecture. While, to cater remaining peaks in the modified load profile, an optimal peak shaving algorithm with day-to-day energy management scheme is applied in the second stage. The second stage determines the inputs needed for the proposed rule-based BES optimized peak demand shaving control by means of PSO. The proposed scheme is targeted to achieve improved performance for community architecture in MGs. To make the model more relatable, closer to real world, and practical, the proposed model will be focused on the community-based architecture utilizing non-homogenous loads analysis i.e., lower (LCS), middle (MCS), upper-middle (UMCS), and high class (HCS) consumer. The load is non-homogeneous due to the non-identical features of consumer products and various user preferences from different classes. Each class of consumers has its own set of PV installations to consider. To account for seasonal fluctuations in consumer behavior, different usage parameters for SDs in

summers and winters will be examined in the study. Simulation results are compared to the values without dynamic-HEMS optimization and a closely related work of Rampelli et. al [57].

)

Chapter 3

Demand Response Based Load Scheduling in Residential Energy Management System

This chapter gives an introduction to DCHEMS to be discussed in the next chapter. It details the basic architecture of a residential network in terms of energy management systems.

2.2 Home Energy Management Systems

A home energy management system consists of an energy management controller (EMC), advanced metering infrastructure (AMI), home gateway (HG), home devices, and in-home displays (IHD). The typical structure of an energy management system in a home user's network is shown in Fig. 3-1.

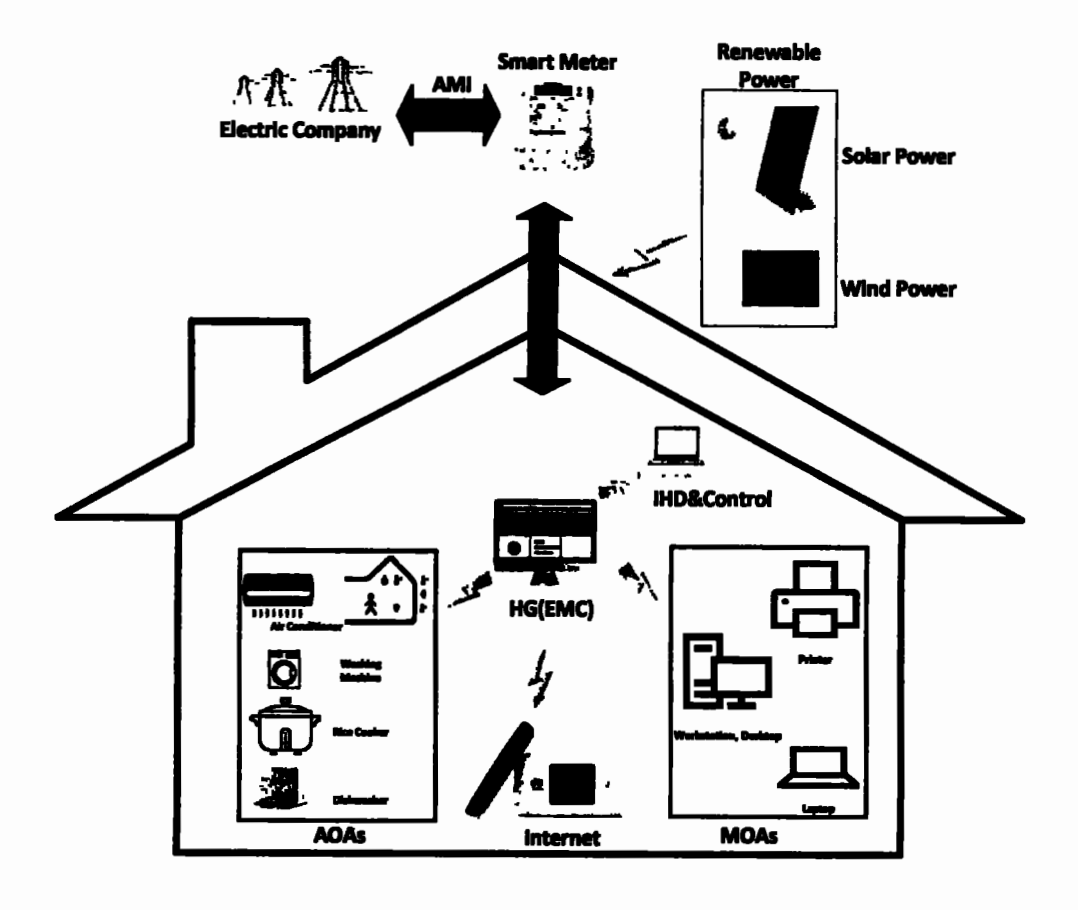


Fig. 3- 1 Architecture of residential energy management [66]

The proposed model explores controllable devices (CD) and non-controllable devices (NCD). CDs are automatic and do not require any manual intervention to conduct their operations. For instance, clothing washers, dishwashers, electric kettles, or rice cookers. The devices can also be categorized as: non-interruptible (rice cooker) and interruptible (clothing dryer) [67]. The NCD operates under consumer dependence and is operational while in use, such as a hand beater, telephone, or non-robotic vacuum cleaner. As a result, the CD can only be scheduled, whereas NCD necessitates manual intervention. Furthermore, the CDs taken into account in this technique are smart home devices. CDs do not communicate with each other in the architecture shown below; instead, they solely interact with the home gateway. The home gateway is responsible for scheduling all the CDs connected to the house at the beginning of the day.

To formulate a connection between the smart meter and the home gateway, a variety of wireless solutions are available. Zig-Bee, Z-Wave, Wi-Fi, or a wired (plugged-in) protocol are the possible options [68]. The home gateway can provide an optimized power consumption schedule to each CD via the home area network. The scheduling process can be monitored through the inhome display or remotely controlled gadgets such as mobile phones, laptops, etc.

The proposed technologies presented in this research assume that smart meters and household devices are combined into an EMC that accepts RTP data from the utility.

3.1. The Usage Pattern for Home CDs

The study has considered 16 devices in one house with a population set of 1000 houses.

Once the utility delivers the user preferences information and electricity price profile to the home

gateway, the EMC can draw inferences about device load scheduling. Consumers prefer to avoid peak hours wherever possible, yet some jobs require being accomplished before certain time periods. Some tasks, such as clothe washing with automatic washers, can be performed at night because as residents are asleep, the electricity price is low. As a result, customers must specify time constraints for each CD. As shown in Fig. 3-2, the parameters for time given as consumer input include starting time of device operation (STDO) α_{a_k} , ending time of device operation (ETDO) β_{a_k} , time length of device operation (TLDO) l_{a_k} , time interval of device operation (TIDO) $[\alpha_{a_k}, \beta_{a_k}]$, and device rating x_{a_k} . One more parameter of time, i.e., activation time slot; t_{a_k} , is allocated to each device after being generated by the optimization technique, which is discussed in the next chapter. The subscript 'a' denotes the device number and 'k' denotes the house number. The EMS via the home gateway receives the data collected from these parameters by the in-home display device.

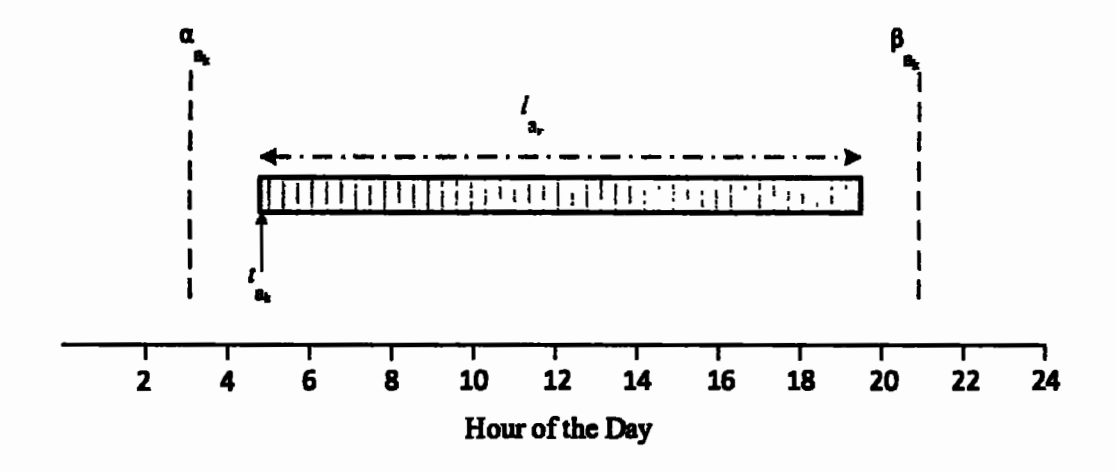


Fig. 3-2 Parameter constraints of devices

Only CDs are scheduled under the proposed concept; NCDs are not. The simulation findings, on the other hand, show that the approach remains effective for NCDs as well. The optimal power scheduling for CDs follows a specified pattern, which is detailed in the next chapter.

As previously stated, consumer preferences metrics are collected for each CD. To do this, we use the indexes a_{a_k} and $\beta_{a_k} \in U\left(a_{a_k} < \beta_{a_k}\right)$, as the start and end TSs, respectively. Device power consumption is believed to be accurate for proper scheduling inside this operation time range. Let TLDO, or needed TSs for device operation, be l_{a_k} . The characteristics listed above are determined based on user choices obtained via in-home display and afterward submitted to EMC. Furthermore, β_{a_k} - α_{a_k} should either exceed or is equivalent l_{a_k} . For instance, if the clothing washer takes 60 minutes to complete the task, of β_{a_k} - α_{a_k} could attain any number equal or larger than 6 and smaller than 144 in the meantime. The bigger the value of β_{a_k} - α_{a_k} , the more load scheduling options are available. These correlations of the above-mentioned characteristics are shown in Fig. 3-3 for four distinct types of CDs i.e., a₁, a₂, a₃, and a₄ for the k^{th} dwelling.

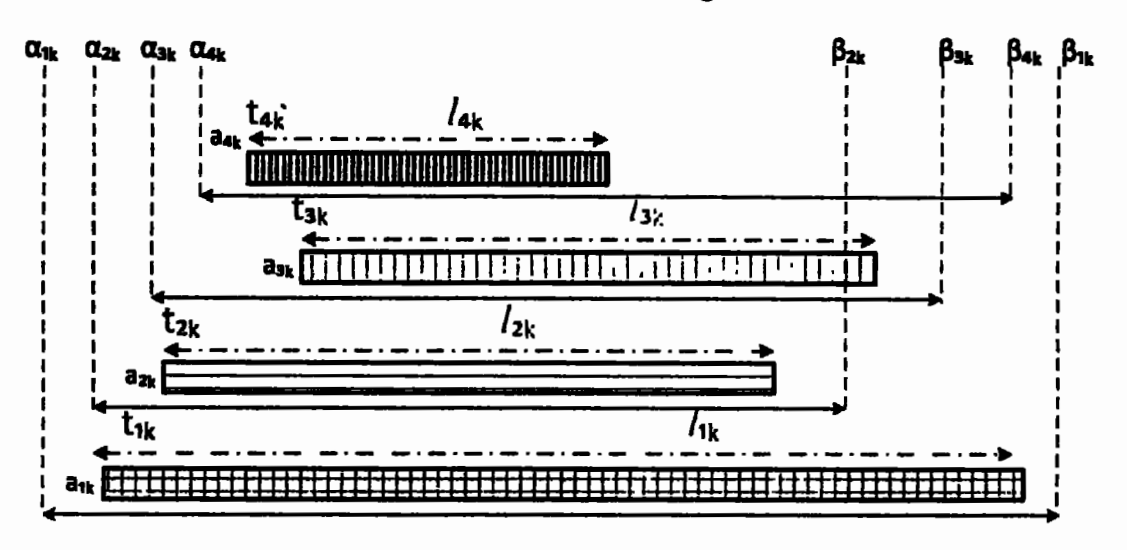


Fig. 3-3 The relationship of devices parameters shown in an example

3.2. Inclined block rate Pricing Scheme

Although RTP is more flexible than time of use pricing and critical peak pricing, it has the disadvantage of clustering many devices in low electricity price zones as shown in Fig. 3-4 (a). It

can be observed that new peaks have emerged around 20 and 100 TSs due to low electricity prices in these timings. Hence, RTP allows the accumulation of devices in the respective TSs. Given this limitation, the suggested system uses a combination of inclined block rate with RTP, which can alter electricity price rates within low electricity price TS according to the devices' power usage [69]. This eliminates the possibility of a second peak in low electricity price time periods as shown in Fig. 3-4 (b). It can be noticed, that application of inclined block rate reduces peak to average ratio of power profile as well as prevents new peaks emergence. This leads to the fact that the use of an inclined block rate, which may control the power demand of one device by suggesting its penalty factor, reduces PAR. However, if a large number of devices appear during the same time slots, the power consumption pattern of the entire power system will skyrocket.

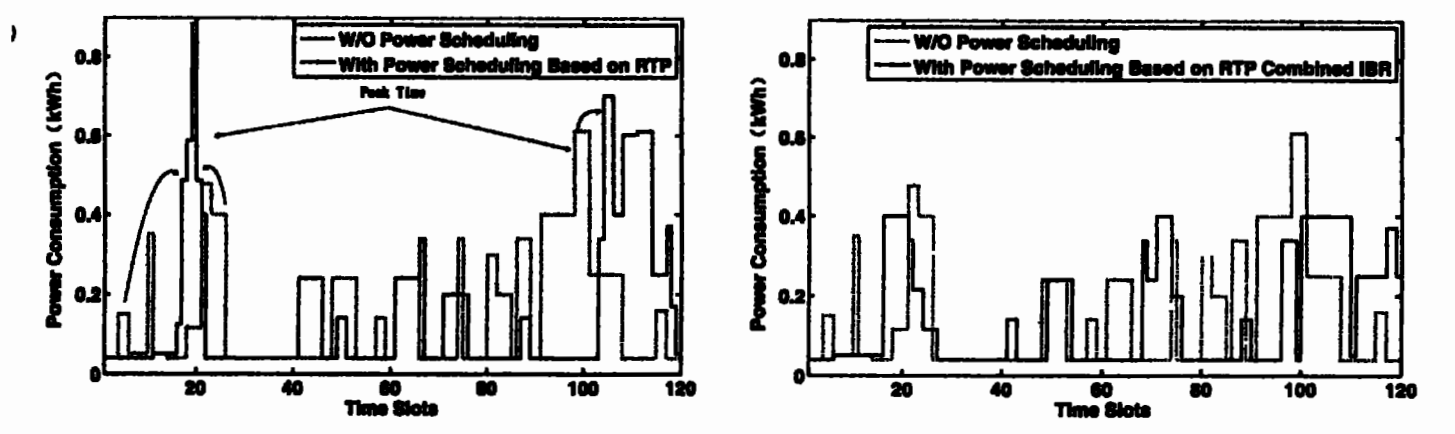


Fig. 3- 4 Comparison of load scheduling techniques, (a) Load scheduling with RTP (b) Load scheduling with RTP combined with inclined block rate [66].

This scenario is explained with the help of Fig. 3-5. For the sake of easiness, we've just examined one device per home in a community of m homes. The devices in question are supposed to have their α_{a_k} in a TS with the lowest electricity price compared to its successor slots. In this case, any scheduling method used in combination with the inclined block rate will tend to push t_{a_k}

of all houses near the slot with the lowest electricity price. Despite this, the Inclined block rate is able to keep the power consumption pattern of each dwelling below the required level. However, a power consumption pattern peak in the general community will be caused by the constellation of devices t_{a_k} arranged around the lowest electricity price. It eventually affects the entire electricity system. If an RTP data for example, has the lowest electricity price around hour 5 of the day, and the devices in Fig. 3-5 will be scheduled around that time, generating a greater peak. This condition necessitates a power scheduling system that can scan the surrounding area while optimizing activation time start for all devices. As a result, the next chapter discusses how the proposed algorithm solves the situation.

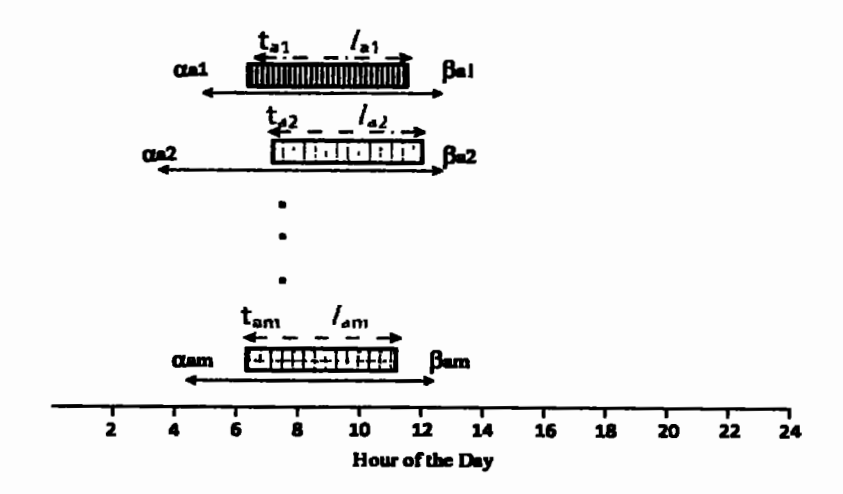


Fig. 3-5 Generation of power peaks in device's cluster shown as an example.

3.3. Summary

The findings of the chapter show that there is a need to explore an optimized community-based energy management scheme that is capable of handling large data sets. A clustered dynamic management system is proposed with application to communities in an MG in the following chapter.

Chapter 4

Dynamic Clustered Community Home Energy Management System

In this chapter, the dynamic clustered community home energy management (DCHEMS) model for controllable devices (CDs) is presented which is phase 1 of the dissertation. The patterns of residential electric equipment usage, as well as the chosen pricing mechanism, the inclined block rate, is detailed. A mathematical model and flow diagrams are used to demonstrate the suggested PSO-based approach for energy consumption management. The enhancement in results based on the proposed technique in contrast to the prevailing techniques is also shown.

The aim of an energy management system (EMS) is to keep the electricity costs down while lowering the PAR. It accomplishes this by planning power use in accordance with pre-determined electricity pricing. The stability and reliability of the electricity supply are guaranteed by such energy management systems. As a result, every DR-based scheme's primary purpose is to lower PAR and electricity cost, which benefits both the electric utility companies and the consumer.

The proposed community-based system architecture is compliant with MGs. In an environment where several MGs are connected to the grid, the proposed technology can be applied to a community inside an MG. The connected MGs act as substations, delivering DR to community users in accordance with their size. The structure of the community-based scheme for HEMS utilization in smart grid is shown in Fig. 4-1. The suggested technique can be implemented in a power system with many MGs, consisting of communities. Furthermore, each community has a number of houses.

4.1. Proposed System Model and Formulated Problem

The following section outlines an optimal load shifting strategy for all the CDs of the residential consumer. It exploits RTP and modified inclined block rate pricing schemes.

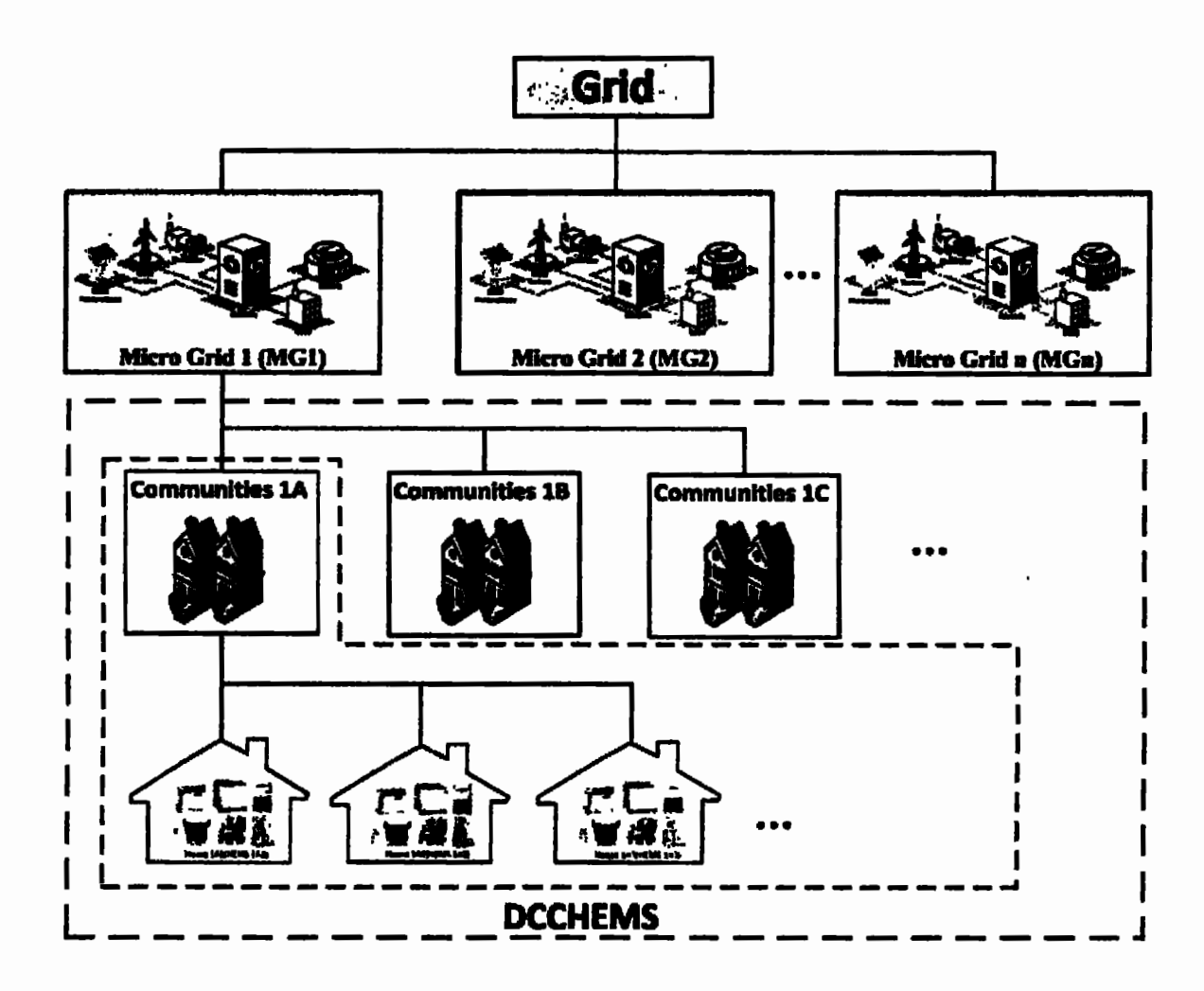


Fig. 4- 1 Community based HEMS framework

The content presented in this chapter is based on my research also published in IEEE access.

4.1.1. Objective of Proposed Approach

Electricity price rates are changed hourly in an RTP configuration. The degree of freedom for optimizing activation time start is lowered if the scheduling of CDs is performed on an hourly basis as per RTP. Conversely, smaller time period consideration may experience convergence problems due to a high number of possible parameters involved. As a result, the plan is to divide a one-hour period into six TSs, each lasting ten minutes. Consequently, a day has 144 TSs denoted by the symbol $\tau \in T$ defined as $\{1, 2, 3 144\}$ [70]. When a day is partitioned into 144 TSs, computationally efficient optimization problems such as PSO can be performed. As a result, the smallest operation time of every device is selected as 10 minutes. The operation times should be denoted by integer multiples of ten.

Considering common household appliances, it is assumed that the number of CDs connected to a house is 16. a is used to denote CDs. We assume that each appliance $a_k \in a$ has the power consumption scheduling vector \mathbf{p}_{a_k} of dimension 1×144 as,

$$\mathbf{p}_{a_k} \triangleq \left[p_{a_k}(1), p_{a_k}(2), \cdots \dots, p_{a_k}(144) \right] \tag{4.1}$$

Where $p_{a_k}(\tau)$ represents the power consumption value for the a^{th} device of the k^{th} house, during the τ^{th} TS. $p_{a_k}(\tau)$ has the unit kWh. Since each house has 16 devices, $a \in \{1,2,\ldots,16\}$. We assume that each device's hourly power consumption remains fixed because each device has a specified specification, as illustrated in Fig. 4-2.

If the per hour power consumption of the device a_k is signified by x_{a_k} , the corresponding power consumption during τ^{th} TS is estimated as,

$$p_{a_k}(\tau) = \frac{x_{a_k}}{6} \tag{4.2}$$

Here, x_{a_k} is the a^{th} device power rating for the k^{th} dwelling. Optimization of the power consumption scheduling vector \mathbf{p}_{a_k} is the target. It has been transmitted to a^{th} device via a proper wireless connection.

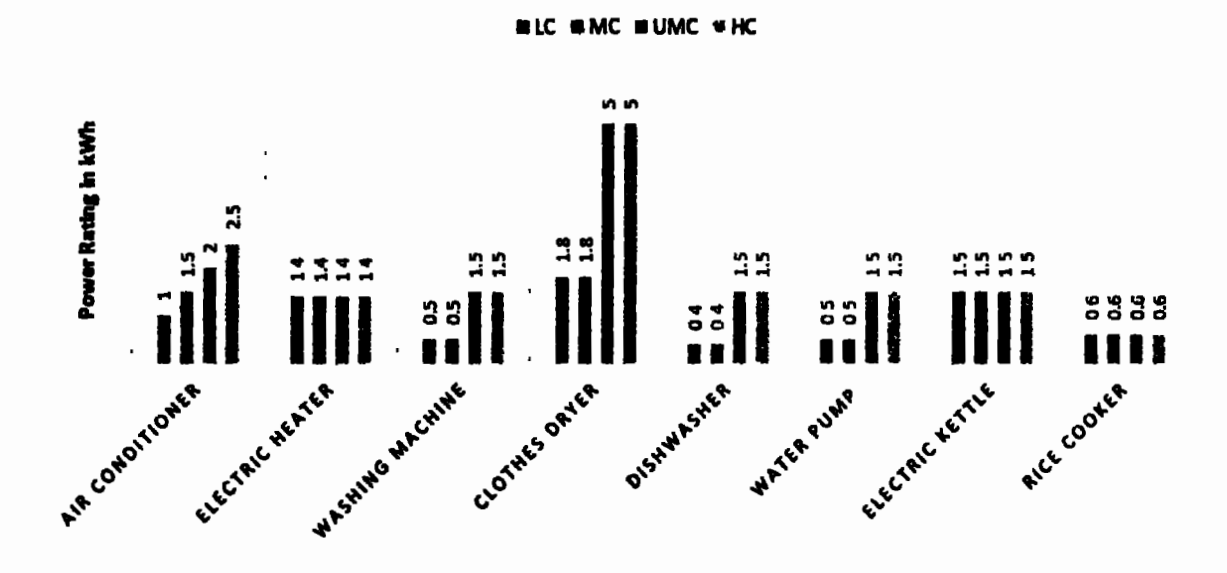


Fig. 4-2 Devices with non-homogeneous loads, for all four classes, with power rating in kWh

We define a variable t_{a_k} as the activation time slot (ATS) for the a^{th} device of k^{th} house. Since, a_{a_k} , β_{a_k} , l_{a_k} and x_{a_k} are all known already, the power consumption scheduling vector of a device 'a' can only be determined once t_{a_k} is known.

STDO α_{a_k} , ETDO β_{a_k} , AOTI $[\alpha_{a_k}, \beta_{a_k}]$, TLDO l_{a_k} , and power consumption value per hour x_{a_k} are now available for each device $a_k \in \mathbf{a}$. Additionally, we made activation time start denoted by t_{a_k} , a variable. t_{a_k} should be larger than or equal to α_{a_k} and less than or equal to $\beta_{a_k} - l_{a_k}$ and

it can be determined if α_{a_k} , β_{a_k} , and l_{a_k} are known. To put it another way, the variable parameter t_{a_k} is written as

$$t_{a_{b}} \in \left[\alpha_{a_{b}}, \beta_{a_{b}} - l_{a_{b}}\right] \tag{4.3}$$

In Fig. 4-3, the t_{a_k} range is illustrated as a sample for a^{th} device of k^{th} dwelling.

We must calculate the optimum value of ATS for every CD subject to the constraint specified in the equation for the a^{th} device and k^{th} house (4.3). ATS for all the CDs is stored in a variable vector $[t_{a_1}, t_{a_2}, \dots t_{a_k}]$. Therefore, a power consumption scheduling matrix for all CDs would have the expression as

$$\mathbf{P} = \begin{cases} p \mid p_{a_k}(\tau) = \frac{x_{a_k}}{6}, \forall a_k \in \mathbf{A}, \tau \in [t_{a_k}, t_{a_k} + l_{a_k}] \\ p_{a_k}(\tau) = 0, \quad \forall a_k \in \mathbf{A}, \tau \notin [t_{a_k}, t_{a_k} + l_{a_k}] \end{cases}$$
(4.4)

where P denotes a matrix in which each row stands for the power schedule of a certain device. τ specifies the column indices. $\tau \notin [t_{a_k}, t_{a_k} + l_{a_k}]$ denotes that τ belongs to T but not to the range $[t_{a_k}, t_{a_k} + l_{a_k}]$. Each column vector of the power utilization scheduling matrix is added up to calculate the total power utilization scheduling vector \mathbf{p}_{scd} .

$$\mathbf{p}_{scd} = \{ p_{scd} \mid p_{scd}(\tau) = \sum P(\tau), \forall \tau \in \mathbf{T} \}$$
 (4.5)

 $P(\tau)$ denotes the τ^{th} column in the power utilization scheduling matrix in equation (4.5).

When the power utilization scheduling problem is defined for a single residence, following is the expression for objective function

minimize Electricity cost (
$$p_{scd}$$
) (4.6)
s.t. $t_{a_{b}} \in [\alpha_{a_{b}}, \beta_{a_{b}} - l_{a_{b}}]$

where,

Electricity cost
$$(p_{scd}) = \sum_{\tau=1}^{144} rtep(\tau) \cdot p_{scd}(\tau)$$
 (4.7)

The electricity cost at the τ^{th} TS is denoted by RTP in equation (4.7). An optimization strategy can be used to reduce the electricity price shown in equation (4.7).

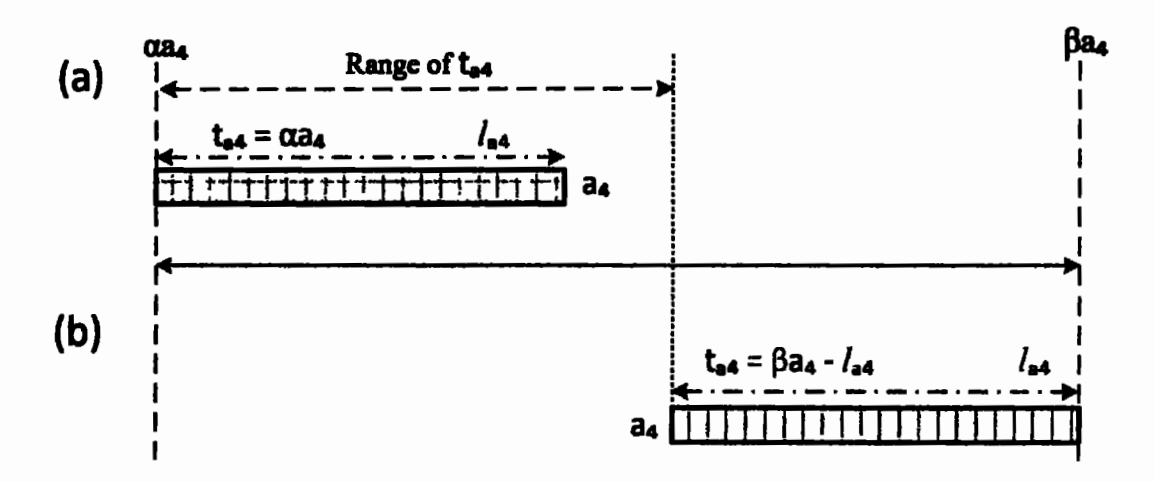


Fig. 4-3 The range illustration of STDO for home devices 'a': (a) device starting right at STDO and (b) device starting at the latest possible time.

4.1.2. Selected Pricing Scheme and Modified Inclined Block Rate

Application of inclined block rate pricing scheme affects RTP rates by multiplying it with a factor $\lambda > 1$, whenever the power usage pattern of any house goes beyond a predefined threshold. RTP is unaffected in any other way. Inclined block rate acts as a monitoring term, preventing sudden peaks in power consumption patterns from being caused by the scheduling algorithm. As a result of the scheduling algorithm optimization, unwanted power peaks can arise. When numerous devices in a house operate with overlapping α_{a_k} and β_{a_k} , this can happen. They may be assigned to identical TSs during which RTP offers low electricity rates. As a result, unfavorable power peaks

emerge. The PAR of the power consumption pattern is increased when these unwanted peaks occur. Inclined block rate controls such a situation by involving the penalty term and prevents the scheduling algorithm from creating power peak patterns. In the proposed approach, inclined block rate is modified to reflect the penalty term which applies only when power usage pattern crosses a γ_c scaled threshold i.e. the number of houses lying under the current community. Two electricity price levels are considered and there is a change in electricity price every hour. Modified inclined block rate control is incorporated into the RTP formulated as:

$$rtp_{pc}(\tau) = \begin{cases} rtp(\tau), & \text{if } p_c \le th \times \gamma_c \\ rtp(\tau) \times \lambda, & \text{if } p_c > th \times \gamma_c \end{cases}$$
(4.8)

where,

$$p_{c} = \sum_{\forall a \in C_{c}} \sum_{\forall k \in C_{b}} p_{a_{b}(\tau)} \tag{4.9}$$

Here $\operatorname{rtp}(\tau)$ is the real-time electricity price received from electricity supply company for time slot τ , $\operatorname{rtp}_{pc}(\tau)$ is the electricity price based on the power consumption p_c of the community being optimized, th is the threshold set to 2 kWh, and γ_c is the count of houses under current community. C_h represents a set of houses in the current community of consumers and C_c refers to the current cluster of CDs.

Numerous price forecast systems are given in the literature [71], [72], despite the fact that it appears unrealistic to forecast electricity prices a day prior. Fig. 4-4 shows the pricing data of electricity: RTP on the 9th of July 2015, retrieved from Illinois [73].

4.2. Proposed PSO Based EMS for Energy Consumption

This section introduces PSO and its application to the topic at hand.

4.2.1. Particle Swarm Optimization (PSO)

Eberhart and Kennedy [74] proposed the PSO, which is a particle population-based iterative approach. The optimization process begins with the particles' positions and velocities being given initial values. PSO enables candidate solutions, or particles, to congregate in surroundings of best solution space. Flight trajectories particles are monitored by the global best (gbest) and particle best (pbest). For this, they define the particle and local best positions, respectively.

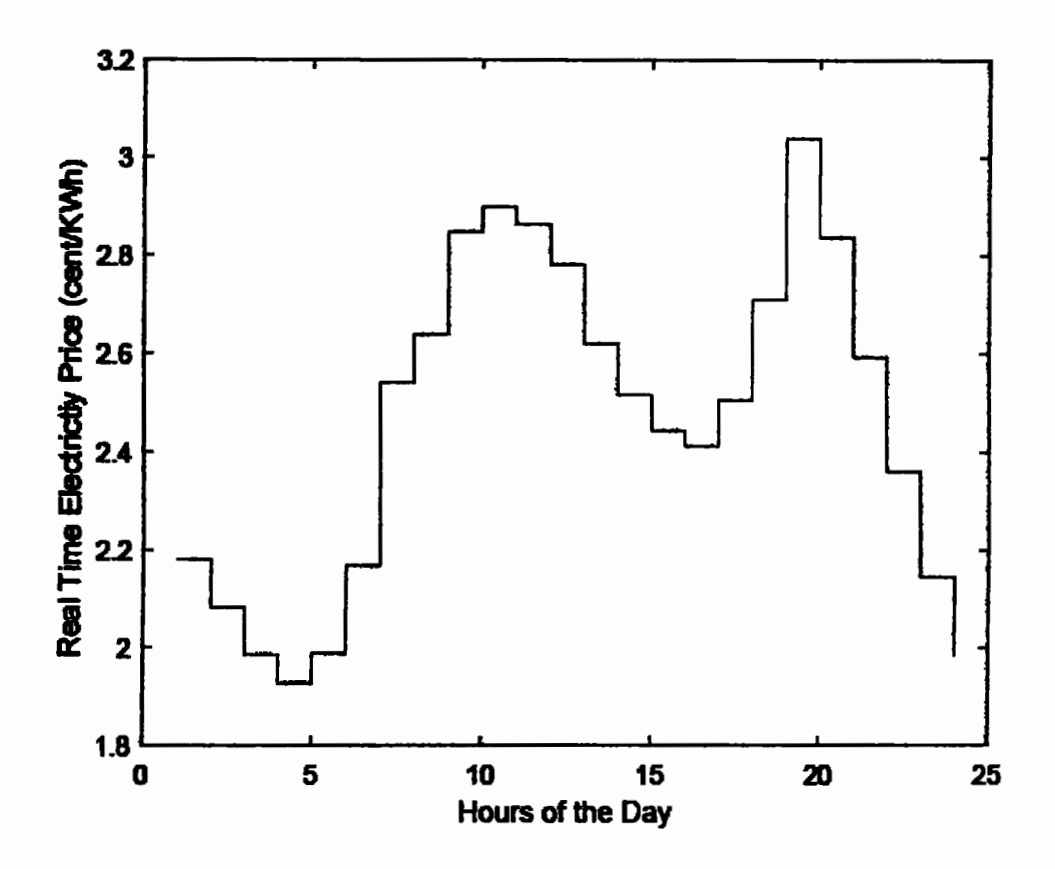


Fig. 4- 4 RTP on 9th July 2015

In our problem, electricity cost is reduced using PSO for optimum activation time start allocation of each house in the community. The goal of optimization is to keep TLDO within the range of STDO and ETDO as specified in equation (4.3). Customers provide the user preference which is the initial value for optimization termed as STDO. Then the cost function is saved that minimizes electricity cost as shown in (4.7) and adjusts *pbest* location for all the CDs. This process will continue until the termination condition is met.

As particle i goes throughout the search space, its velocity is updated according to equation (4.10). If x_i^t is i^{th} particle of position vector in the search space (i. e R_n) at time step t, then equation updates the location of each particle in the search space (4.11).

$$V_{ij}^{t+1} = \omega V_{ij}^{t} + c_1 r_1 \left(\text{pbes}t_{ij}^{t} - x_{ij}^{t} \right) + c_2 r_2 \left(\text{gbes}t_{j}^{t} - x_{ij}^{t} \right)$$
(4.10)

$$x_{ij}^{t+1} = x_{ij}^t + V_{ij}^{t+1} (4.11)$$

The i^{th} particle's velocity and position vectors in dimension j at time t are V_{ij}^t and x_{ij}^t . phest $_{ij}^t$ is the particle i's personal best position in dimension j as determined from initialization to time t. Similarly, ghest $_j^t$ is the global best in dimension j discovered over time t from initialization. The random numbers denoted by variables r_1 and r_2 are uniformly generated during the range of [0,1]. Coefficients represent the particle weight, the *phest* momentum is represented by c_1 , c_2 represents the pull towards ghest.

The velocities and particles are initialized randomly with the help of constraint described in equation (4.3). Each cycle is expected to improve the same initially created population. By keeping an eye on *pbest*, each particle improves its own version. If a newer form of *pbest* is improved than the old one, the old one is removed and replaced with the current one. Also, if *pbest* outperforms

gbest, pbest will take its position. When the process is ended and the termination criteria as stated in Fig. 4-5 are met, the *gbest* is returned as the final answer.

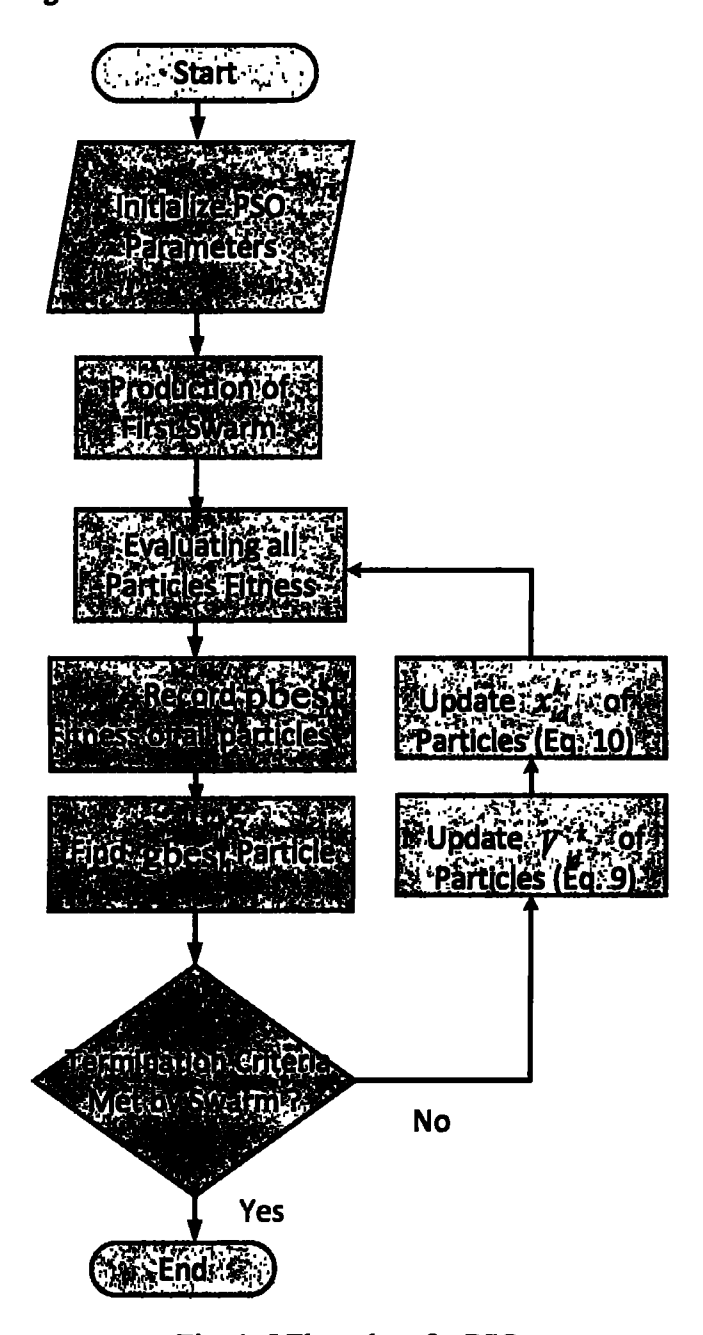


Fig. 4-5 Flow chart for PSO

4.2.2. Formulation of DCHEMS

Many firms, including California Edison and Pacific Gas & Electric [75], [76], have used the inclined block rate as a pricing mechanism for a long period. As discussed in the previous chapter, if a large number of devices appear during the same time slots, modified inclined block rate alone cannot handle the increase in power consumption pattern of the entire power system. Therefore, it is required to explore an optimization technique that is workable for such a situation.

It is assumed that grid or electricity supply company communicates DR-related tasks to the substations. And they further communicate it to the respective communities. The 1000 house complete population is separated into four sorts of community classes for non-homogeneous load analysis: Lower, middle, upper-middle, and higher class.

There are an equal number of dwellings in each of these classifications. According to their daily habits, each of these four classes has its own set of user preferences. For example, because their morning chores begin about noon, higher-class, which usually have their own independent businesses, wind up their chores till late at night. Their homes are typically equipped with heavy-duty loads, such as 2 to 5 tone air conditioners, automatic clothe washers that require a large amount of water to allow for extended water pump operation, and automatic water heating. In comparison to other community types, all of these devices are high in power ratings. Middle-class, on the other hand, does it a little sooner, with lower-power-rated devices linked at their residences. Devices such as automatic washers and dishwashers, for example, are installed without the need for electric water heating. As a result, they consume less power to operate than the higher or upper-middle-class [77]. Fig. 4-2 depicts the power ratings utilized for CDs in all four classes. Lower class usually begins and ends the day earlier. They start around 4 a.m. while finishing all of the chores around 9 p.m. Table 4-1 reflects these data for the above-mentioned classes. In each class, we assumed varying

percentages of CDs. CD is supposed to be 20% in the lower-class, 40% in the middle-class, 60% in the upper-middle-class, and 80% in the higher-class community.

Table 4- 1 Characteristic parameters used for CDs [24].

	Controllable Devices	Operation Time Slots (scattered between)
Lower-class	Electric Heater	95 – 125
	Air Conditioner	1 - 25, 125 - 144
	Clothe Washer	1 – 44
	Water pump	65 – 95
	Dishwasher	115 – 144
	Clothes Dryer	55 – 85
	Electric Kettle	25 - 50, 95 - 115
	Rice Cooker	1 - 35, 55 - 75, 92 - 115
Middle-class	Air Conditioner	1 - 35, 135 – 144
	Electric Heater	95 – 135
	Clothe Washer	1 – 65
	Clothes Dryer	55 - 95
	Dishwasher	125 - 144
	Water pump	75 - 110
	Electric Kettle	45 - 65, 95 - 115
	Rice Cooker	15 - 35, 55 - 75, 95 - 125
Upper-middle-class	Air Conditioner	1 - 55, 135 - 144
	Electric Heater	95 - 135
	Clothe Washer	1 - 75
	Clothes Dryer	75 - 100
	Dishwasher	125 - 144
	Water pump	85 - 115
	Electric Kettle	55 - 75, 95 - 115

	Controllable Devices Operation Time Slots (scattered bet		
	Rice Cooker	25 - 55, 75 - 85, 100 - 135	
Higher-class	Air Conditioner	1 - 144	
	Electric Heater	95 - 144	
	Clothe Washer	1 - 95	
	Clothes Dryer	95 - 125	
	Dishwasher	1 - 25	
	Water pump	95 - 125	
	Electric Kettle	65 - 85, 100 - 125	
	Rice Cooker	35 - 65, 85 - 100, 100 - 135	

A randomly generated one-day load profile that is exposed to PSO to discover the optimal clustering set among all possible clustering combinations of C1, C2, and C3 as shown in Fig. 4-6. C3 cluster sizes range from 2 to 7 per community, with both uniform and unequal cluster sizes [24]. As shown in section 4.3, the optimal clustering combination based on PAR reduction percentage is used in a randomly generated population load profile for 90 days. Each class's whole population of 250 dwellings is separated into C1 communities, with devices inside the communities being categorized according to C2 and subsequently grouped into C3 clusters. According to the C1 optimal value, each community has 50 dwellings. Under C2, ETDO is chosen as the sorting criterion. As the ideal value, the number of device clusters in each community designated by C3 is set to 5.

In general, the devised algorithm comprises of two phases. The data formulation begins with a pre-processing stage based on dynamic clustering. Second, for CD load scheduling, dynamic clustering is used on the formed data.

In Fig. 4-7, the pre-processing stage is indicated, which entails sorting of all houses before making sets of communities according to C1. The selection of houses into communities is dynamic as it is based on average PAR of each cluster. There are 16 devices in each house. These 16 devices per house are divided into 5 clusters as per their STDO and ETDO. PAR is calculated for 5 clusters and all houses are sorted in ascending order based on maximum PAR. Second, the 1000-house population is divided into five groups of 200 dwellings each. In addition, all sets are ranked by their second-highest PAR. Finally, the 10 groups of 100 dwellings are ordered by the third-highest PAR. Every 21st house from the sorted list is chosen to bring distinctions of data set in one community. Houses are chosen at the turn of the century aiming to populate each town with a diverse population depending on PARs. Due to the availability of residences with varying PAR values, dynamic clustering is made easier. Since the size of one community is 50 houses, therefore, the LC consists of five communities of 250 houses. Similarly, each of the other three classes consists of 250 houses.

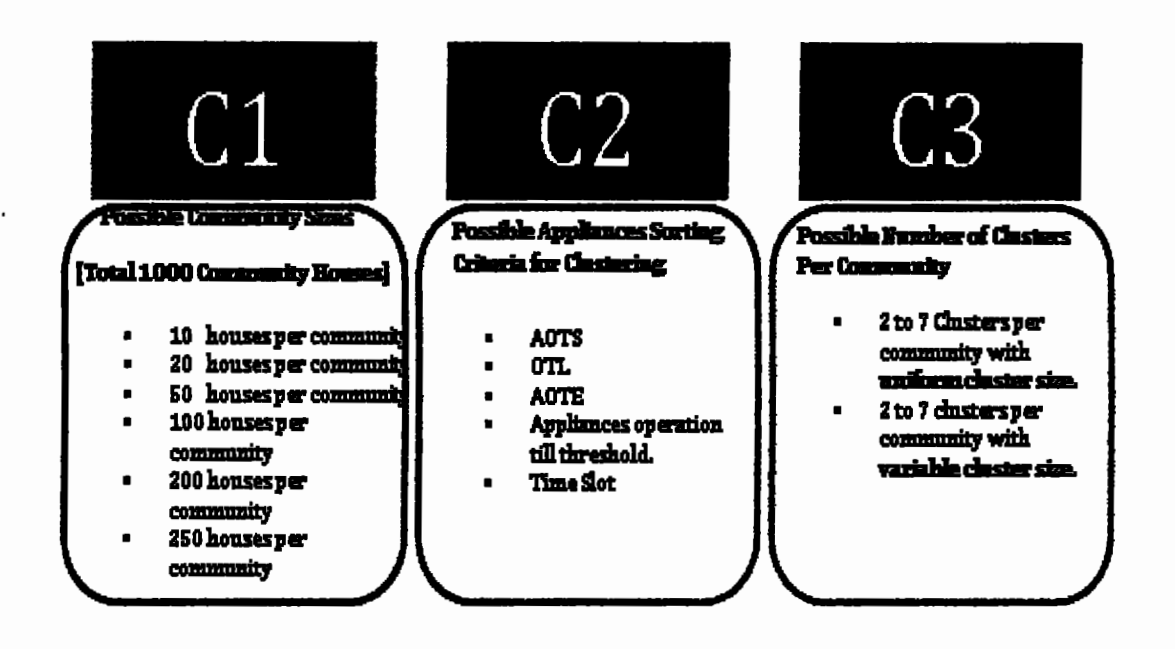


Fig. 4- 6 DCHEMS parameters for clustering.

Therefore, the five communities belong to each class. One community of 50 houses has a total of 800 devices, i.e., 50 ×16.

According to criterion C3, each community's devices are further separated into five clusters of varied configurations. Even multiples of the integer interval [-3, +3] are used to vary the borders of the cluster with the greatest average PAR. The combination with the lowest PAR is chosen.

The stages taken by the DCHEMS algorithm are depicted in Fig. 4-7's flow diagram. The following is a summary of the overall power scheduling goal:

minimize Electricity cost (
$$p_{cc}$$
)

s.t. $t_{a_b} \in [\alpha_{a_b}, \beta_{a_b} - l_{a_b}]$ (4.12)

Electricity cost (
$$p_{cc}$$
) = $\sum_{\forall k \in C_h} \sum_{\forall a \in C_c} \sum_{\tau=1}^{144} \text{rtp}_{pc}(\tau) . p_{a_k(\tau)}$ (4.13)

Here Electricity cost (p_{cc}) is the total electricity cost based on power consumption pattern. The power consumption pattern for the cluster of the community being scheduled is denoted by p_{cc} , $rtp_{pc}(\tau)$ represents electricity rate for the τ^{th} time slot according to (4.8). $p_{a_k}(\tau)$ is the power rating of CD for k^{th} house and a^{th} device. The houses in the current community are represented by C_h . Current cluster is denoted by C_c . Therefore, the objective function of our proposed algorithm is to minimize overall consumer electricity cost of power consumption. Modified inclined block rate is applied on the entire community to keep the PAR under control, as the population is divided into several smaller communities.

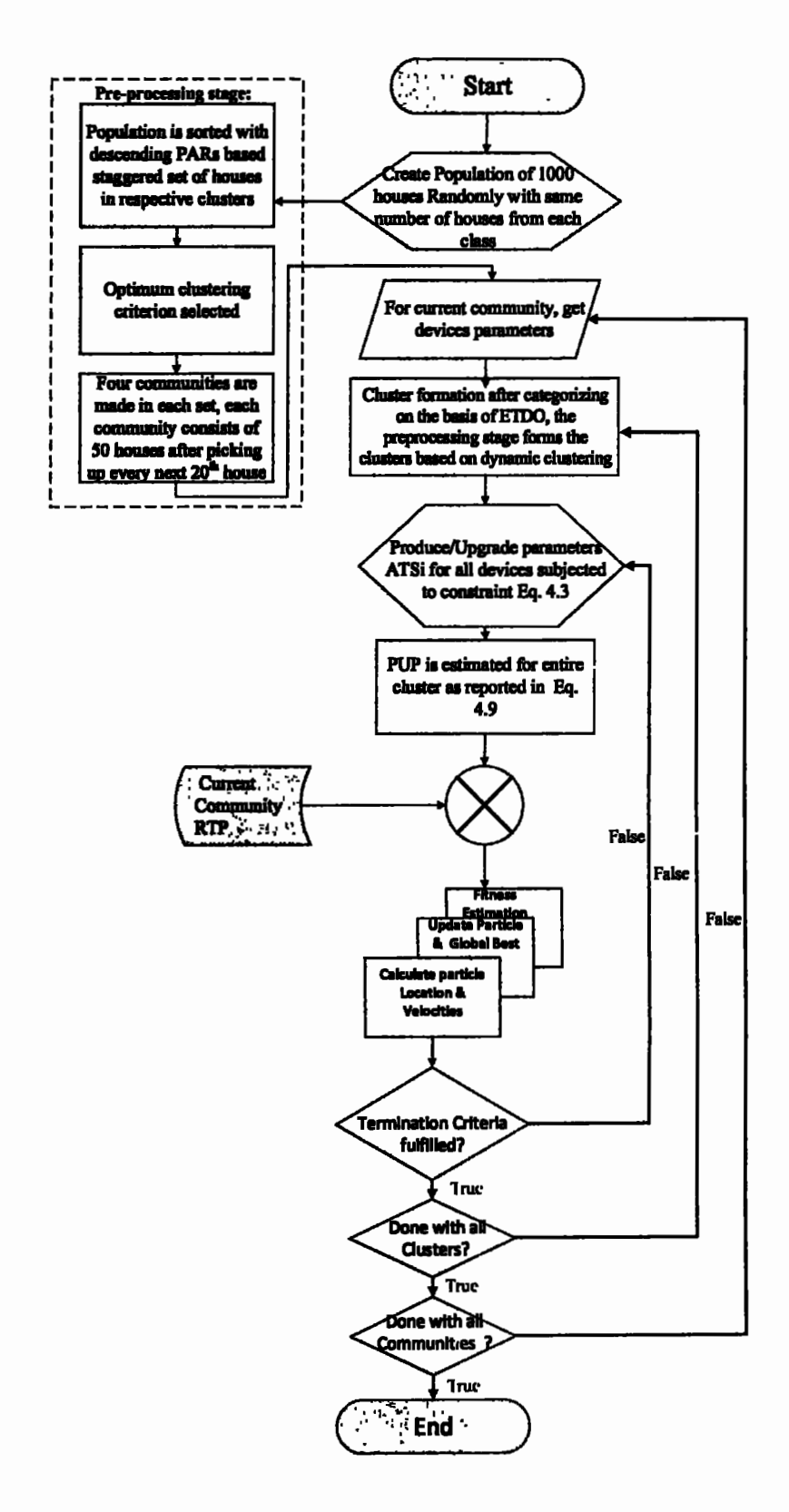


Fig. 4-7 Flow diagram of DCHEMS scheme

4.3. Results of Simulations

The simulation findings of the proposed energy management system are detailed in this section. For 90 days, PSO is employed with tested parameters on a randomly generated house population of 1000 dwellings. Each class of community comprises of 250 dwellings out of the 1000 total. According to Aziz et al. [24], the clustering parameters are set for a single day's load profile. The proposed algorithm's results and simulation results are presented in this section. When compared to existing approaches in the literature, the results show an improvement in PAR of power consumption pattern and electricity cost. Three performance indicators were utilized to demonstrate the comparison with existing techniques: percentage cost reduction (PCR), percentage PAR reduction (PPARR), and power consumption pattern's variation to mean ratio (VMR). The calculation of these parameters is as follows:

$$PCR = \frac{\text{Electricity cost} - \text{Power scheduled electricity cost}}{\text{Electricity cost}} \times 100$$
 (4.14)

$$PPARR = \frac{PAR - PARPS}{PAR} \times 100 \tag{4.15}$$

$$VMR = \frac{\sum_{\tau=1}^{144} (Power usage pattern(\tau) - \mu PUP))^2}{144} \times \frac{1}{\mu PUP}$$
 (4.16)

The peak to average ratios are PAR and PARPS before and after power scheduling, and the mean power consumption pattern is μ_{PUP} . Table 4.2 shows the percentage improvements in the proposed technique over reference procedures for the above-mentioned performance indicators. For population load profile generation, a maximum of 16 and a minimum of 8 devices are considered.

Some devices can run multiple times each day, depending on the users' normal routines. The possible time periods for CD power consumption are shown in Table 4-1. All of the simulations in this study were done in MATLAB. PSO employs the following parameters to meet the needs of the optimization algorithm: swarm size of 100, a neighbor minimum fraction of 0.25, variable count 16, relative change tolerance value of 10-16, and iteration stops at 3200.

The best clustering set out of the possible clustering parameters combination is generated when PSO is applied on a load profile generated randomly for a day as shown in Fig. 4-6. Values of 2 to 7 clusters for one community can be obtained in C3 for uniform and unequal cluster sizes. For each community, 50 houses were generated for each of the four sorts of community classes, and the results are displayed here. ETDO is used to organize home devices. The number of clusters will be set at five. The randomly generated load profiles for a period of 90 days generate the specified parameters and they are stated to be the best clustering combination [24].

The following four sorts of profiles are created in this study: profiles for unoptimized data, inclined block rate combined with PSO for load shifting [24], static clustering-based load scheduling [24], and the proposed DCHEMS. Note that the electricity pricing data is from Ameren Illinois Power Company (2015) and covers the period from April 11th to July 9th, 2015.

In Fig. 4-8, an optimization for the 45th day power consumption pattern against time TSs is given, demonstrating that the proposed algorithm greatly increases PAR when compared to non-dynamic clustering-based alternatives. In static clustering-based scheme denoted by CCHEMS in Fig. 4-8, the peak at TS 109 of 215 kW/TS is lowered to 168 kW/TS at TS 87 in DCHEMS. Sharp peaks in power utilization are replaced by either no or extremely low power utilization peaks in unoptimized and PSO-inclined block rate approaches, indicating a difference. The algorithm adjusts

a load of users to off-peak from on-peak hours, preventing new peaks from forming. This demonstrates the value of integrating inclined block rate with RTP, as stated in section 3.2.

The load curve's diversity factor improves after dynamic clustering is used. The gradual change in the load profile validates effectiveness of proposed load scheduling management. In comparison to the static clustering-based approach, the suggested technique shows a considerable improvement in PAR, as shown in Fig. 4-9(b), where mean PAR for the unoptimized scheme, optimized with inclined block rate and PSO, static clustering, and dynamic clustering are 3.78, 3.65, 2.51, and 1.71, correspondingly. Fig. 4-9 (a) shows the electricity cost reduction for the proposed and reference techniques in \$/Day over a 90-day timeframe (a). 844.82 \$/Day, 461.46 \$/Day, 379.13 \$/Day, and 344.35 \$/Day, respectively, for unoptimized method, optimized with inclined block rate and PSO, SCHEMS, and DCHEMS. When compared to dynamic clustering, the mean electricity cost reduction with static clustering is roughly 4.12%.

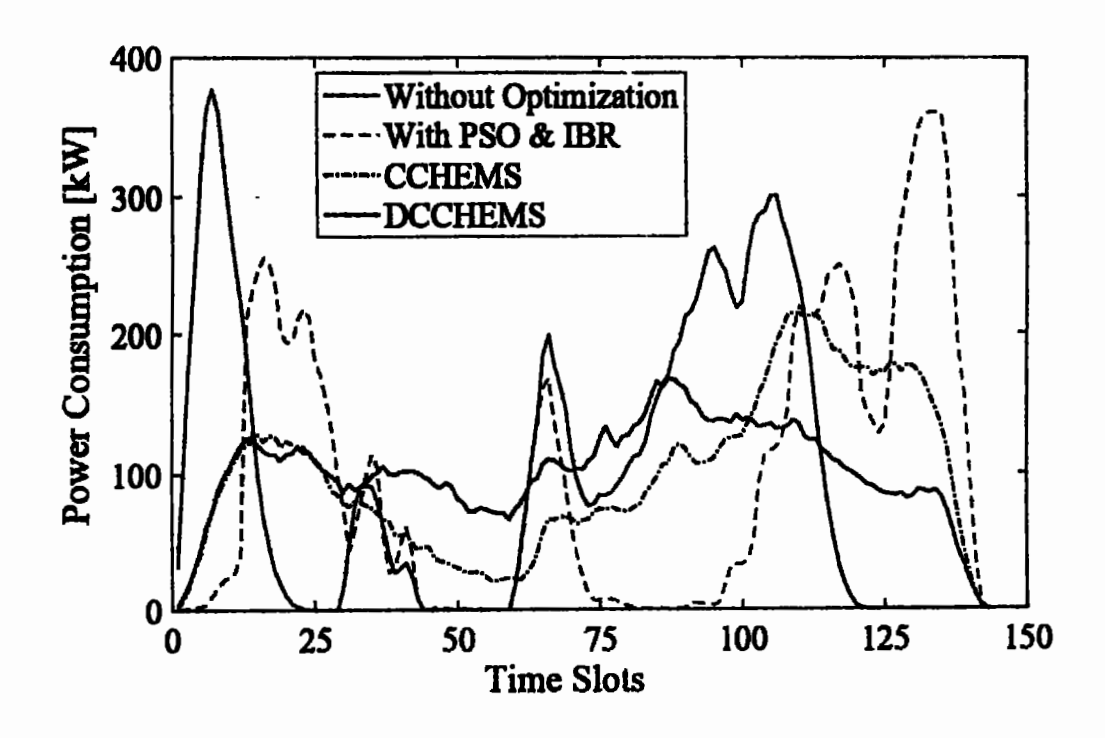


Fig. 4-8 Power consumption pattern at 45th day.

Fig. 4-9 (b) depicts the PAR effects. PAR is reduced by 33.49 percent with a static clustering scheme and 54.75 percent with DCHEMS. With reference to cost reduction capability, the suggested DCHEMS outperforms non-dynamic optimization by 4.11 percent. When the PAR reduction is assessed with DCHEMS, the results are more positive, with a 21.26 percent improvement over non-dynamic optimization.

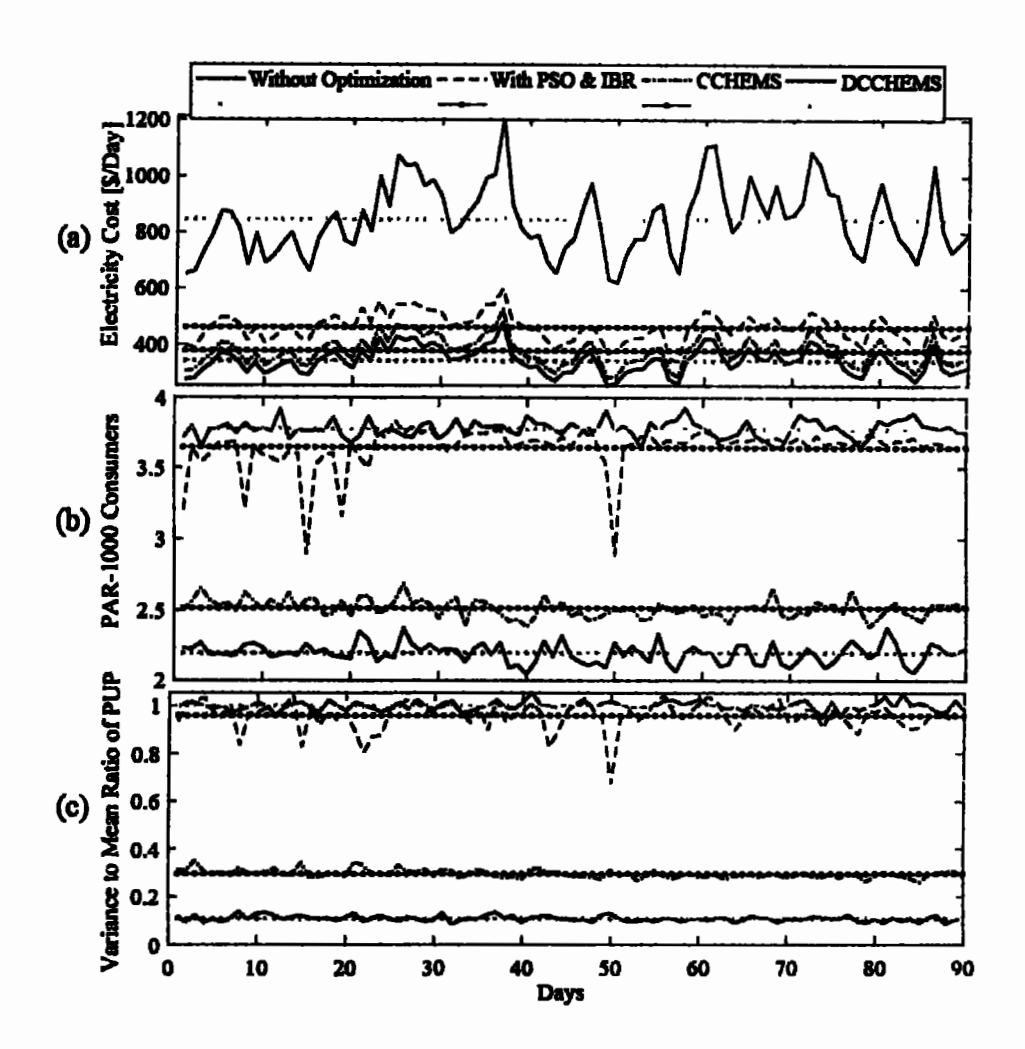


Fig. 4- 9 Simulated Results with PSO over a period of 90 days: (a) Cost of electricity, (b) Peak to average ratio and (c) VMR ratio of power consumption pattern

Given the increased PAR and cost savings, utilities are motivated to provide more incentive to consumers for participating in DR events. The last measure, the power consumption pattern's variance to mean ratio (VMR), shows that DCHEMS outperforms non-dynamic optimization in terms of power consumption pattern smoothness by 19%. As shown in Fig. 4-9 (c), our suggested DCHEMS provides power consumption pattern smoothness in the context of PSO. VMR of zero leads to a flat power consumption pattern in theory, while DCHEMS reduces VMR to 0.11 from 0.3 in that of CCHEMS, which was reduced only up to 0.85 on average for non-dynamic clustering. Smooth power consumption pattern and decreased PAR ensure the overall system's stability and durability.

Table 4-2 shows the averaged outcomes of PSO optimization of 90 days.

Table 4-2 Results Summary

Schemes	PCR	PPARR	VMR
Non-Clustered PSO	45.38	3.49	0.95
Static clustering with PSO	55.12	33.49	0.3
Proposed DCHEMS with PSO	59.24	54.76	0.11

Two design changes are responsible for the suggested technique's substantial decrease in PAR and electricity cost. To begin with, consumers are divided into numerous kinds of communities. Second, based on their operational time overlap and corresponding PAR values, the device clusters were further divided into separate sets. The decrease in PAR promotes a better balance between demand and supply, which is required for an MG to perform well [78].

4.4. Summary

In this chapter, a dynamic clustered community HEMS-based system for residential energy management is proposed. The proposed system incorporates DR and user preferences. By leveraging the differences in consumer preferences and load utilization patterns of distinct social classes, the suggested technique results in compensated consumer and electric utility companies. Consumers gain lower electricity cost, while electric utility company benefits from efficiently trimmed PAR, which improves MG reliability and stability. Simulations were run to validate the proposed DCHEMS framework, and the results were compared to those of a static clustering-based approach and a PSO-inclined block rate-based optimization. PAR is enhanced by 21.26% and electricity cost is improved by 4.11% using the suggested DCHEMS-based approach. A 19% improvement in the variance to mean ratio of power consumption was achieved.

Chapter 5

A Study on Renewable Integration on Clustered Community HEMS

Phase 2 of dissertation begins with this chapter. Another technique used in DSEM is incorporation of renewable energy resources and BES. This chapter focuses on incorporation of renewable energy resources to the MG system with a coordinated control strategy for generating a balance between supply and demand. Therefore, utilization of BES and PV is incorporated into the dynamic clustering optimization algorithm. PV is utilized when available and BES scheduling is modeled for peak shaving in the peak hours of the day.

5.1. Modelling and Simulation Method Development for the Analysis of Power Consumption in a Residential Community Microgrid System

A large number of benefits are offered by community MG systems to enhance energy efficiency, reduce consumer electricity cost and enhance the reliability of power provision to local domestic consumers. Building awareness about energy consumption information may lead to efficient utilization, control, and management of various energy resources available in an MG community. This section presents a simulation-based electricity utilization management scheme in the presence of locally generated power in the MG. The benefits of electricity cost reduction when consumers accept power from community MG systems and electric utility company facilitation when the power grid is capable of absorbing excessive power when it is sent back to it are also discussed.

5.2. Design Specifications

Once the load scheduling and optimal TS assignment to all the CDs is completed, another stage of the study consists of PV and BES incorporation for a small community belonging to a

higher class [19]. Solar irradiance values have been taken from ESMAP Tier1 Meteorological Station in Islamabad, Pakistan, for the year 2017. A rooftop Trina solar panel, TALLMAX TSM-320 PD14 Module, having peak power at 1000 W/m², panel size of 1.9 * 0.9 m² generates a maximum of 320 Watts power, is considered. Maximum efficiency of the module is taken as 17.5%. A BES of 1kWh is also involved in energy management. It supports the grid in case of PV unavailability.

As per the statistics available and considering general trends in Pakistan, the higher class is considered to consume 1200 units/month [79]. Load Profile data is used for a total of five home users belonging to a higher class with rated powers as illustrated in Fig. 4-2.

5.3. Microgrid Layout

Study has been carried out on the layout for a MG system presented in Fig. 5-1 [80].

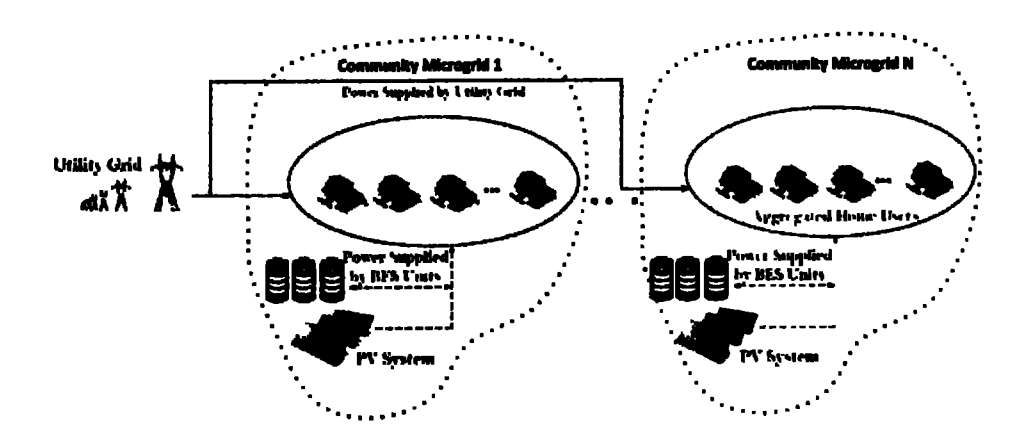


Fig. 5-1 Illustration of MG layout with BES and PV supply

The layout consists of four major elements;

1. Utility grid, delivers alternating supply to each consumer

- PV during sufficient solar irradiance hours, it supplies power to each house as well as charges BES.
- 3. BES for storing extra PV power and later supply it to the consumers during the night.
- Electrical loads of five home users from the higher-class communities are considered. The MG in this study is connected to a 220V utility grid that normally operates in grid-connected mode.

5.4. Control Scheme

The main aim of the proposed control scheme resides in carrying out the balance of power generation and consumer demand. The MG provides the maximum consumer electricity when alternate energy sources including BES power and PV power generation are ample thus decreasing the utility grid power supply. The proposed coordinate management-based control strategy with PV and BES in the MG system is depicted in Fig. 5-2. The load demand profile and PV power are input at the beginning of the flow. On the basis of the inputs taken, judgements are made using PV power generation P_{PV} and the consumer load demand P_{L} . In case $P_{PV} > P_{L}$, then BES is monitored for protection from overvoltage. If SoC is within the upper limit, which is 90% here, the MG control ensures provision of power to the consumers from the P_{PV} , and the remaining P_{PV} is used to charge BES. The utility grid power P_{g} is not supplied during this time. The indication of higher SoC than 90% reflects maximum charging state of BES and leads to the BES over-voltage protection. In case of poor solar irradiance, i.e., if $P_{PV} > P_{L}$ is false, BES should be monitored for protection from low voltage. If SoC is less than SoC₁ which is considered as 40% here, then the load demand is supplied by limited PV. Also, there will be a requirement of P_{g} to compensate for insufficient PV power. Meanwhile, no power is drawn from the BES since it enters a low voltage protection state. When

SoC is more than the SoC_l, the required load power is drawn from limited P_{PV}, P_g, and BES. In the meantime, the remaining energy storage in the BES units determines the battery power, P_b output.

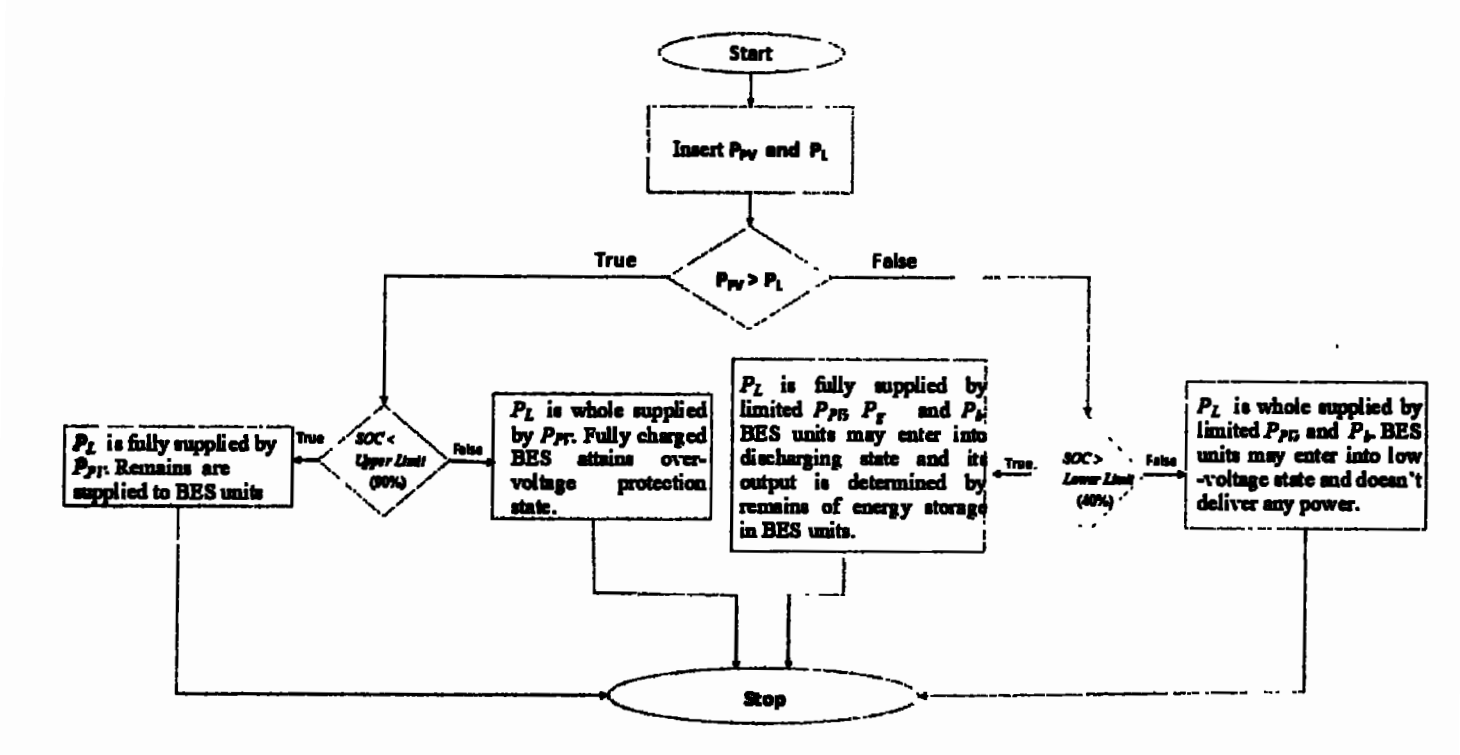


Fig. 5-2 Flow diagram for MG control strategy

The following operation states are considered during the day and night time.

- During the daytime almost all the power demanded by the consumers is supplied by PV.
 The utility has to supply minimal power to the load only if demanded power exceeds PV source power. Meanwhile, BES may also get charged by PV.
- In case of insufficient solar irradiance utility grid mainly supplies power to the consumer
 and little power is taken from the PV system. Meanwhile, limited PV charges BES. Once
 all the PV is consumed, BES unit charging may stop.

- 3. During the night, if BES carries sufficient power, all the consumers are fed by BES, until exhausted completely. Once BES is completely consumed, the utility takes up the remaining required power by the consumers.
- 4. Night time with no BES storage, utility supplies electricity to all the consumers.

5.5. Simulation Results

The simulations are presented for one MG with independent five single-phase domestic consumers aggregated together with specifications of 220V and 60 Hz. Two days are selected for simulation purposes. One is hot plus cloudy. Other is cold and sunny. In order to analyze results thoroughly, an hour is divided into 6 TSs, as done in chapter 4. Therefore, the simulations are performed against 144 TSs.

5.5.1. Case-I

Case-I depicts MG operation simulations for a summer's day. The day is hot with high solar irradiance and a gust of clouds also appears during the day. Solar irradiance values are taken from ESMAP Tier1 Meteorological Station NUST University, Islamabad, for a hot day of June 2017 is shown in Fig. 5-3(a). The consumer load profile is shown in Fig. 5-4.

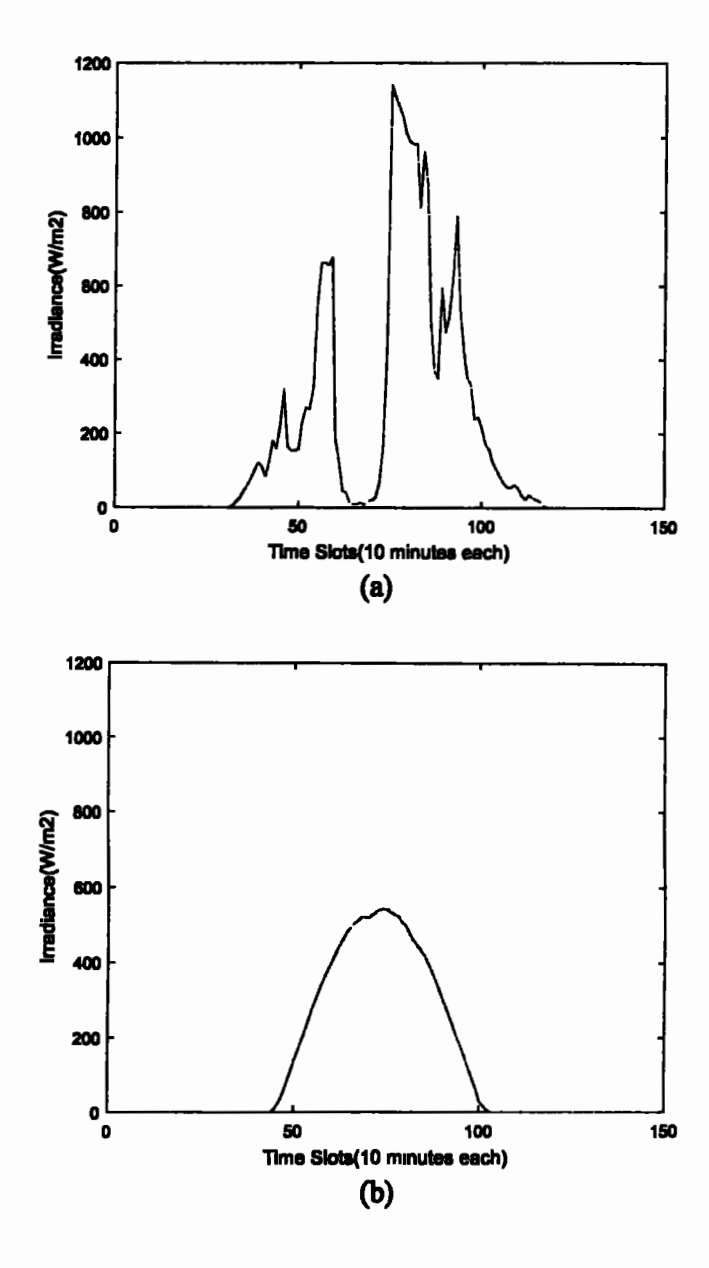


Fig. 5- 3 Used solar irradiance for the PV power. (a) Normal irradiance—Sunny plus cloudy day state; (b) Low irradiance—Cold day state

The dawn time was at 5:30 (TS 33) and dusk was at a round of 19:30 (TS 117). From dawn to dusk, the PV framework gave plenty of power to both domestic power consumers. It also charges BES units except for the TSs where a gust of clouds appears around 10:00 (TS 60) that ends around 12:20 (TS 74). The BES takes up the load instead of PV, as exhibited in Fig. 5-5. Behind the dusk time, BES units have sufficient charge storage so they start serving domestic consumers around 4:50 (TS 101) until BES units dry out at roundabout of 20:00 (TS 120) whereas, the PV framework is inoperative during this period as illustrated in Fig. 5-5, BES power supply section. The electric utility company has to fulfil the domestic consumers' power demands for the time ahead of 5:30 (TS 33) and later of 20:00 (TS 120) when the PV framework and BES both stop supporting the home users as illustrated in Fig. 5-5, in utility grid power supply section.

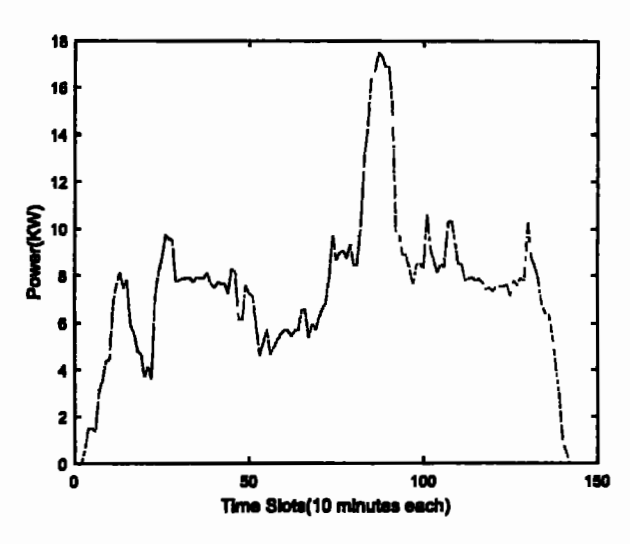


Fig. 5-4 Electricity load profile used for higher class home users

Furthermore, little power is supplied by PV at the beginning of sunrise. From 5:30 (TS 33) to 7:09 (TS 43), both the utility grid and PV system supply domestic consumers. Therefore, the power grid and PV framework have to corporately handle the burden of domestic power demand. Moreover, Fig. 5-6 shows the SoC variations of general BES activity.

5.1.1. Case-II

Case-II depicts MG operations simulations for a winter's day with comparatively lower solar irradiance. Solar irradiance values taken from ESMAP Tier1 Meteorological Station NUST University, Islamabad, for a cold day of December 2017 are shown in Fig. 5-3(b).

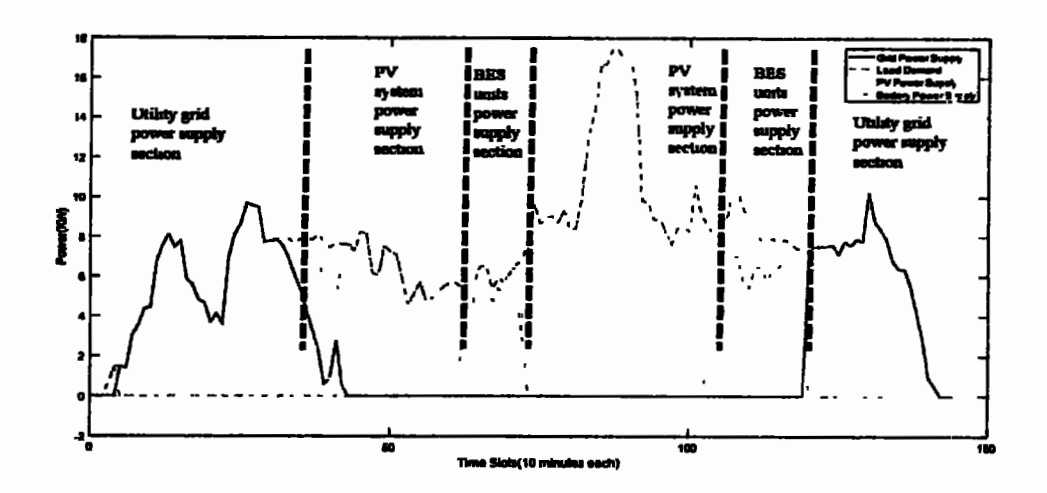


Fig. 5-5 Electricity response for simulated MG case-I

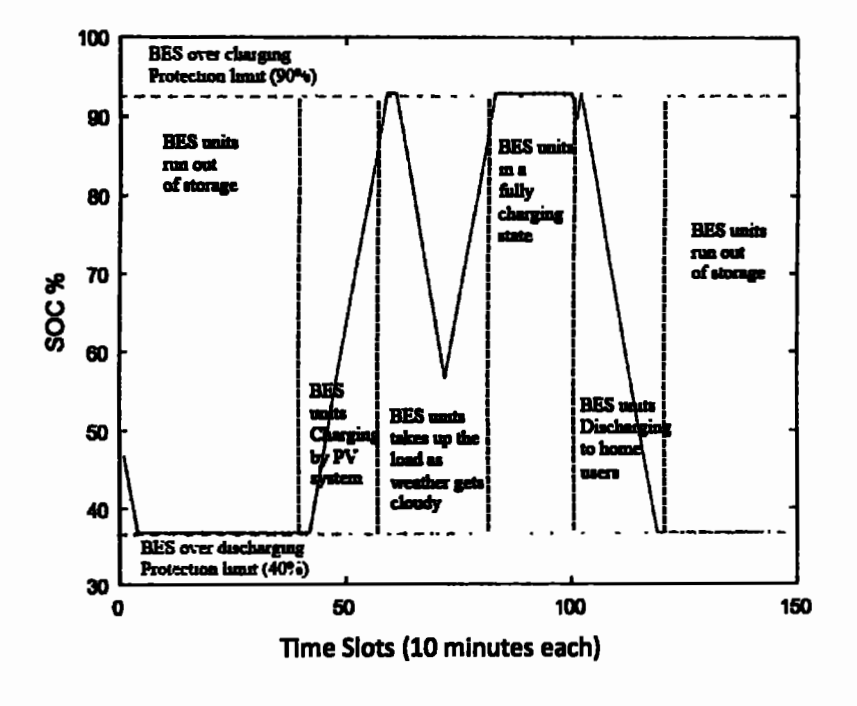


Fig. 5-6 Charging and discharging states of BES for case-I

The dawn time was at 7:30 (TS 45) and dusk was at a round of 17:00 (TS 102). From dawn to dusk, the PV framework gave plenty of power to both domestic power consumers' and charges BES as exhibited in Fig. 5-7 in the PV system Power Supply section. Behind the dusk time, BES units turn to a realizing state and start serving domestic consumers around 4:10 (TS 97) until BES units dry out at roundabout of 19:00 (TS 114) whereas, the PV framework is inoperative during this period as illustrated in Fig. 5-7, BES power supply section. The utility grid has to fulfil the domestic consumers' power demands for the time ahead of 7:30 (TS 45) and later of 19:00 (TS 114) when the PV framework and BES both stop supporting the home users as shown in Fig. 5-7, in utility grid power supply section. Furthermore, little power is supplied by PV in the beginning of sunrise. From 7:30 (TS 45) to 8:20 (TS 50), both utility grid and PV system collectively supply domestic consumers. Therefore, the power grid and PV framework have to corporately handle the burden of domestic power demand. Moreover, Fig. 5-8 shows the SoC variations of General BES activity.

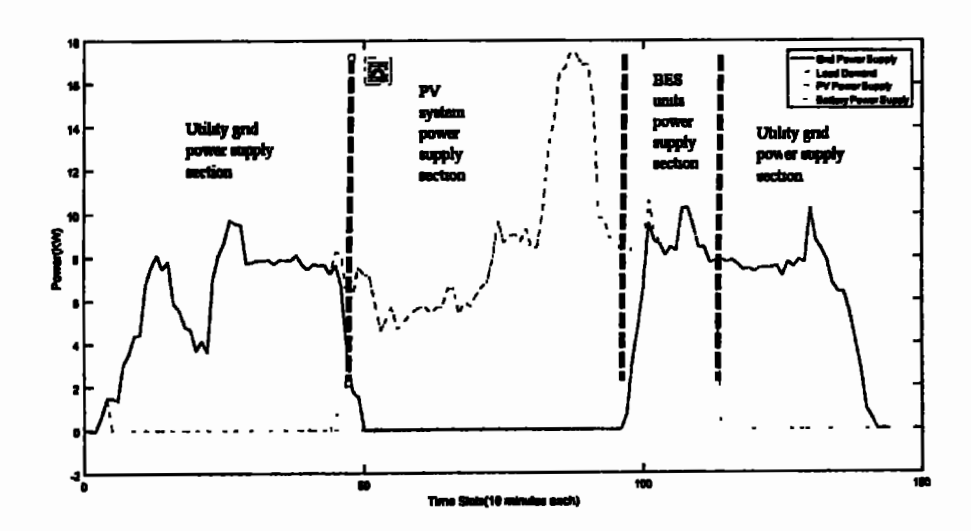


Fig. 5-7 Electricity Response for simulated MG Case-II

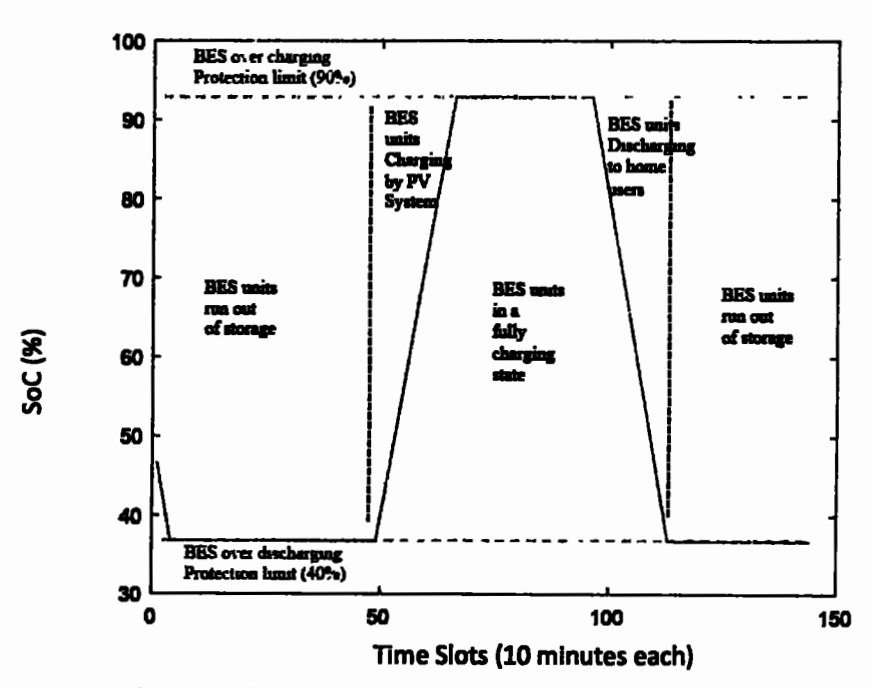


Fig. 5-8 Charging and discharging states of BES for case-II

The proposed coordination-based management scheme in section 5.4 offers the benefits of effective utilization of renewable and alternate energy sources like PV and BES for maintaining a balance in generation and load. But it has a major drawback of BES degradation as a consequence of a greater number of battery cycles utilization. This makes the system uneconomical. Therefore, there is a need to find an optimal solution that can only utilize BES power when there is a peak so that battery lifetime may be prolonged and the design is economical.

For this, the following section presents BES scheduling for peak shaving and PV utilization.

5.2. Optimal BES Scheduling for Peak Shaving and PV Utilization

The aims of the proposed optimization problem while defining objective function and constraints are; reduction of peak load, minimization of electricity cost, elongation of BES lifetime while considering SoC of BES. The algorithm considers the fact that the more the number of cycles consumed by the battery storage, the more quickly it derates. Therefore, it keeps the BES charged

during off-peak and only uses it during peak load. Consequently, the battery provides grid support during peak hours.

For solar power utilization, three PV penetration levels are used in the study, i.e., 5%, 10%, and 15% PV penetration in community, as shown in section 5.6.3. In case of abundant alternate energy sources, the concept of sending the excessive power back to the source is also presented. For effective demonstration of control strategy, the implementation of the suggested BES scheduling method is applied on load profile data of 1000 houses belonging to a local community in Pakistan. Peak load reduction and smooth charging/discharging of BES which is significant for BES lifetime is depicted by the simulation results.

5.2.1. Challenges in BES Technology

BES incorporation has another issue of fast derating the life expectancy of the batteries. Therefore, the batteries life cycle is a major concern these days. A BES may need to charge and discharge multiple numbers of times a day according to the variations in the load profile due to the consumer's demand. Low depth of discharge (DoD) keeps the BES life cycle unaffected, but large DoD can lead to BES life degradation. A high discharge rate may also damage the batteries and this, in turn, reduces energy storage system reliability.

5.2.2. Control Strategy

Considering all discussed issues, a model has been developed for PV incorporation and BES peak shaving algorithm as explained in the following section.

The elementary form of the HEM system procedure is depicted by the constraints presented henceforth. Other more specific implementations can be extracted and adapted by the model. The

suggested scheme's flow diagram is depicted in Fig. 5-9. The highlighted red block shows monitoring of load profile for peaks. The portion of the load profile above the threshold defined as LP-th is considered to be the load peak. During the TSs of $P_{PV} \leq P_L$, the BES is only utilized for serving peaks of load demand. In case if BES is not sufficient, then limited PV serves the required load. LP-th is termed as P_{peak} , illustrated in Fig. 5.10. The simple selection of appropriate time t can be decided as per the feasibility of the defined problem. E.g., if one hour is divided into intervals of 10 minutes each, t would be 6.

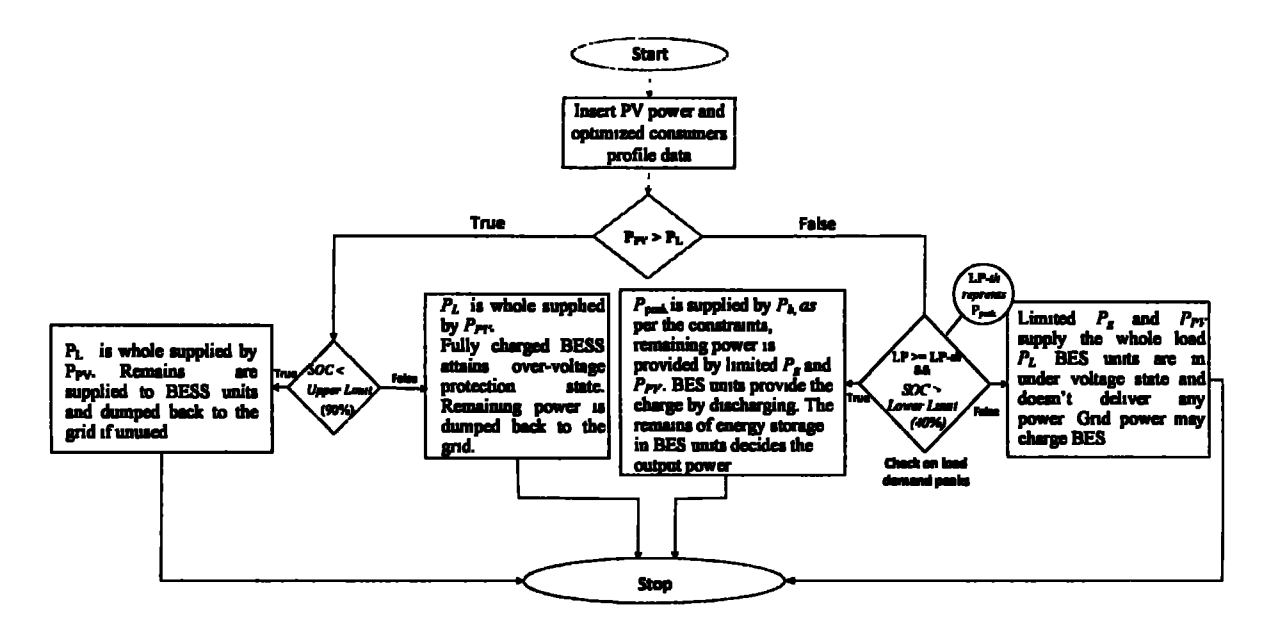


Fig. 5-9 Flow diagram for peak shaving MG control strategy

The following mathematical model is utilized for simulating the proposed coordination-based energy management scheme.

5.2.2.1. Power Balance

$$\hat{P}_{g}^{(t)} + P_{PV}^{(t)} + P_{b}^{(t)} = \hat{P}_{L}^{(t)} + P_{b-c}^{(t)} \qquad \forall t \in \{1, 2 \dots 144\}$$
 (5.1)

Equation (5.1) states the fact that the domestic load i.e., $\hat{P}_L^{(t)}$, the charging needs of the BES $P_{b-c}^{(t)}$ is either fulfilled by the utility grid power $\hat{P}_g^{(t)}$ or by the energy saved due to by the PV and BES, i.e. $P_{PV}^{(t)}$ and $P_b^{(t)}$. In case, if PV is sufficient and BES is already charged then power may go back to the source as presented in simulations section.

5.2.2.2. BES Scheduling

When $\hat{P}_{L}^{(t)}$ is acquired, the following optimization problem is used to perform BES scheduling [81].

$$\min_{\substack{p_b^{(t)} \\ t \in \{1, \dots, 144\}}} \sum_{t=1}^{t=144} \hat{P}_g^{(t)} - P_{peak} \tag{5.2}$$

$$\hat{P}_{q}^{(t)} = \hat{P}_{L}^{(t)} + P_{b}^{(t)} \tag{5.3}$$

$$\beta_g^{(t)} \ge 0 \tag{5.4}$$

$$P_{shave}^{(t)} = \begin{cases} \hat{P}_{L}^{(t)} - P_{peak}, & \hat{P}_{L}^{(t)} > P_{peak} \\ 0, & \hat{P}_{L}^{(t)} < P_{peak} \end{cases}$$
(5.5)

$$P_{\text{shave}}^{(t)} + P_{b}^{(t)} \ge 0 {(5.6)}$$

$$-P_{max} \le P(t)_b \le P_{max} \tag{5.7}$$

$$SoC^{(t)} = SoC^{(t-1)} + \frac{\eta}{\kappa_c} P_b^{(t)}$$
 (5.8)

$$SoC_{min} \le SoC^{(t)} \le SoC_{max}$$
 (5.9)

BES amount of charging and discharging is represented by $P_b^{(t)}$. $P_{shave}^{(t)}$ is the load power between P_{peak} and maximum value of load profile. P_{peak} is taken to be a tuning parameter that

represents desired peak load. Therefore, BES supplies its available power, that of P_{peak} for peak shaving. As shown in Fig. 5-10, $P_{shave}^{(t)}$ denotes the load power shaved by BES. $SoC^{(t)}$ defines the BES SoC. $\hat{P}_g^{(t)}$ is the electricity dispatched by the grid. SoC_{max} defines the maximum and SoC_{min} defines the minimum limit of BES SoC, which is taken to be 30% and 90%.

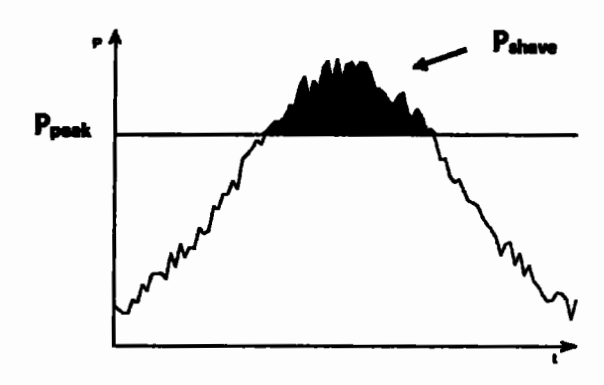


Fig. 5- 10 Description of Pshave and Ppeak

The objective function tries to achieve peak shaving as much as possible. Note that reducing the size of $\hat{P}_g^{(t)} - P_{peak}$ by discharging means increasing the amount of the peak shaving. In order to avoid peak load that is an issue for the utility as well as the consumers. Therefore, larger peak shaving is attained by minimizing the difference between $\hat{P}_g^{(t)} - P_{peak}$ by BES discharging.

Equation (5.3-5.6) are the constraint equations catering to various situations that occur in BES scheduling. Equation (5.3) represents estimated amount of provided electricity from the utility grid, $P_b^{(t)} \ge 0$ represents charging and $P_b^{(t)} \le 0$ represents discharging. Equation (5.4) depicts that electricity provided by the utility grid is always positive. Equation (5.5) defines BES discharging constraint of dispatching only when load power is greater than P_{peak} . Equation (5.6) depicts that BES cannot dispatch more than $P_{shave}^{(t)}$. Maximum and minimum charging limit of BES are depicted

in Equation (5.7) and Equation (5.8) denotes the maximum and minimum allowable limits of $SoC^{(c)}$ where, E_c denotes BES capacity and η represents charging discharging efficiency, taken as 0.95.

The simulations for the proposed control strategy are presented in the following section.

5.2.3. Simulation Results

In Pakistan, various classes of people generally have different PV installations as per their requirements and devices installed. Considering the variations in society, three case studies are presented. Case 1 utilizes 5% of PV penetration. This means only 5% of houses, out of 1000 have installed PV at their homes. Similarly, calculations are carried out for the next two cases for 10% and 15% of PV penetration. Two days are selected for simulating PV penetration for each case, one cold and other is hot plus cloudy, considering similar weather conditions as shown in Fig. 5-3 (a) and 5-3 (b). A BES of 148kWh is used for the peak shaving for each case. The electricity profile used as load demand for the simulations is shown in Fig. 5-11.

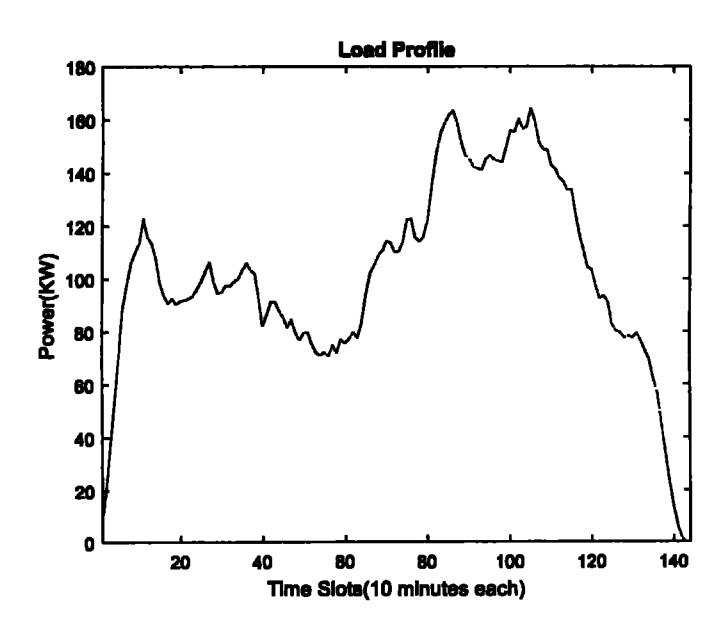


Fig. 5-11 Electricity profile used load for a total of 1000 residential consumers

5.2.3.1. Case Study I - 5% PV Penetration

Simulation results are presented in Fig. 5-12, where all the left-hand figures reflect cold day conditions and those on right-hand side are reflecting hot plus cloudy day conditions.

Fig. 5-12 (a) and (b) show the electricity response in the simulated scenario of the proposed MG for hot and cold days. The load demand of the entire population, the PV output for 5% penetration and the power supplied by the utility grid is reflected in curves. The shaded area represents BES units supplied against the P_{peak} of 122 kW. As per the scheduling constraints, BES is only dispatched for the load above P_{peak} . Due to the small penetration of the PV system, it may only be used for limited power supply. PV in case of its availability is supposed to take up the load and the peak power is supplied by the BES. The off-peak region is supported by the limited PV and utility grid. Power supplied and absorbed by the BES along with SoC is illustrated in Fig. 5-12 (c) and Fig. 5-12 (d), respectively. The y-axis on the right-hand side in the graphs depicted in Fig. 5-12 (c) and Fig. 5-12 (d), denotes the SoC evolution of BES against the TSs. And the y-axis on the left represents the power generated by BES in kWs. Positive values of power reflect the BES discharging and negative power shows its charging TSs. The excessive PV for about a maximum value of 8 kW is sent back to the source as shown in Fig. 5-12 (e) and Fig. 5-12 (f).

Similarly, electricity response for a hot day where a gust of cloud appears almost around TS equals 60 is shown in Fig 5-12 (b). The PV and utility grid alternately take up the load during the unexpected cloudy TSs.

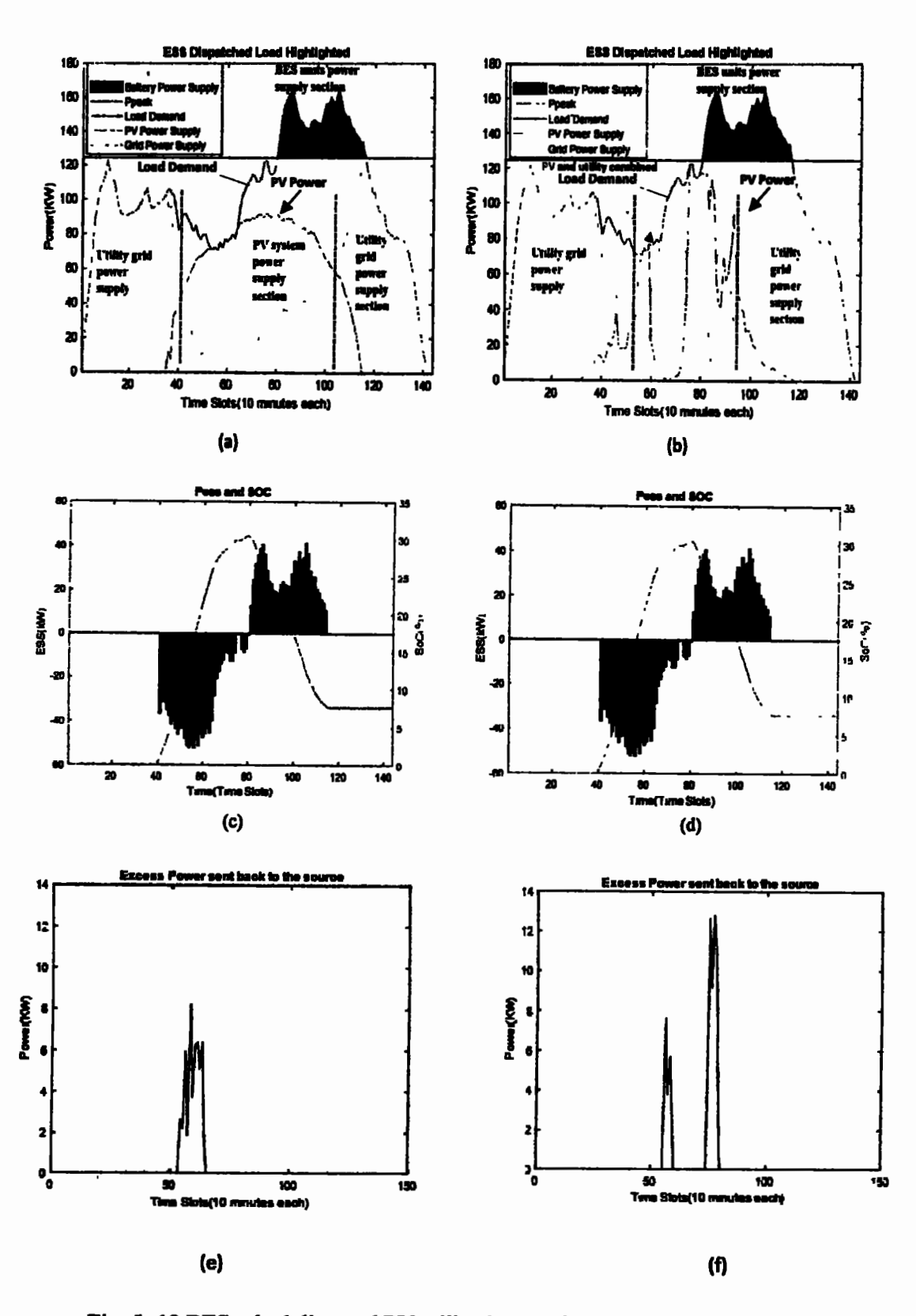


Fig. 5- 12 BES scheduling and PV utilization results for 5% PV penetration.

The figure shown in 5-12 (a) and (b) is the electricity response in the simulated MG, left: cold day, right: hot day. (c) and (d) show P_b and SoC of Energy storage system, L: cold day, R: hot day. (e) and (f) is the excess power sent back to the source, L: cold day, R: hot day

5.2.3.2. Case Study II- 10% PV Penetration

Similarly, a case study is carried out for 10% PV penetration, where 10% of houses of the entire population have available PV installation. The simulation of MG operation in summers and winters day conditions is performed by using solar irradiance data as presented in Fig. 5-3 (a) and 5-3 (b). The similar electricity profile in Fig. 5-11 is considered as the consumer load demand. In this case, PV penetration is comparatively larger, therefore, the solar irradiance is improved than that of case I. In the simulation results shown in Fig. 5-13, the shaded area represents BES units supplied against the P_{peak} of 120 kW. The effectiveness of the proposed solution for peak shaving and PV utilization can be viewed from the hot and cloudy day in Fig. 5-13 (b), where the BES supports the grid in case of PV unavailability due to an unexpected gust of cloud during P_{peak} region. Due to the better solar irradiance as compared to case I, the power supplied by the utility grid is further reduced. The excess power sent back towards the utility grid which is considerably large in comparison to case I is presented in Fig. 5-13 (e) and Fig. 5-13 (f).

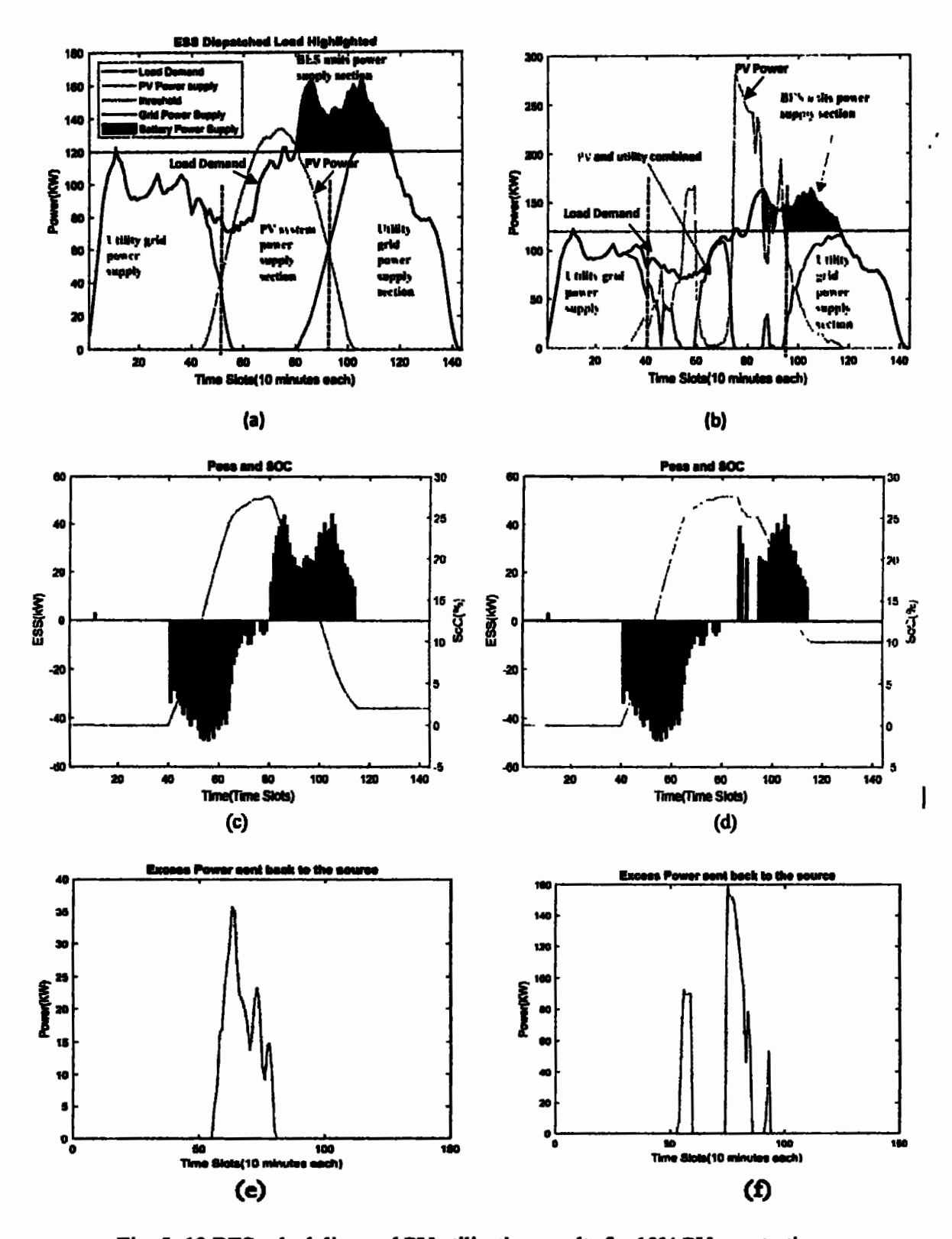
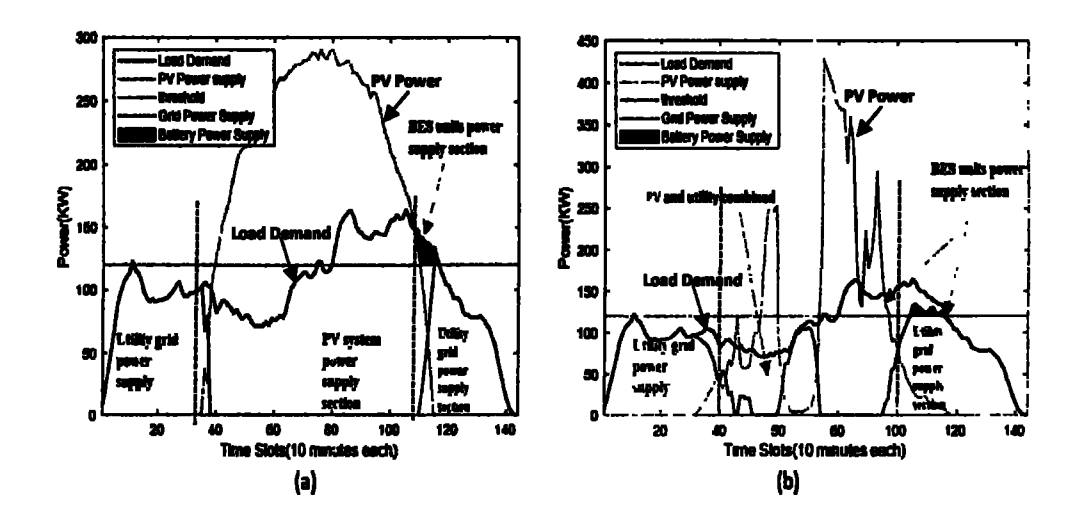


Fig. 5-13 BES scheduling and PV utilization results for 10% PV penetration.

The figure shown in 5-13 (a) and (b) is the electricity response in the simulated MG, L: cold day, R: hot day. (c) and (d) reflect Pb and SoC of Energy storage system, L: cold day, R: hot day. (e) and (f) is the excess power sent back to the source, L: cold day, R: hot day

5.2.3.3. Case Study III- 15% PV Penetration

Similarly, case study is carried out for 15% PV penetration, where 15% of houses of the entire population have available PV installation. As shown in Fig. 5-14, the shaded area represents BES units supplied against the P_{peak} of 120 kW. In this case, PV penetration is further larger, therefore, the solar irradiance is higher than that in case II. P_{shave} is further reduced since most of P_{peak} is supported by PV. BES participates least in supplying the peak load due to enough PV power. Due to excessive PV, the BES in the summer case over-charges even more than the upper limit of BES charging.



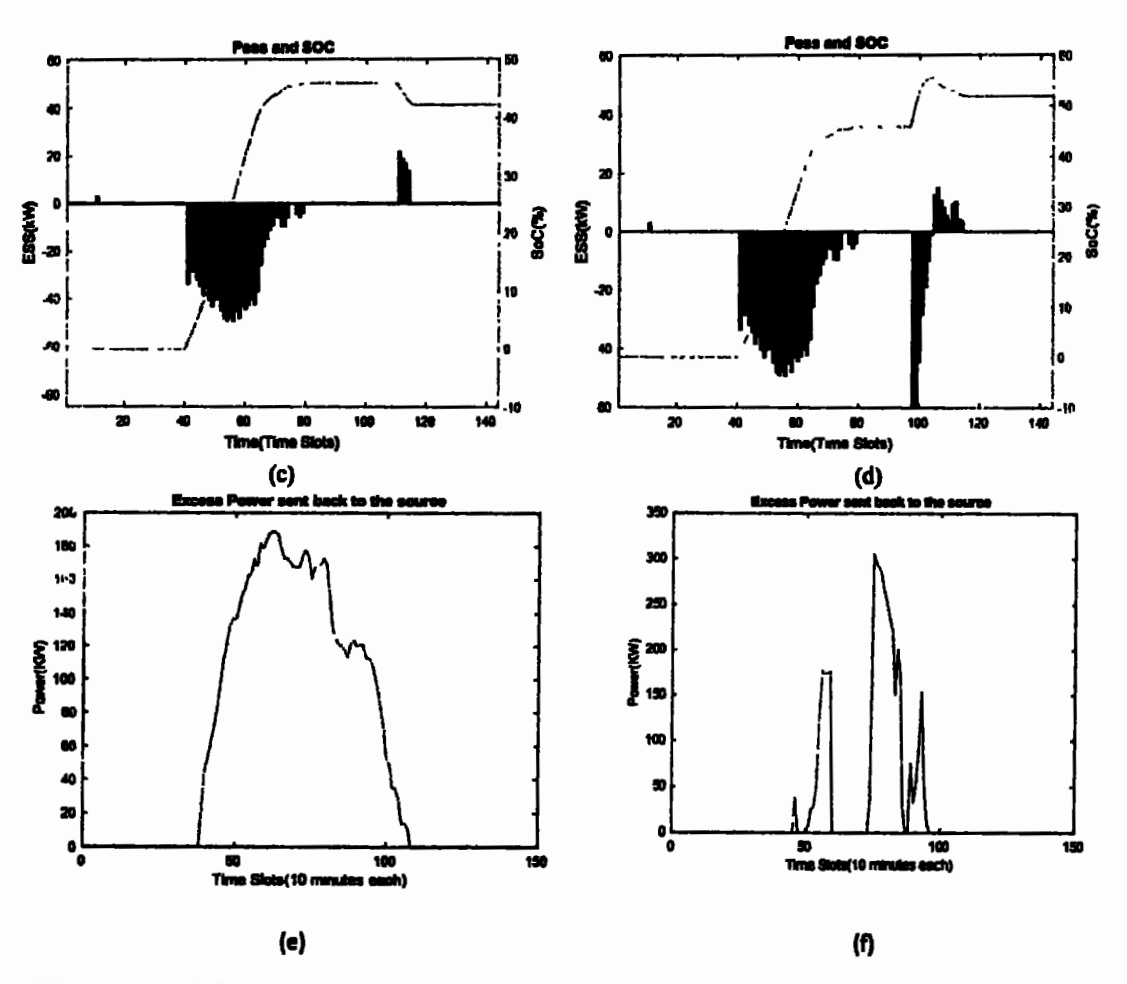


Fig. 5- 14 BES scheduling and PV utilization results for 15% PV penetration. The figure shown in (a) and (b) is the electricity response in the simulated MG for 15% PV penetration, left: cold day, right: hot day. (c) and (d) P_b and SoC of energy storage system, L: cold day, R: hot day. (e) and (f) Excess power sent back to the source, L: cold day, R: hot day

5.3. Summary

It can be observed from the cases presented above that large sized PV installation may lead to excessive unutilized power which is sent back to the utility. This may cause the issues of voltage rise on the generation rise and makes the system uneconomical. Therefore, proper PV sizing is required, so that the available power be fully utilized. The problem of effective utilization of available PV power may also be solved by incorporating dynamic (variable) demand limits (P_{peak})

which is considered to be fixed in the above cases. It is suggested that based on the available distributed energy resources and the consumer demand, an optimized dynamic demand limit solution may be proposed which can be fixed for a day but varies over a number of days.

The proposed technique presented in this chapter is based on the idea of PV power utilization for the off-peak load as well. In the meantime, the utility grid power is assumed to be used for some other purposes or loads so that the maximum available PV power can be utilized. But this leads to a number of issues, e.g., overcharging and over discharging of BES, alternate roles of PV and grid, i.e., the PV taking available off-peak load and grid is used to charge BES at times. A way around this issue could be that grid should only take a load less than the peak, so that the load profile may be smooth as per the requirement of the electric utility company. And PV should be utilized to charge the BES that can serve the peak load whenever it arises. Therefore, it is required to present a rule-based peak shaving control mechanism that can work in various modes and perform according to the required situation.

Another most promising solution to the overcharging of BES due to grid or PV may be resolved by considering a limit to BES charging as per the requirements of the peak hours. Therefore, there is also a need to decide on a feed-in limit to the BES to avoid its overcharging. Also, if the energy required for charging battery is pre-calculated for each day, then the issue of overcharging may solve completely. Hence, it is required to consider dynamic demand and feed-in limitations for effective utilization of BES and PV in the MG system.

A drawback of the study is the lack of consideration of day-to-day management of the BES charging/discharging mechanism. The daily management should ensure some energy is stored in BES at the end of the day. This enables BES capable of serving any unexpected peaks appearing in

the beginning of the next day before it charges. The above-mentioned issues have been incorporated in the scheme of a study presented in the following chapter.

Note: For brevity and clarity purposes, all the power and energy units of kW/TS and kWTS have been mentioned as kW and kWh in this and the following chapters. This change is due to the time granularity of TS considered in this work, i.e., 1 hour has six TS.

Chapter 6

Optimal Peak Shaving\Clipping using Dynamic Feed in and Demand limits

Peak clipping or peak shaving are two terms used interchangeably in the literature. Peak shaving is a DSEM based technique used in grid-connected MG systems. It is advantageous for both the electric utility company and the consumers while enhancing the stability of the overall electricity system. This chapter is focused on an optimized rule-based demand peak shaving scheme implemented for grid-connected MG systems incorporating BES and PV powers. A method is proposed for determining feed-in and demand limitations for a priori knowledge of predicted load consumption and PV availability P_{pv}. The charging/discharging schedules for BES are also presented based on the optimized demand peak shaving control management. The rules formulation is so performed that the feed-in and demand powers remain restricted to the respective determined limits of the day. The SoC of BES follows the constraint of attaining a similar value at the beginning and end of the day. To determine required optimized inputs, PSO algorithm is used by the suggested rule-based control scheme to minimize peak demand energy drawn from the grid. Various load and PV power profiles are used to test the overall control scheme.

The content presented in this and following chapter is based on my research also published in IEEE access.

6.1. System Illustration

A utility grid-connected MG system consisting of PV and BES, as illustrated in Fig. 6-1. The utility grid is capable of power deliverance as well as absorption.

In order to make the comparison with the previous results, the same load profile of 200kW is used as in Chapter 4. The same PV is also used for only 5% and 15% penetration levels so that effects of significant difference in PV can be analyzed. A 220 V, 600 Ah BES is selected for the purpose of peak demand shaving. The power balance equation among available sources is given as

$$P_{g}(t) + P_{pv}(t) + P_{b}(t) = P_{L}(t)$$
 6.1

Assuming discrete time granularity, time interval is denoted by "t" in equation (6.1) $[(t-1) \times T_C, t \times T_C]$, where T_C is the 10 minutes TS.

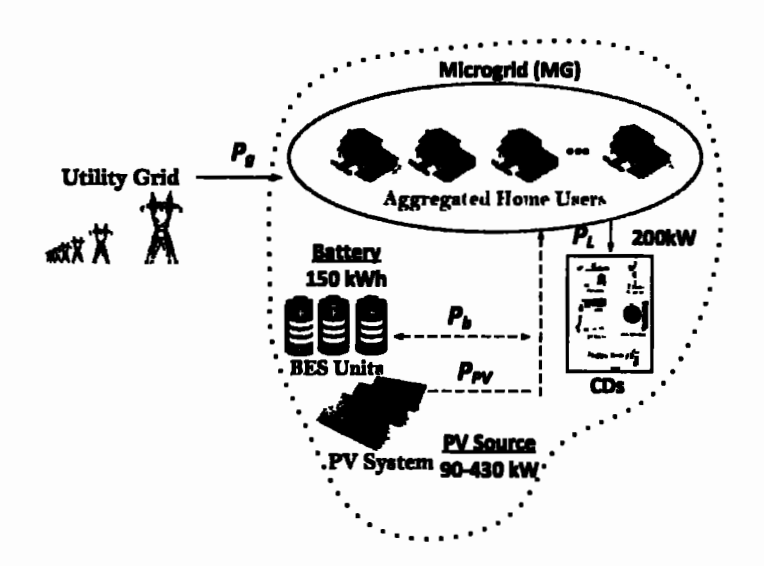


Fig. 6-1 Residential system with PV source, BES, and controllable devices (CDs) as load

6.2. BES Operating Modes

The purpose is to limit the utility grid power $P_g(t)$ to the peak power so that the portion of power above the peak can be taken up by the MG power sources. Since peak power is the limit on the consumer demand to be catered by the utility grid, therefore it is termed as demand limit power, denoted by P_{dl} . Therefore, the purpose of considering the PV source accompanying the BES, is to

restrict $P_g(t)$ to P_{dl} . The modes of BES for operating TSs for typical load consumption profiles and PV power availability are illustrated in Fig. 6-2.

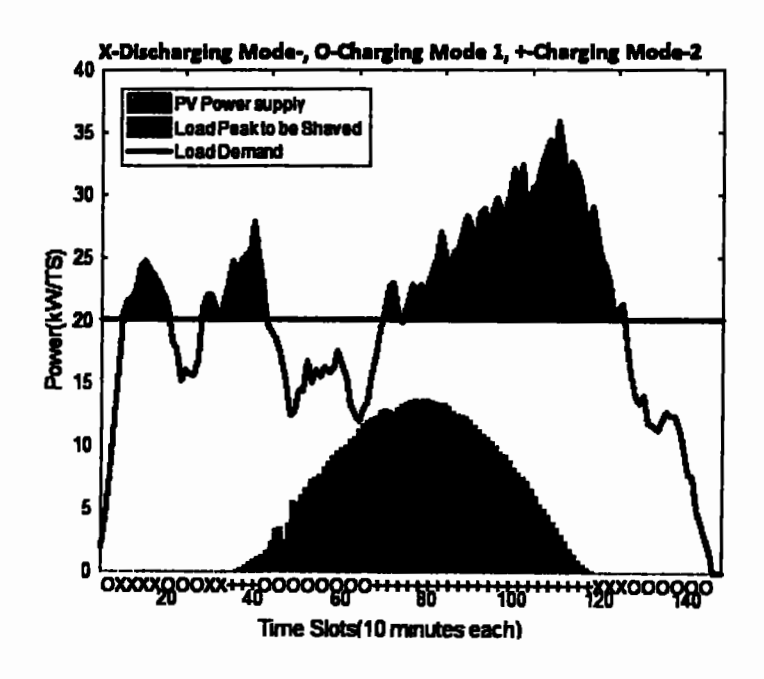


Fig. 6- 2 Operating TSs of modes of BES: t_{dls-c} when $P_L(t) > P_{dl} && P_{pv}(t) \le P_L(t) - P_{dl}$; t_{c1} when $P_L(t) \le P_{dl}$; and t_{c2} when $P_L(t) > P_{dl} && P_{pv}(t) > P_L(t) - P_{dl}$.

Three operating modes are considered to limit $P_g(t)$ to P_{dl} by using BES with availability of PV source. The modes are depicted in the following manner.

- 1. Discharging mode (DCM): DCM denoted by t_{dis-c} , is the time when load demand exceeds the demand limit. And the insufficiency of PV source does not allow it to cater the load demand i.e., $P_L(t) > P_{dl} \&\& P_{pv}(t) \le P_L(t) P_{dl}$. Logical AND operator is depicted by the symbol "&&".
- 2. Charging mode 1 (CM1): CM1 is denoted by t_{c1} , is the time when load demand is within the range of the demand limit, i.e., $P_L(t) \leq P_{dl}$.

3. Charging mode 2 (CM2): CM2 is denoted t_{c2} , is the time when load demand exceeds the demand limit and PV source successfully supplies the needed power, i.e., $P_L(t) > P_{dl}$ && $P_{pv}(t) > P_L(t) - P_{dl}$.

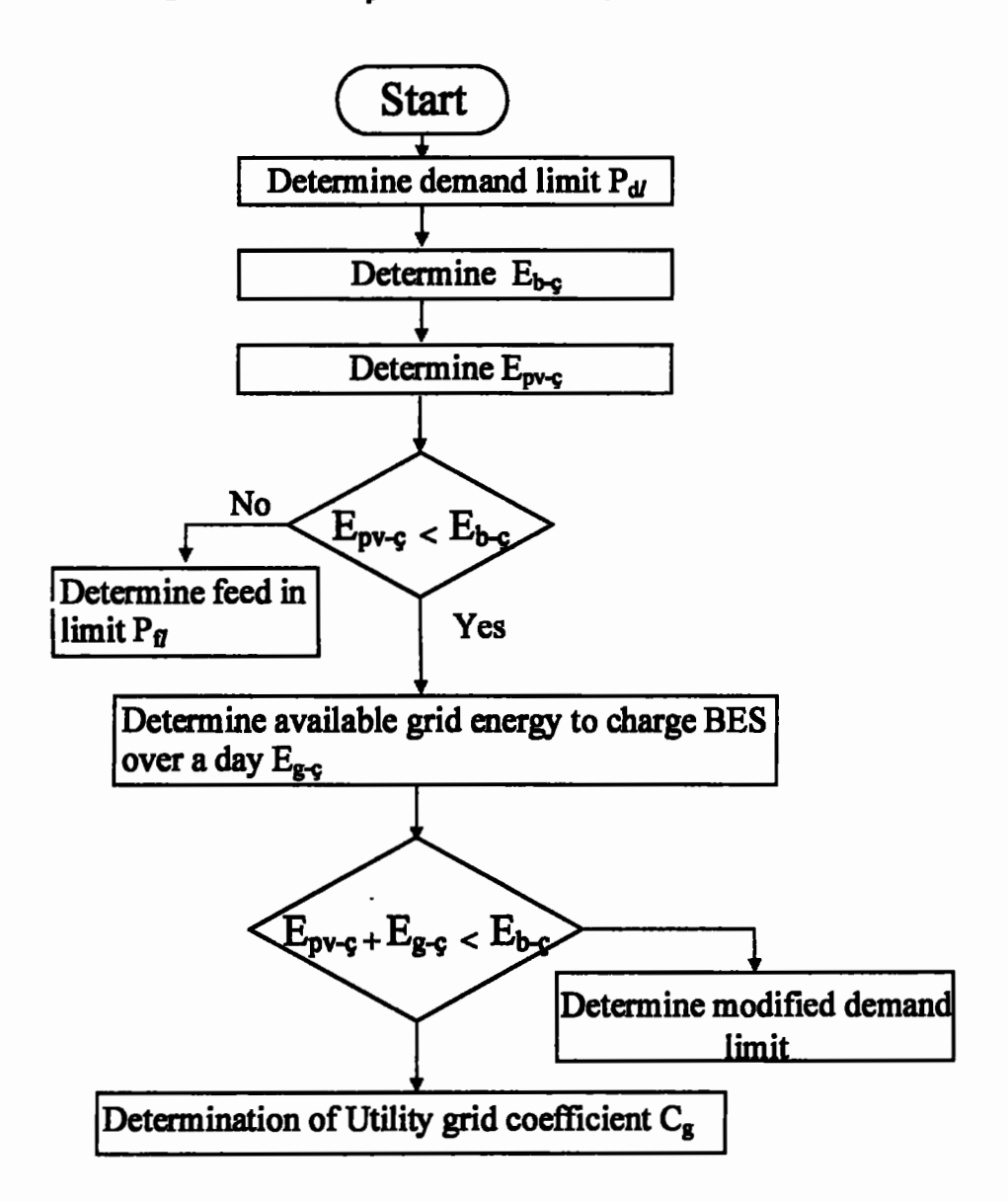


Fig. 6-3 Input's coordination needed for rule-based management control method [57]

6.3. Determination of Optimal Inputs

Predicted PV power and load demand are used to determine the inputs that are required for the suggested rule-based peak shaving management. The required inputs are P_{dl} , E_{b-c} , E_{pv-c} , E_{g-c} , C_g , P_{dl}^m and P_{fl} . The flowchart depicted in Fig. 6-3 reflects the coordination among these inputs. First, P_{dl} , E_{b-c} , and E_{pv-c} are determined. Then, E_{g-c} is determined if $E_{pv-c} \le E_{b-c}$. And P_{dl}^m is determined if $E_{pv-c} + E_{g-c} \le E_{b-c}$; otherwise C_g is determined. Where P_{fl} is determined, if $E_{pv-c} > E_{b-c}$. BES charge/discharge schedules for the purpose of peak shaving are determined by using these inputs. The utilized method to determine the input is presented ahead.

6.3.1. Demand Limit

Here, a control variable is required to be defined which is called the BES's dischargeable energy over 24 hours $(E_{b-dis-c}^*)$, which is selected from 0 kWh to the BES's rated energy capacity $E_{b-rated}$ (0 kWh and $E_{b-rated}$ both included), i.e.

$$0 \le E_{b-dis-c}^* \le E_{b-rated} \tag{6.2}$$

Since $E_{b-rated}$ is 150 kWh, $E_{b-dis-c}^* \in [0.150]$ kWh.

The determination of demand limit is performed such that $E_{b-dis-c}$ is equal to $E_{b-dis-c}^*$. Resultantly, it can be expressed as:

$$E_{b-dis-c} = E_{b-dis-c}^* \tag{6.3}$$

$$\sum P_{b-dis-\varsigma}(t) - E_{b-dis-\varsigma}^* = 0, \quad \forall t \in t_{dis-\varsigma}$$
 (6.4)

To limit $P_g(t)$ to P_{dl} , the required amount of load power $P_L(t) - P_{dl}$ is provided either by BES or PV source, when $P_L(t) > P_{dl}$. Nevertheless, BES only supplies the power which could not be taken up by the PV source.

Therefore, we have

$$P_{b-dis-c}(t) = P_L(t) - P_{di} - P_{pv}(t), \quad \forall t \in t_{dis-c}$$

$$= 0, \text{ otherwise.}$$
(6.5)

Substituting equation (6.5) into (6.4) gives

$$\sum (P_L(t) - P_{dl}) - P_{pv}(t) - E_{b-dis-c}^* = 0, \forall t \in t_{dis-c}$$
(6.6)

Equation (6.6) is in form of $f(P_{dl}) = 0$, where

$$(P_{dl}) = \sum ((P_L(t) - P_{dl}) - P_{pv}(t) - E_{b-dis-c}^*, \ \forall t \in t_{dis-c}$$
 (6.7)

The root-finding algorithm of the regula falsi method is exploited to find the solution of P_{dl} which is an independent variable as depicted in equation (6.7) [82]. Both secant and bisection search theorem methods combine to form the regula falsi method. It has fast response as compared to the bisection method with guaranteed root convergence. As per the regula falsi method, (P_{d-l1}, P_{d-l2}) are selected in way that $f(P_{d-l1})$ is assigned positive value and $f(P_{d-l2})$ as negative. Then, P_{d-l0} is solved as follows:

$$P_{d-l0} = \frac{1}{m} (0 - f(P_{d-l1})) + P_{d-l1}$$

Where,

$$m = \frac{f(P_{d-12}) - f(P_{d-11})}{P_{d-12} - P_{d-11}} \tag{6.8}$$

Using equation (6.8), we determine $f(P_{d-l0})$. When $|f(P_{d-l0})| < e$, P_{d-l0} becomes P_{dl} . When $|f(P_{d-l0})| > e$, either replace P_{d-l1} by P_{d-l0} (if $f(P_{d-l0}) > 0$) or replace P_{d-l2} by P_{d-l0} (if $f(P_{d-l0}) < 0$). Then, continue the above process till P_{d-l0} becomes P_{dl} .

6.3.2. The Energy Required for Charging BES for a Day

To be flexible for daily management, the energy necessary to charge the battery over 24 hours must be equivalent to the energy required to discharge the BES over 24 hours, i.e.,

$$E_{b-c} = E_{b-dis-c} = E_{b-dis-c}^{\bullet} \tag{6.9}$$

6.3.3. PV Energy Available to Charge BES Over 24 Hours

It can be deduced from equation (6.9), the BES will be charged by the total energy $E_{b-\varsigma}$, from either the utility grid or from PV source. Firstly, the PV energy that is available for charging the BES over the duration of 24 hours (without having to inject it into the grid) is determined. If the available PV energy is insufficient, then the utility grid energy that may be available for charging the BES is calculated. The $P_{pv-\varsigma}$ is $P_{pv}(t)$ and $P_{pv}(t) - (P_L(t) - P_{dl})$ during t_{c1} and t_{c2} , respectively, i.e.

$$\begin{split} P_{pv-\varsigma} &= P_{pv}(t) \quad \forall t \in t_{\varsigma 1} \\ &= P_{pv}(t) - (P_L(t) - P_{dl}) \quad \forall t \in t_{\varsigma 2} \\ &= 0, \text{ otherwise} \end{split} \tag{6.10}$$

The PV energy available to charge the BES over 24 hours is then the sum of $P_{pv-c}(t)$ over 24 hours. It is given as;

$$E_{nv-c} = \sum_{t=1}^{T} P_{nv-c}(t) \tag{6.11}$$

Where T is 144 TSs.

6.3.4. Utility Grid Energy Available for Charging BES Over 24 Hours

From equations (6.9) and (6.11), if $E_{pv-\varsigma} \leq E_{b-\varsigma}$, it shows that the required BES energy cannot be provided by PV supply. This deficient energy is provided by the utility grid while ensuring the demand is not exceeding the demand limit. This clarifies that BES does not take any charge from the utility grid during $t_{\varsigma 2}$. Therefore, the excess utility power during $t_{\varsigma 2}$ is used to charge BES with $(P_{g-\varsigma}(t))$, for limiting P_g to P_{dl} is $P_{dl}-P_L(t)$, i.e.

$$P_{g-c}(t) = P_{dl} - P_L(t) \quad \forall t \in t_{c1}$$

$$= 0, \quad \text{otherwise}$$
(6.12)

Hence, the utility grid energy available to charge BES over 24 hours is then the sum of $P_{g-\varsigma}(t)$ over 24 hours. It is given as;

$$E_{q-c} = \sum_{t=1}^{T} P_{q-c}(t)$$
 (6.13)

6.3.5. Utility Grid Energy Coefficient for Charging the BES

If $E_{pv-\varsigma} \leq E_{b-\varsigma} \&\& E_{g-\varsigma} + E_{pv-\varsigma} > E_{b-\varsigma}$, the deficit energy amount to fully charge the BES, i.e., $E_{b-\varsigma} - E_{pv-\varsigma}$, must be supplied by the grid, as stated in equations (6.9), (6.11), and (6.13). But, when using the total amount of the available PV energy for charging the BES, only a portion of the grid energy is needed. In the mentioned situation, if $C_g E_{g-\varsigma}$ is used as the required grid energy for charging the BES, it equals $E_{b-\varsigma} - E_{pv-\varsigma}$, as

$$C_g E_{g-\varsigma} = E_{b-\varsigma} - E_{pv-\varsigma}$$

$$C_g = \frac{E_{b-\varsigma} - E_{pv-\varsigma}}{E_{g-\varsigma}}$$
(6.14)

6.3.6. Modification of Demand Limit

From equations (6.9), (6.11), and (6.13), if $E_{g-\varsigma} + E_{pv-\varsigma} \leq E_{b-\varsigma}$, this depicts that the BES is not able to acquire the required amount of charging to limit $P_g(t)$ to P_{dl} . In this situation, SoC_f cannot match with SoC_i, resulting in a breach of flexibility for day-to-day control. To prevent this violation, it is required to modify P_{dl} so that the dischargeable energy of BES over T should be equal to the sum of available PV source and grid energy for charging BES over T, i.e.,

$$\sum_{t=1}^{T} P_{g-c}^{m}(t) + \sum_{t=1}^{T} P_{pv-c}^{m}(t) = \sum_{t=1}^{T} P_{b-dis-c}^{m}(t)$$
 (6.15)

Superscript "m" depicts the corresponding variables for modified demand limit P_{dl}^m . Using equations (6.5), (6.10), and (6.12), substituting, $P_{b-dis-c}^m(t), P_{pv-c}^m(t)$, and $P_{g-c}^m(t)$ into (6.15) for t_{c1}^m , t_{c2}^m , and t_{dis-c}^m gives

$$\sum (P_{dl}^{m} - P_{L}(t)) + P_{pp}(t) - 0 = 0 \quad \forall t \in t_{c1}^{m}$$
(6.16)

$$\sum_{t=0}^{\infty} (0) + (P_{pv}(t) - (P_L(t) - P_{dl}^m)) - (0) = 0, \ \forall t \in t_{c2}^m$$
 (6.17)

$$\sum(0) + (0) - \left(-\left(P_{pv}(t) - (P_L(t) - P_{dl}^m) \right) \right) = 0, \quad \forall t \in t_{\text{dis}-\varsigma}^m$$
 (6.18)

The zero terms in the above equations refer to the absence of power for the occurring modes, respectively. For example, zero on the left-hand side of equation (6.16) refers to $(P_L(t) - P_{dl})$ which is not possible since $P_L(t) < P_{dl}$ during mode t_{c1}^m . Similarly, the zero on the right-hand side of (6.16) refers to the absence of $P_{b-dls-c}^m(t)$ because it is the charging mode, therefore, discharging is not possible. Equations (6.17) and (6.18) are developed in the similar way.

Combining (6.16)–(6.18) over T gives

$$\sum_{t=1}^{T} \left(P_{pv}(t) - (P_L(t) - P_{dl}^m) \right) = 0 \tag{6.19}$$

Consequently, the adjusted demand limit is represented as

$$P_{dl}^{m} = \frac{\sum_{t=1}^{T} (P_{L}(t) - P_{pv}(t))}{T}$$
 (6.20)

6.3.7. Feed-in Limit

Based on the equations (6.9) and (6.11), if $E_{pv-c} > E_{b-c}$, then the battery can be charged with the appropriate quantity of energy without using all of the available PV energy. As a result, a

PV power limit P_{fl} is established in a way that the PV source is not utilized for charging the BES when $P_{pv-c}(t) \leq P_{fl}$. When $P_{pv-c}(t) > P_{fl}$ during the period t_c , the battery is fully charged with $P_{pv-c}(t) - P_{fl}$, i.e.

$$\sum P_{pv-c}(t) - P_{fl} = E_{b-c}, \forall t \in t_c \& t_1$$
 (6.21)

In equation (6.21), t_l is the time when $P_{pv-c}(t) > P_{fl}$. Moreover, $P_{pv-c}(t) = P_{pv}(t)$ when $t_c = t_{c1}$ and $P_{pv-c}(t) = P_{pv}(t) - (P_L(t) - P_{dl})$ when $t_c = t_{c2}$.

$$\sum (P_{pv-c}(t) - P_{fl}) - E_{b-c} = 0, \forall t \in t_c \& t_1$$
 (6.22)

Equation (6.22) is in form of $f(P_{fl}) = 0$, where

$$(P_{fl}) = \sum (P_{pp-c}(t) - P_{fl}) - E_{b-c} \quad \forall t \in t_c \& t_1$$
 (6.23)

In equation (6.22), as P_{fl} is an independent variable, the regula falsi method's root finding procedure is employed to solve for P_{fl} . The regula falsi approach is used to determine P_{fl} in the same manner as was used to determine P_{dl} . Initially, (P_{fl1}, P_{fl2}) are picked with $f(P_{fl1})$ being positive and $f(P_{fl2})$ being negative. P_{fl0} is then calculated as follows:

$$P_{fl0} = \frac{1}{m} (0 - f(P_{fl1})) + P_{fl1},$$

Where,

$$m = \frac{f(P_{fl2}) - f(P_{fl1})}{P_{fl2} - P_{fl1}} \tag{6.24}$$

Using (6.24), we determine $f(P_{fl0})$. When $|f(P_{fl0})| < e$, P_{fl0} becomes P_{fl} . When $|f(P_{fl0})| > e$, either replace P_{fl1} by P_{fl0} (if $f(P_{fl0}) > 0$) or replace P_{fl2} by P_{fl0} (if $f(P_{fl0}) < 0$). Then, continue the above process till P_{fl0} becomes P_{fl} .

6.4. Control Strategy for Rule-Based Peak Shaving

The peak shaving rules for the formulation of the upcoming day's charging/discharging schedules of BES are developed by using the above-determined inputs. These regulations are written in a way that they ensure flexibility in the daily management while restricting the feed-in powers and peak utility grid demand to the relevant feed-in and demand limits of the day. This section details the BES charging/discharging rules formulation.

1. **DCM** (During t_{dis-c})

<u>Rule 1</u>: The amount dispatched by the BES $(P_L(t) - P_{dl}) - P_{pv}(t)$ as per (6.5).

2. CM1 (During t_{c1})

<u>Rule 2</u>: If $E_{pv-c} \le E_{b-c} \&\& E_{pv-c} + E_{g-c} > E_{b-c}$, the BES takes charge from PV source and the utility grid with the amount $P_{pv}(t) + C_g(P_{dl} - P_L(t))$ as per (6.10), (6.12), and (6.14).

Rule 3: If $E_{pv-\varsigma} \le E_{b-\varsigma} \&\& E_{pv-\varsigma} + E_{g-\varsigma} \le E_{b-\varsigma}$, the BES takes charge from PV source and the utility grid with the amount $P_{pv}(t) + (P_{dl}^m - P_L(t))$ as per (6.16).

<u>Rule 4</u>: If $E_{pv-c} > E_{b-c} \& P_{pv}(t) > P_{fl}$, the BES takes charge from PV source with the amount $P_{pv}(t) - P_{fl}$ as per (6.10) and (6.21).

<u>Rule 5</u>: If $E_{pv-c} > E_{b-c} \&\& P_{pv}(t) \le P_{fl}$, the BES takes no charge from PV Source.

3. CM2 (During t_{c2})

<u>Rule 6</u>: If $E_{pv-c} \le E_{b-c}$, the BES takes charge from PV source with the amount $P_{pv}(t) - (P_L(t) - P_{dl})$ as per (6.10).

<u>Rule 7</u>: If $E_{pv-c} > E_{b-c} \&\& (P_{pv}(t) - (P_L(t) - P_{dl})) > P_{fl}$, the BES takes charge from PV source with the amount $(P_{pv}(t) - (P_L(t) - P_{dl})) - P_{fl}$ as per (6.10) and (6.21).

<u>Rule 8</u>: If $E_{pv-c} > E_{b-c} \&\& (P_{pv}(t) - (P_L(t) - P_{dl})) \le P_{fl}$, the BES takes no charge from PV Source.

Using the coulomb-counting approach [83], the SoC of the BES in its charge/discharge modes is determined as follows:

$$SoC(t) = 1 - \frac{\sum_{t_0}^{t} i}{Ah_{b-rated}}$$
 (6.25)

Where, discharging is reflected by positive i, and negative i reflects charging.

The resulting utility grid power while considering the above-mentioned Rules 1-8 and equation (6.1), is given in Table 6.1.

Table 6- 1 Utility Grid Power

Mode of Operation	Rule	Utility Grid Power	
DCM	1	P_{dl}	
CM1	2	$P_L(t) + C_g(P_{dl} - P_L(t))$	
CM1	3	P_{dl}^m	
CM1	4	$P_L(t) - P_{fl}$	
CM1	5	$P_L(t) - P_{pv}(t)$	
CM2	6	P_{dl}	
CM2	7	$P_{dl}-P_{fl}$	
CM2	8	$P_L(t) - P_{pv}(t)$	

6.5. Determination of Optimal Inputs

Peak shaving of utility grid electricity while ensuring optimized utilization of the BES is critical. The following is a discussion of the formulation of such an optimal problem.

The objective function along with the constraints are detailed as follows:

$$minimize, f = E_{g-pk} (6.26)$$

Subjected to

$$P_a(t) + P_{pv}(t) + P_b(t) = P_L(t)$$
 (6.27)

$$SoC_l \le SoC(t) \le SoC_u, SoC_f = SoC_l$$
 (6.28)

$$P_{b-\varsigma}(t) \le P_{b-\varsigma-mx}, P_{b-dis-\varsigma}(t) \le P_{dis-\varsigma-mx}$$
(6.29)

$$E_{b-dis-c}^* \le E_{b-rated} \tag{6.30}$$

The goal, according to Equation (6.26) is to minimize E_{g-pk} . The power balance constraint is shown in equation (6.27). The constraints of the battery's SoC as well as the battery's flexibility in day-to-day operations are shown in Equation (6.28). The restrictions of the battery's charge/discharge powers and dischargeable energy through the duration of a day are shown in equations (6.29) and (6.30), respectively. Table 6.2 [57] lists the system parameters as well as the limitations.

Table 6- 2 System parameters [57]

Parameter	Value	Parameter	Value
P_{d-pk}	165 kW	SoC_l/SoC_u	0.2/0.9
P_{pv-ins}	90-430 kW	SoCi	0.5
$E_{b-rated}$	150 kWh	$P_{b-\varsigma-\mathrm{mx}}$	40 kW
Ah _{b-rated}	600 Ah	$P_{b-dis-c-mx}$	40 kW

 E_{g-pk} is the peak energy drawn from the utility grid over the course of a day as per equation (6.26), i.e.;

$$E_{g-pk} = maximum(E_g(t)), \forall t \in [0, T]$$
(6.31)

 E_q is determined as

$$E_g(t) = (P_g(t)) \times T_c \tag{6.32}$$

Because the inputs needed for peak shaving control are dependent on $E_{b-dis-c}^*$, as previously mentioned, $E_{b-dis-c}^*$ is regarded as a control variable. The problem represents an offline optimization problem that is defined with a nonlinear fitness function. The problem is handled in MATLAB with particle swarm optimization (PSO). For tackling a nonlinear optimization problem, the PSO method is a prominent heuristic optimization method [12].

In Fig. 6-4, a flow chart depicts the method of determining the battery's optimal dischargeable energy $(E^*_{ob-dis-c})$ using the PSO. After determining $(E^*_{ob-dis-c})$ the inputs related to $(E^*_{ob-dis-c})$ are regarded as the optimized inputs needed for the postulated rule-based control, i.e. P_{od-lm} , E_{ob-c} , E_{opv-c} , E_{og-c} , C_{og} , P^m_{od-lm} , and P_{ofl} . It signifies that the optimal rule-based

inputs are obtained as a result of optimization, i.e., solving the optimization problem. The proposed rule-based peak shaving management method then uses these optimal rule-based inputs to generate optimal battery schedules. The suggested peak shaving management is depicted in Fig. 6-5 in the form of a flowchart.

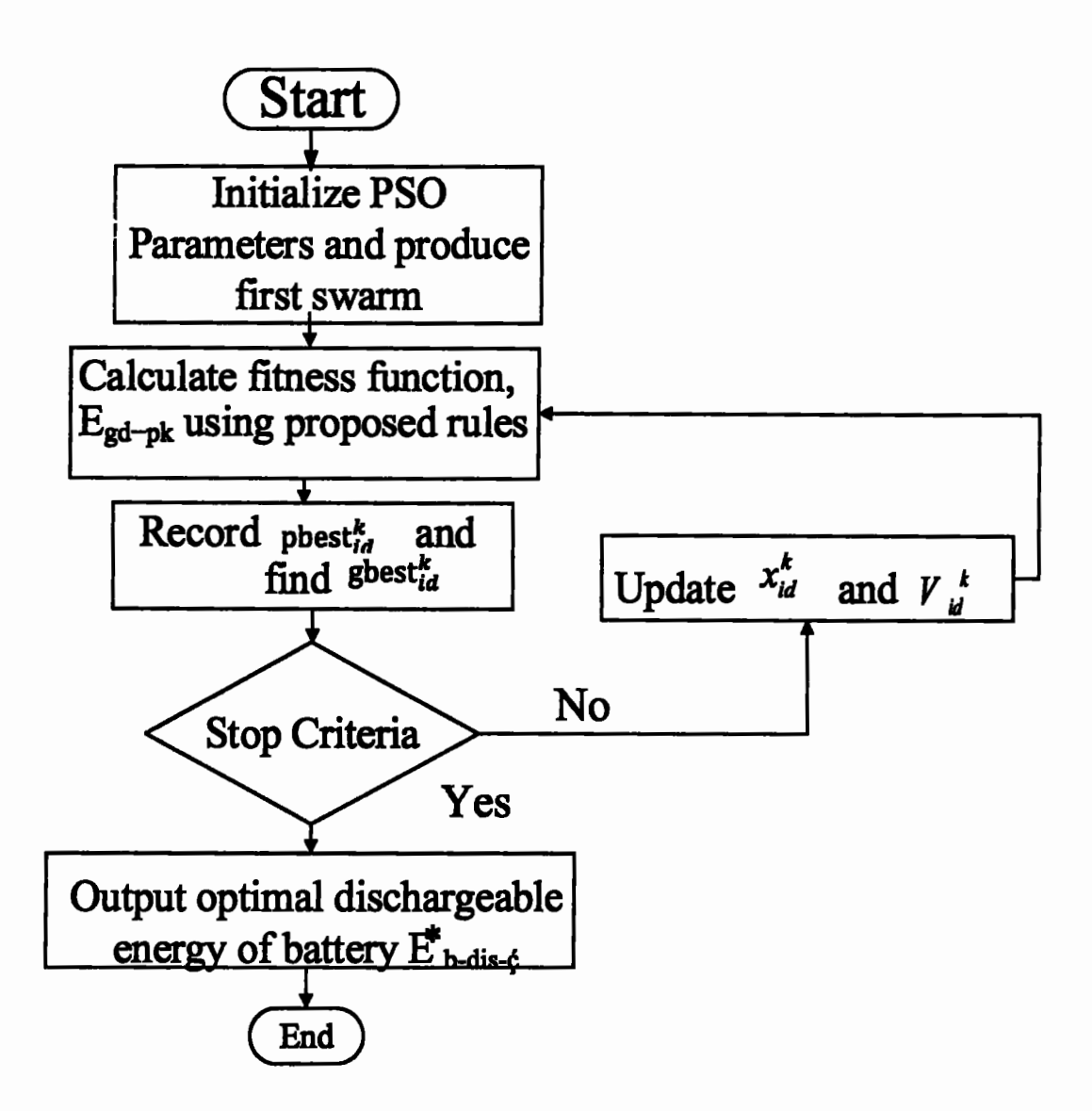


Fig. 6-4 Particle swarm optimization for finding optimal dischargeable energy of BES

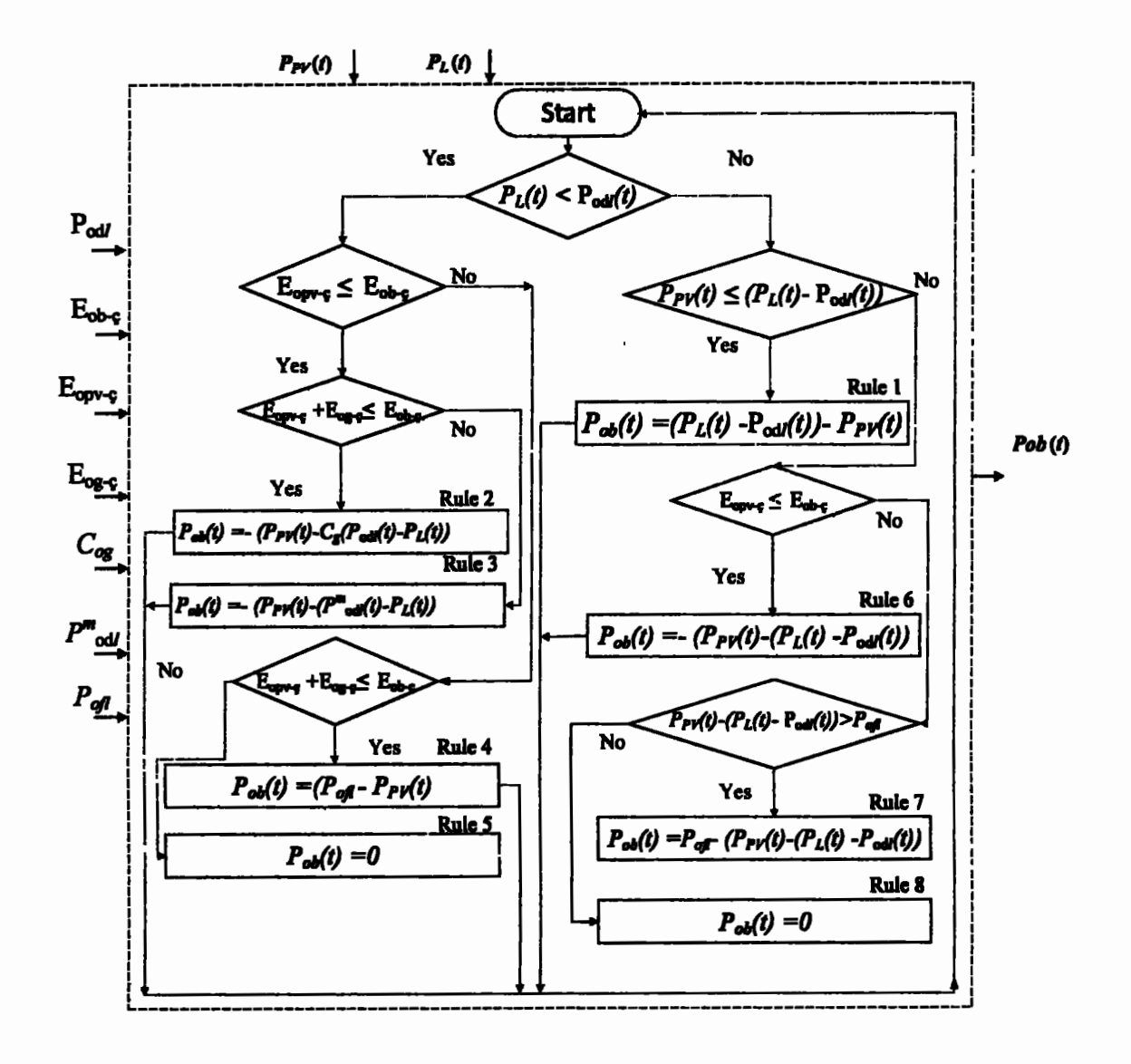


Fig. 6-5 Flow diagram for optimal rule-based peak shaving control [57]

6.6. Simulation Results

The method presented above is tested on a grid-connected MG framework incorporating PV and BES. Simulations are performed for four cases. PV penetration levels of 5% and 15% are utilized for the hot and cold days, respectively. The optimal inputs required for applying the control algorithm for the simulated case studies are depicted in Table 6.3. The best fitness value is acquired

for multiple runs of the PSO algorithm for the case of 10 % PV availability for the cold day. The minimum value among these best fitness values (considering all runs), i.e., 111.31 kWh, is the optimal peak energy drawn from the utility grid. The attained results of these cases with the proposed method are discussed as follows.

Table 6-3 Optimal inputs of management algorithm with application to four cases

Input Parameter	Case 1	Case 2	Case 3	Case 4
P _{odl} (kW)	137.4463	111.3113	122.668	107.8125
E_{ob-C} (kWh)	65.2600	81.7368	59.6737	91.0526
<i>E_{opv−Ç}</i> (kWh)	66.3143	70.1186	60.1927	92.1413
$E_{og-\zeta}$ (kWh)	NA	NA	NA	NA
Cog	NA	NA	NA	NA
P_{odl}^{m} (kW)	NA	NA	NA	NA
P_{ofl} (kW)	15.5921	25.3714	32.3715	35.5489

The obtained results with the proposed method are discussed for these cases as follows.

6.6.1. Case 1: 5% PV Penetration for Hot and Cloudy Day

In this scenario, the management scheme is simulated over a hot and cloudy day as illustrated in Fig. 6-6(a). The estimations corresponding to P_{od-lm} , E_{ob-c} , E_{opv-c} , and P_{ofl} are 137.4463 kW, 65.2600 kWh, 66.3143 kWh, and 15.5921. The amount of available PV energy for charging BES exceeds the energy required for charging the BES $E_{opv-c} > E_{ob-c}$. As a result, in this scenario, E_{og-c} , C_{og} , and P_{od-lm}^m are not applicable (NA), as shown in Table 6.3. According to Fig. 6-5 for the estimated E_{ob-c} , the DCM occurs during t = 102-109 TS, and CM1 is during t = 32-39 and 113-117 TS. There is no CM2 because the BES charging is already at SoC_u during excess PV TSs. The grid charges the BES during t = 131-136 TS for daily management of BES SoC. Fig. 6-6

(b) shows the BES's optimal charge/discharge schedules for the different modes. As observed, the PV source exclusively charges the BES. Fig. 6-6 (c) illustrates that $SoC_i = SoC_f = 50\%$, which is desirable to ensure flexibility in day-to-day management. Flexible day-to-day management with $SoC_i = SoC_f = 50\%$ is reflected in Fig. 6-6(c). Fig. 6-6 (d) depicts the corresponding utility grid demand. The illustration suggests that the utility grid demand is capped for $P_{od-lm} = 137.4463$ kW.

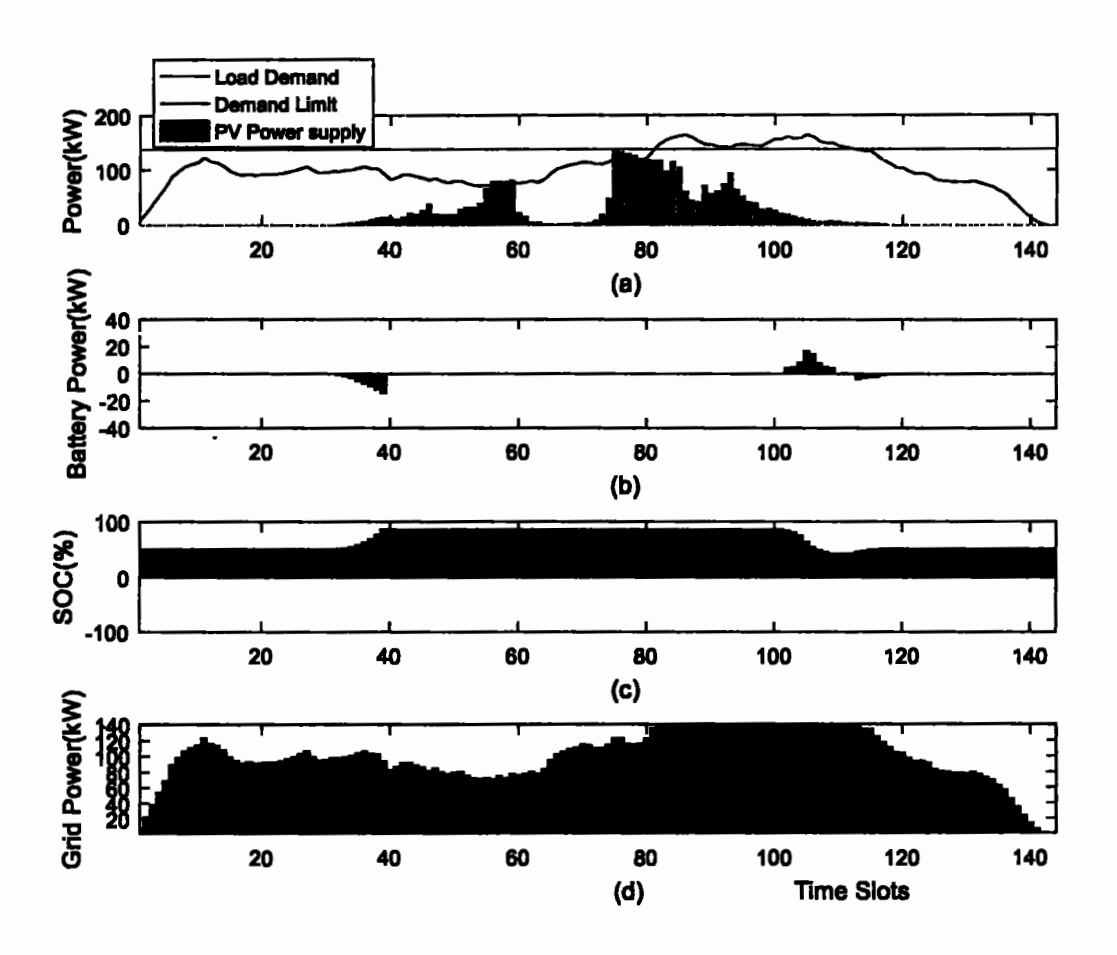


Fig. 6-6 Case-1. (a) Profiles for PV power supply and load consumption. (b) Schedules of BES charge/discharge. (c) BES state of charge. (d) Utility grid power

6.6.2. Case 2: 5% PV penetration for Cold day

In this scenario, the management scheme is simulated over a cold day with comparably lesser magnitude PV power as illustrated in Fig. 6-7(a). The estimated values corresponding to P_{od-lm} , E_{ob-c} , E_{opv-c} , and P_{ofl} are 111.3113 kW, 81.7368 kWh, 70.1186 kWh, and 25.3714 kW. The amount of available PV energy for charging the BES again exceeds the energy required for charging the BES $E_{opv-c} > E_{ob-c}$. As a result, in this scenario, E_{og-c} , C_{og} , and P_{od-lm}^m are not applicable (NA), as shown in Table 6.3.

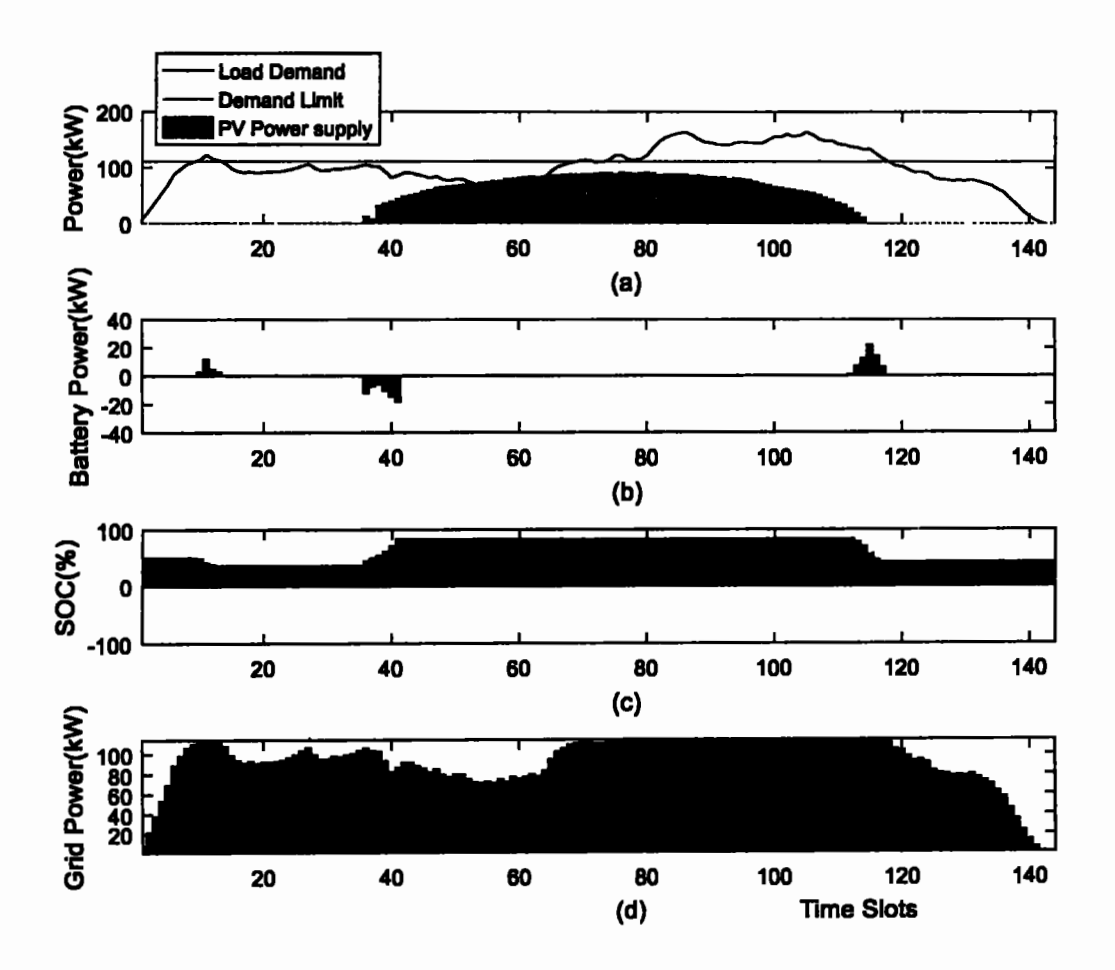


Fig. 6-7 Case-2. (a) Profiles for PV power supply and load consumption. (b) Schedules of BES charge/discharge. (c) BES state of charge. (d) Utility grid power

According to Fig. 6-7 for the estimated E_{ob-c} , the DCM occurs during t = 10-13 and 112-118 TS, and CM1 is during t = 36-41 TS. There is again no CM2 because the BES charging is already at SoC_u during excess PV TSs. The grid charges the BES during t = 1-6, 131-140 for daily management of BES SoC. Fig. 6-7 (b) shows the BES's optimal charge/discharge schedules for the different modes. As observed, the PV source exclusively charges the BES. Fig. 6-7 (c) illustrates that $SoC_l = SoC_f = 50\%$, which is desirable to ensure flexibility in day-to-day management. Flexible day-to-day management with $SoC_l = SoC_f = 50\%$ is reflected in Fig. 6-7(c). Fig. 6-7 (d) depicts the corresponding utility grid demand. The illustration suggests that the utility grid demand is capped for $P_{od-lm} = 111.3113$ kW.

6.6.3. Case 3: 15% PV penetration for Hot and Cloudy day

In this scenario, the management scheme is simulated over a hot and cloudy day with 15% of PV penetration as illustrated in Fig. 6-8(a). The estimated values corresponding to P_{od-lm} , $E_{ob-\varsigma}$, $E_{opv-\varsigma}$, and P_{ofl} are 122.668 kW, 59.6737 kWh, 60.1927 kWh, and 32.375 kW, respectively. The amount of available PV energy for charging the BES exceeds the energy required for charging the BES ($E_{opv-\varsigma} > E_{ob-\varsigma}$). As a result, in this scenario, $E_{og-\varsigma}$, C_{og} , and P_{od-lm}^m are not applicable (NA), as shown in Table 6.3. According to Fig. 6-8 for estimated $E_{ob-\varsigma}$, the DCM occurs during t=32-36 and 117 TS, CM1 is during t=105-115 TS. There is again no CM2 because the BES charging is already at SoC_u during excess PV TSs. Fig. 6-8 (b) shows the BES's optimal charge/discharge schedules for the different modes. As observed, the PV source exclusively charges the BES. Fig. 6-8 (c) illustrates that $SoC_l = SoC_f = 50\%$, which is desirable to ensure flexibility in day-to-day management. Fig. 6-8 (d) depicts the corresponding utility grid demand. The

illustration suggests that the utility grid demand is capped for $P_{od-lm} = 122.668$ kW which is less than 5% PV penetration of case 1, as desired.

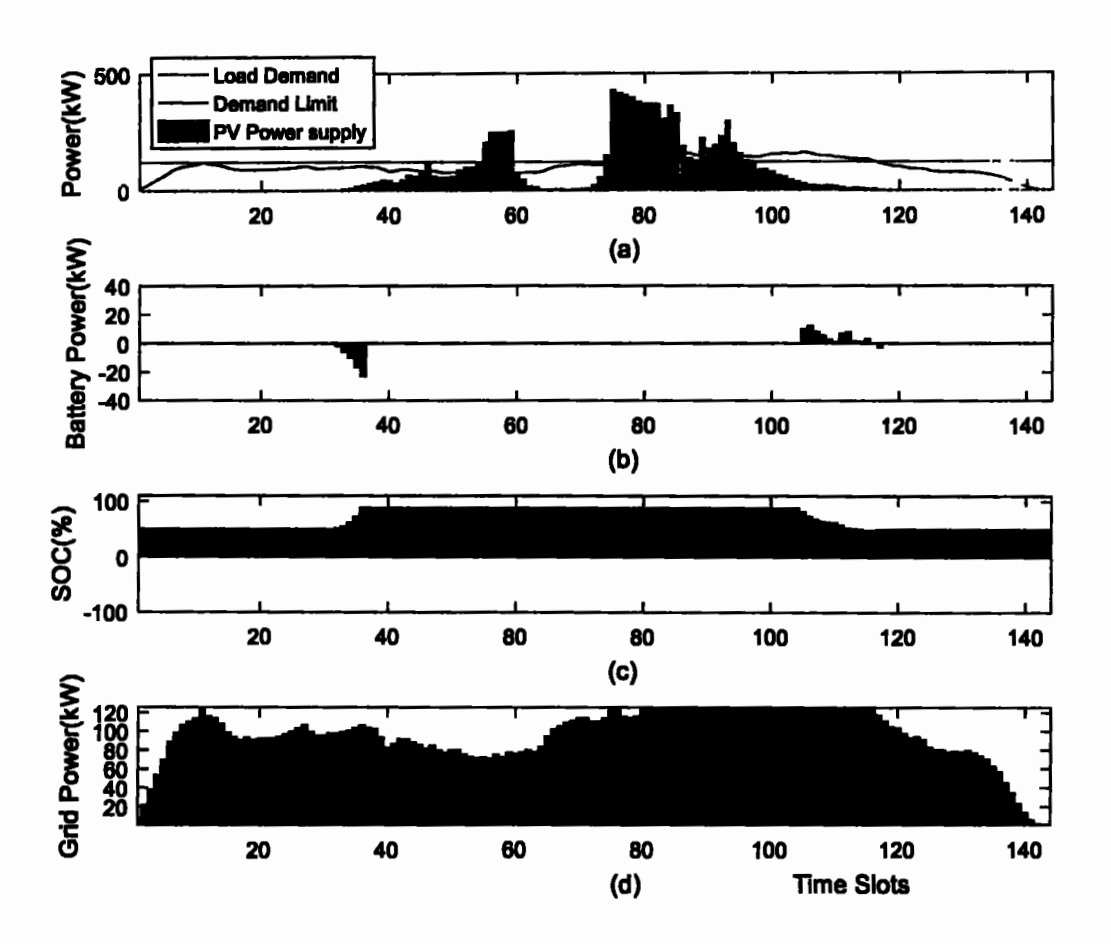


Fig. 6-8 Case-3. (a) Profiles for PV power supply and load consumption. (b) Schedules of BES charge/discharge. (c) BES state of charge. (d) Utility grid power

6.6.4. Case 4: 15% PV penetration for Cold Day

In this scenario, the management scheme is simulated over a cold day with comparably lesser magnitude PV power as illustrated in Fig. 6-9(a). The estimated values corresponding to P_{od-lm} , E_{ob-c} , E_{opv-c} and P_{ofl} are 107.8125 kW, 91.0526 kWh, 92.1413 kWh, and 35.5489 kW,

respectively. The amount of PV energy available for charging the BES again exceeds the energy required for charging the BES $(E_{opv-c}>E_{ob-c})$. As a result, in this scenario, E_{og-c} , C_{og} , and P_{od-lm}^m are not applicable (NA), as shown in Table 6.3. According to Fig. 6-9 for the estimated P_{od-lm} , the DCM occurs during t=9-14 and 115-118 TS, CM1 is during t=36-38 TS. There is again no CM2 because the BES charging is already at SoC_u during excess PV TSs. Fig. 6-9 (b) shows the BES's optimal charge/discharge schedules for the different modes. As observed, the PV source exclusively charges the BES. Fig. 6-9 (c) illustrates that $SoC_i = SoC_f = 50\%$, which is desirable to ensure flexibility in day-to-day management.

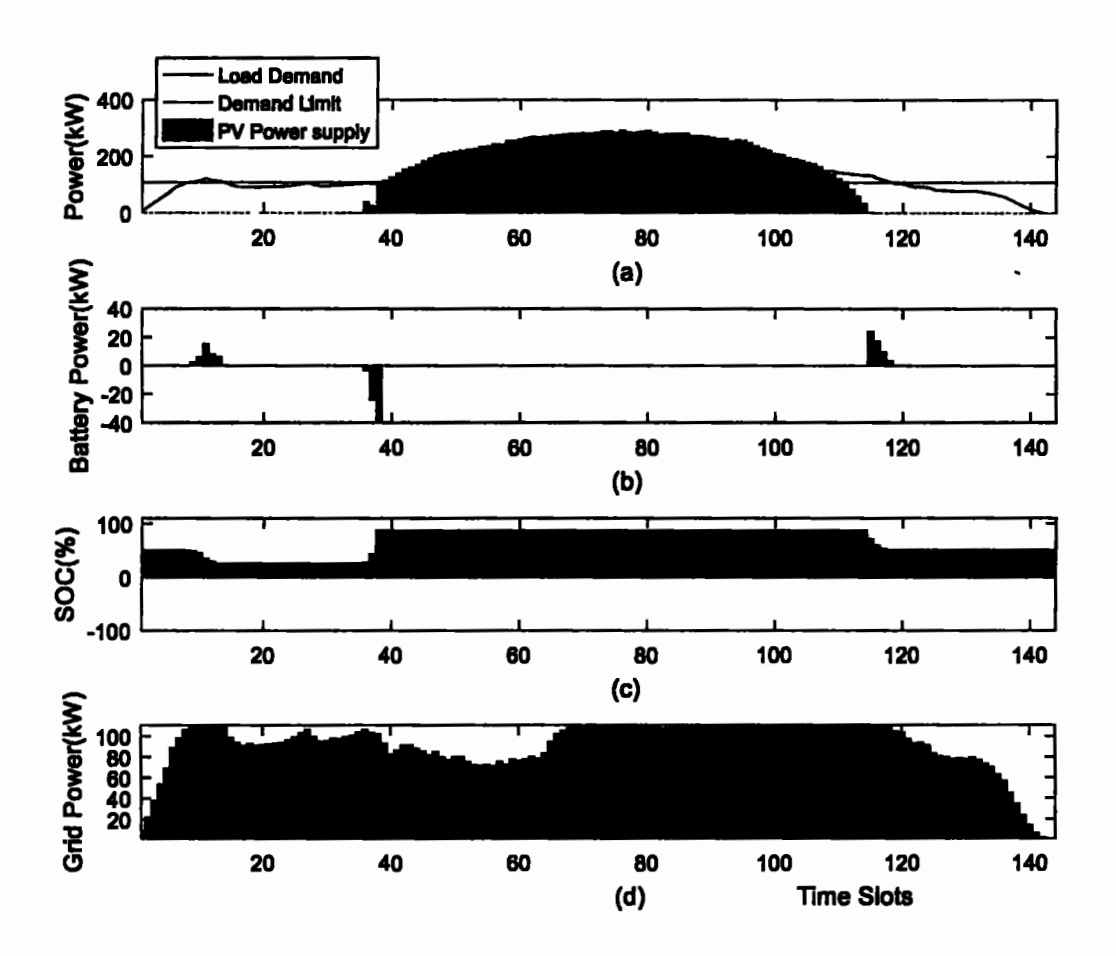


Fig. 6-9 Case-4. (a) Profiles for PV power supply and load consumption. (b) Schedules of BES charge/discharge. (c) BES state of charge. (d) Utility grid power

Fig. 6-8 (d) depicts the corresponding utility grid demand. The illustration suggests that the utility grid demand is capped for $P_{od-lm} = 107.8125$ kW which is less than 5% PV penetration of case 2, as desired.

Table 6- 4 Comparison of Percentage of Peak Shaving (PPS) For Different Cases

Schemes	Case-1	Case-2	Case-3	Case-4
PUGP (kW)	137.4463	111.3113	122.668	107.8125
PPS (%)	16.36	32.27	25.35	34.40

6.7. Summary

Table 6.4 presents the percentage of peak shaving (PPS) for each case. It is obvious from the results that increasing the PV penetration reduces the demand limit and more PV can participate in peak shaving. In the proposed algorithm, systematic coordination exists between various modes and a smooth charging discharging of BES is observed. This shows how dynamic feed-in and demand limits are effective in BES utilization as well as peak load shaving. Day-to-day management of the BES charging/discharging mechanism also adds to the MG stability. The load factor of the utility grid is improved as the off-peak load below the demand limit is only taken by the utility grid. Hence an optimized peak shaving control strategy with a defined set of rules is proposed with dynamic feed-in and demand limits.

However, due to the same load profile used for all the cases, a number of rules could not be demonstrated as shown in Table 6.3. Therefore, for enhancing the scope of the presented study, it is suggested to use different load profiles for winters and summers along with distinct user preferences in response to the change of seasons should be utilized in the peak shaving algorithm. And different PV penetrations should be demonstrated for both.

An optimization based pre-processing stage maybe added to the MG system that can reduce the PAR of load demand before the optimal peak shaving application. This may lead to a more optimized and economical solution which lessens the burden on the BES system. Effects on the PPS can also be observed.

All these discussed issues are addressed in dynamic-HEMS and rule based optimal peak shaving control technique presented in the next chapter.

Chapter 7

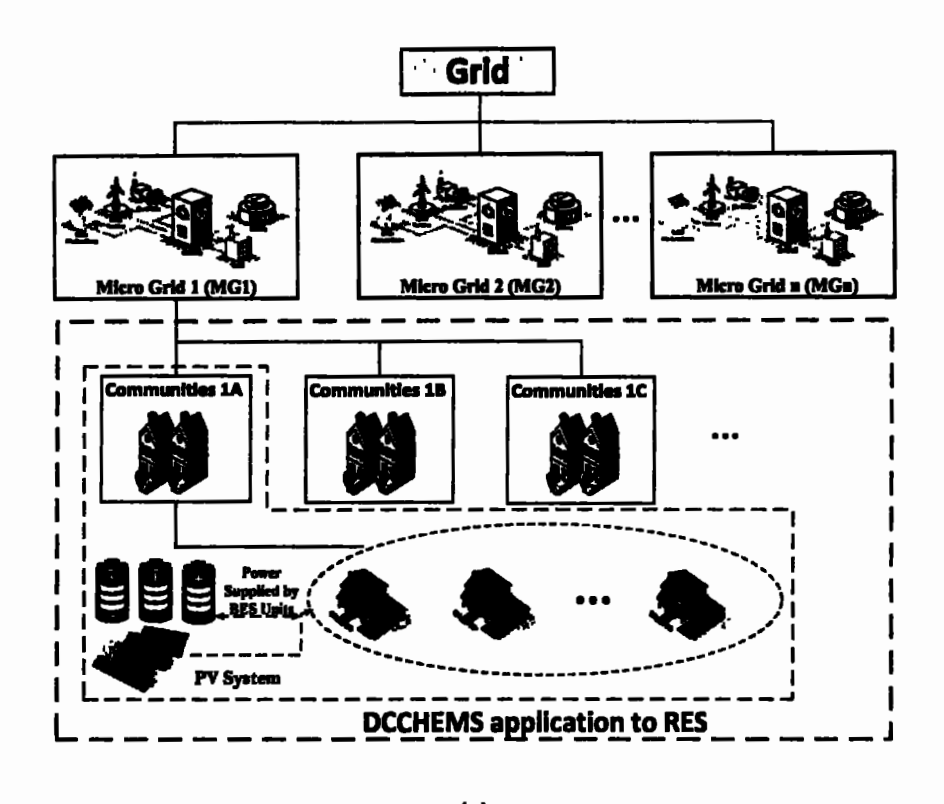
Dynamic HEMS based Optimal Peak Shaving Control in a Microgrid

In the existing literature, the optimal rule-based approaches do not provide dynamicity in the heuristic computation-based schemes applied [57,84,85]. This can have various benefits of improved percentage peak shaving when peak reduction is the target of the heuristic computation-based schemes. This will also reduce the burden on the BES. To avoid that limitation, a two-stage control strategy is proposed in this chapter as shown in Fig 7-1. A pre-processing stage based on a modified dynamic-clustered home energy management system (DCHEMS) scheme with application to the residential communities is incorporated. Based on the resultant load profile, the second stage is responsible for the determination of desired inputs for optimized BES peak shaving control using PSO.

To make the model meaningful, realistic and practical, the proposed model, in the preprocessing stage uses four classes of consumers i.e., lower class, middle class, upper-middle-class and higher class. Due to the non-identical properties of CDs and distinct user preferences from different classes, the load is non-homogeneous. The PV installations considered for each class are also different. Considering the variations in consumers' behaviors due to seasonal changes, different usage parameters for CDs in summers and winters are considered in the study.

7.1. System Illustration

A utility grid-connected MG, with a community-based HEMS architecture consisting of distributed energy resources of PV and BES power sources, is illustrated in Fig. 7-1 [57]. The utility grid is capable of power deliverance as well as absorption.



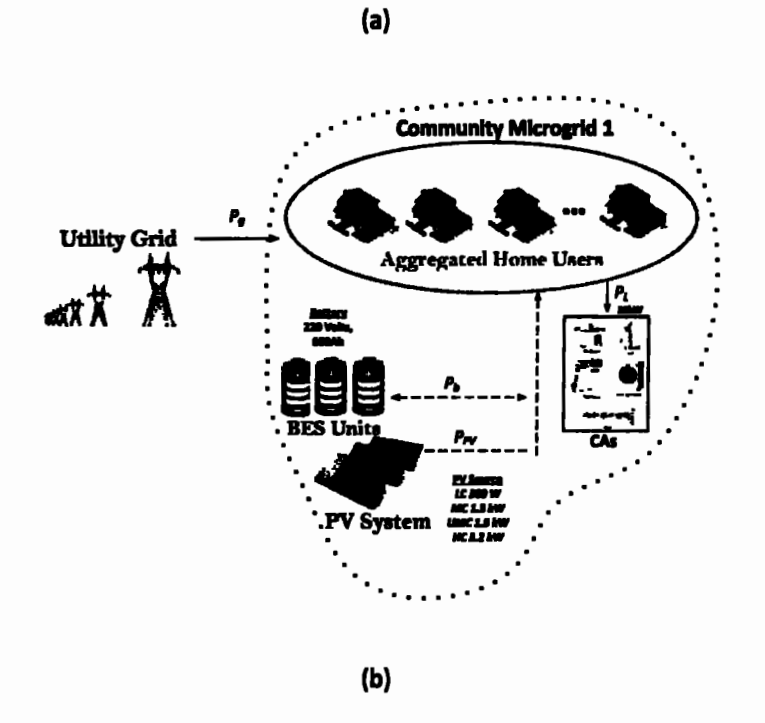


Fig. 7- 1(a) Community based Dynamic-HEMS framework (b) BES and PV considered as distributed energy resources within community MG.

7.1.1. Load Demand

Two distinct load profiles are considered for summer and winter conditions. The same eight devices are considered which were taken in chapter 3. But some of the devices are used more frequently in summers, whereas, some are used in winters. For example, the air conditioner is more frequently used in summers for cooling purposes. The same air conditioner is less frequently used for heating in winters that consume lesser power as compared to that of cooling. This is due to the trend of more sunlight utilization and getting done with most of the tasks during the day. This is the reason why peak hours in the load demand are generally observed during 09:00 to 12:00 hours in winters, whereas they occur during 20:00 to 23:00 in summers, in underdeveloped countries like Pakistan [57]. Similarly, electric heaters, clothes dryers are more frequently used in winters as compared to summers. In contrast, as a general trend of people, the clothe washers and water pumps are used more in summers due to frequent clothes changing and bathing in the hot season. But these do not require hot water as normal tap water is fair enough in good sunny days. Similarly, the dishwashers can use normal tap water in summers, whereas, they require heated water in winter to get rid of utensils greasiness. For rice cookers, consumers belonging to first three classes generally take meals thrice a day, unlike higher-class. In winters, due to smaller days, only lower-class takes thrice, as they wake up too early in the morning. Considering all these facts and the usage parameters given for all the four classes given in [12], Table 7.1 provides the typical usage parameters for CDs for winters and summers.

Classes of communities are analyzed both in winters and summers. The load profile of a small community, consisting of 40 houses is considered. An equal number of houses are considered from each class of consumers for winters and summers. For summers, the peak load is 35.94 kW and for winters there is a peak of 33.89 kW.

Table 7- 1 Typical usage parameters for CDs in summers and winters

	Controllable Devices	Operation hours Summers (scattered between)	Operation hours Winters (scattered between
Lower-class	Air Conditioner	1 to 4, 21 to 24	4 to 6
	Electric Heater	NA NA	5 to 8, 19 to 21
	Clothe Washer	1 to 8, 15 to 20	1 to 11
İ	Clothes Dryer	NA	7 to 12
	Dishwasher	1 to 13, 18 to 24	9 to 15, 16 to 24
	Water pump	1 to 8, 13 to 15, 20 to 24	1 to 7, 17 to 24
İ	Electric Kettle	4 to 6, 10 to 12, 17 to 19	5 to 9, 11 to 1, 18 to 20
İ	Rice Cooker	1 to 6, 9 to 11, 16 to 18	1 to 8, 10 to 12, 15 to 18
Middle-class	Air Conditioner	1 to 6, 20 to 24	5 to 7
	Electric Heater	NA	6 to 8, 15 to 22
	Clothe Washer	1 to 9, 17 to 21	1 to 12
	Clothes Dryer	7 to 15, 20 to 24	8 to 15
	Dishwasher	9 to 12, 15 to 18, 19 to 24	9 to 15, 16 to 1
	Water pump	9 to 10, 21 to 23	8 to 11, 20 to 22
	Electric Kettle	6 to 10, 13 to 15, 18 to 20	6 to 10, 18 to 21
	Rice Cooker	1 to 10, 12 to 14, 16 to 19	1 to 12, 16 to 19
Upper-middie-class	Air Conditioner	1 to 8, 19 to 24	5 to 9
	Electric Heater	15 to 20	7 to 9, 15 to 23
•	Clothe Washer	1 to 10, 17 to 22	I to 13
	Clothes Dryer	11 to 18, 11 to 12	9 to 17
Ì	Dishwasher	9 to 12, 12 to 17, 19 to 24	9 to 15, 19 to 23
1	Water pump	1 to 11, 20 to 24	1 to 12, 20 to 24
	Electric Kettle	8 to 13, 13 to 16, 19 to 21	8 to 13, 18 to 22
	Rice Cooker	1 to 11, 12 to 15, 18 to 23	1 to 13, 17 to 22
Higher-class	Air Conditioner	1 to 24	1 to 24
	Electric Heater	15 to 24	15 to 24
ŀ	Clothe Washer	1 to 24	1 to 15
ļ	Clothes Dryer	1 to 24	9 to 21
}	Dishwasher	10 to 3, 7 to 24	10 to 2, 5 to 24
	Water pump	1 to 24	1 to 24
	Electric Kettle	11 to 14, 18 to 24	10 to 13, 18 to 24
	Rice Cooker	1 to 12, 18 to 24	1 to 14, 18 to 23

7.1.2. Distributed Energy Resources (DERs)

Solar power generation for different classes and communities is explored as follows.

Solar irradiance values have been taken from ESMAP Tier1 Meteorological Station in Islamabad, Pakistan. A rooftop Trina solar panel (SP), TALLMAX TSM-320 PD14 Module, panel size of 1.9 * 0.9 m² generates a maximum of 320 Watts power is considered. The maximum efficiency of the module is taken as 17.5%.

For Islamabad, 1kW SP generates 4 units in a day that means 250W generates 1 unit of energy. For example, if SP deployment size is calculated for producing 200 units; a 50 kW system would produce 200 units. Number of SPs can be calculated by dividing the required power with the power produced by one SP plate. SP area can by calculated by multiplying the number of SP plates by the area of a single plate, i.e.,

No of SPs =
$$\frac{Total\ Power\ Required}{Power\ prodcued\ by\ one\ SP} = \frac{50kW}{320W} \cong 157$$

Total area = No. of SPs × Area of single SP

Total area = $157 \times 1.9 \times .9 = 267.18m^2$

SP Output (Watts) = efficiency × area × Solar Irradiance
SP Output (Watts) = $0.175 * 267.18 * 640$
 $P(Watts) = 29.92\ kW$

This is how PV power is calculated for each class of consumers. As per surveys in Pakistan, generally, the lower class consumes low power throughout the month consumes about 150 units/month. Middle-class without AC consumes 250 units/month. Upper-middle-class with a 1-

ton AC consumes 500 units/month and higher-class with 2 tons AC consumes 750 units/month [77]. Considering this fact and the general trends of mixed communities, units are calculated for each class of the community. 250 units/month are assumed for lower class, 400 units/month for middle-class, 800 units/month for upper-middle and 1250 units/month for higher-class.

Each community has its own locally generated PV in various houses. It is assumed that lower class has 2% of PV installation. Middle-class has 4%, upper-middle-class has 6% and higher-class has 8% of PV installation.

An installed PV of 15 kW is considered where, the values corresponding to each class are 300W, 1.3kW, 1.5kW, and 3.2 kW, respectively.

For the purpose of peak shaving, a 220 V, 600 Ah BES is chosen for the study.

7.2. Stage 1- Dynamic HEMs Based Control Scheme

The proposed DCHEMS algorithm presented in chapter 4 is used in stage 1 optimization. All the device usage patterns and clustering parameters are the same. Therefore, the content is not discussed again in this section. The load demand profiles for summers and winters are processed through DCHEMS algorithm. PAR is reduced by the application of DCHEMS. The peak reduction of load profiles processed by stage 1 is shown in Fig. 7-2. The actual load demand based on user preferences and the peak reduced load profiles are illustrated as graphs. It can be seen that the peak is reduced from 33.8917 kW to 30.4417 kW in winters, and from this 35.9417 kW to 30.1500 kW in the summer load profile as shown in Fig. 7-2 (a) and 7-2 (b), respectively. The improvement in peak reduction leads to PPS increase. Since the time difference among the peaks is increased, resultantly, BES gets sufficient time to recharge itself before the next peak arises. Once the load

scheduling and optimal time slot assignment to all the CDs are done, the resultant optimized load demand is passed on to stage 2.

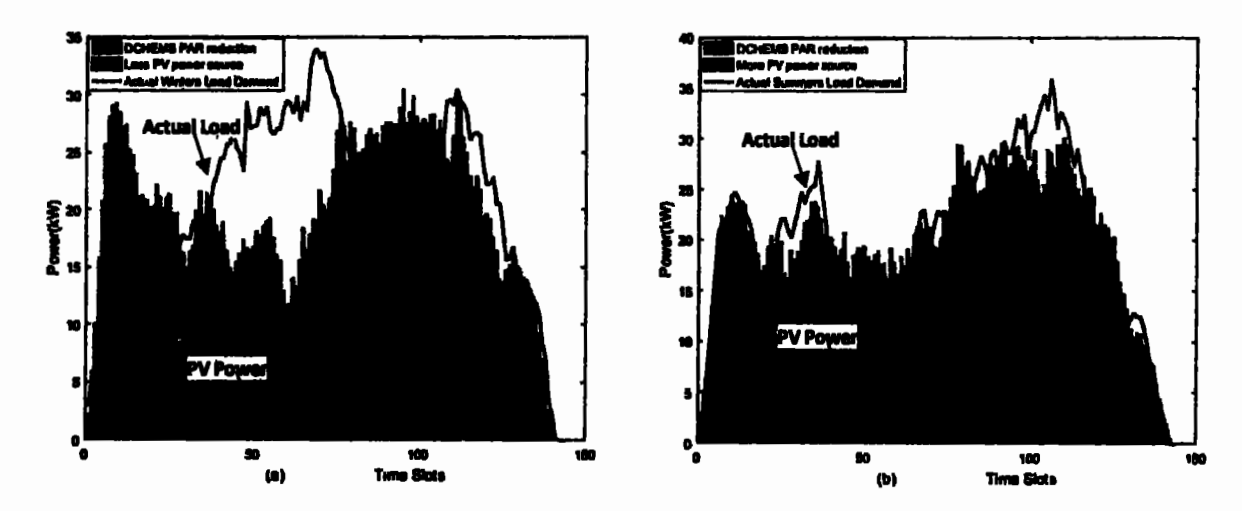


Fig. 7- 2 Dynamic-HEMS based peak reduction of load demand for a) Winters Day condition with less PV b) Summers Day condition with more PV

7.3. Stage 2 - Optimal Peak Shaving Control Scheme

The output of stage 1 after the peak reduction of the summer and winter load profiles is taken as input to the second stage of optimal peak shaving control scheme. The overall block diagram of stage 1 and stage 2 is shown in Fig. 7-4. The optimal peak shaving control scheme is discussed in detail in chapter 6, therefore, only the additions/changes are discussed here. One additional mode with two set of rules is also incorporated to the previous regime, so that further better utilization of available resources can be performed. It is termed as charging mode 3 and it is the time when the load demand is within the range of the demand limit and there is no availability of PV source i.e., $P_L(t) < P_{dl} & P_{pv}(t) = 0$. The additional mode denoted as CM3 is reflected in Fig.7-3.

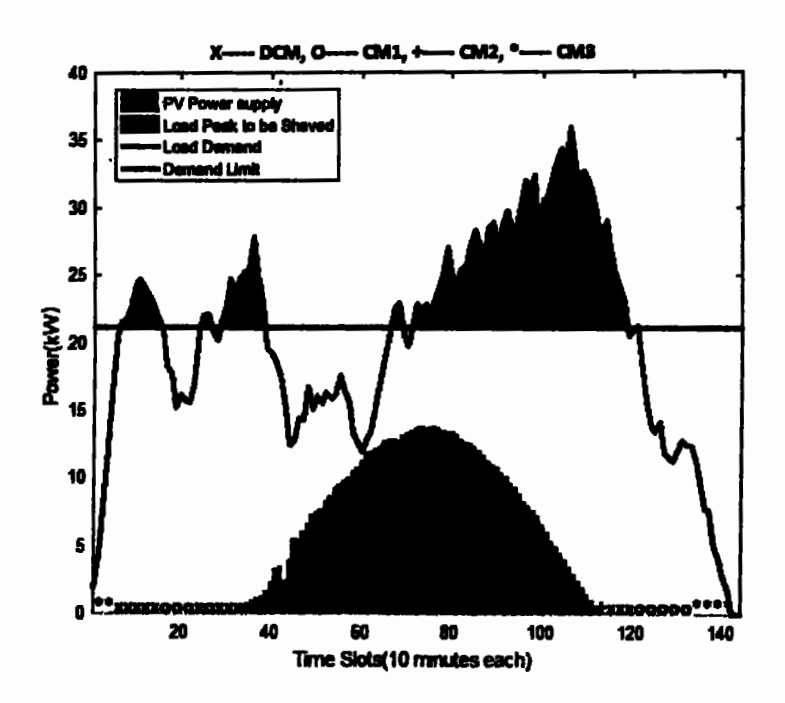


Fig. 7-3 Operating TSs of modes of BES: t_{dls-c} when $P_L(t) > P_{dl}$ && $P_{pv}(t) \le P_L(t) - P_{dl}$; t_{c1} when $P_L(t) \le P_{dl}$; t_{c2} when $P_L(t) > P_{dl}$ && $P_{pv}(t) > P_L(t) - P_{dl}$ and t_{c3} when $P_L(t) < P_{dl}$ && $P_{pv}(t) = 0$

Charging mode 3 consists of two rules, termed as rule 9 and rule 10, discussed as follows

1. Charging mode 3 (CHM3)

Rule 9: If 1 < TS < 10 and a considerable peak in load arises before the PV power appears, i.e., $P_L(t) > P_{dl}$. Then the BES takes charge from the utility grid with the amount $C_g(P_{dl} - P_L(t))$. This enables BES to cater the arising peak before the PV power appears.

Rule 10: If TS > 130 && $SoC(t) \le SoC_f$ BES takes charge from the utility grid with the amount $C_g(P_{dl} - P_L(t))$ so that $SoC_f = SoC_l$ for flexible day to day management.

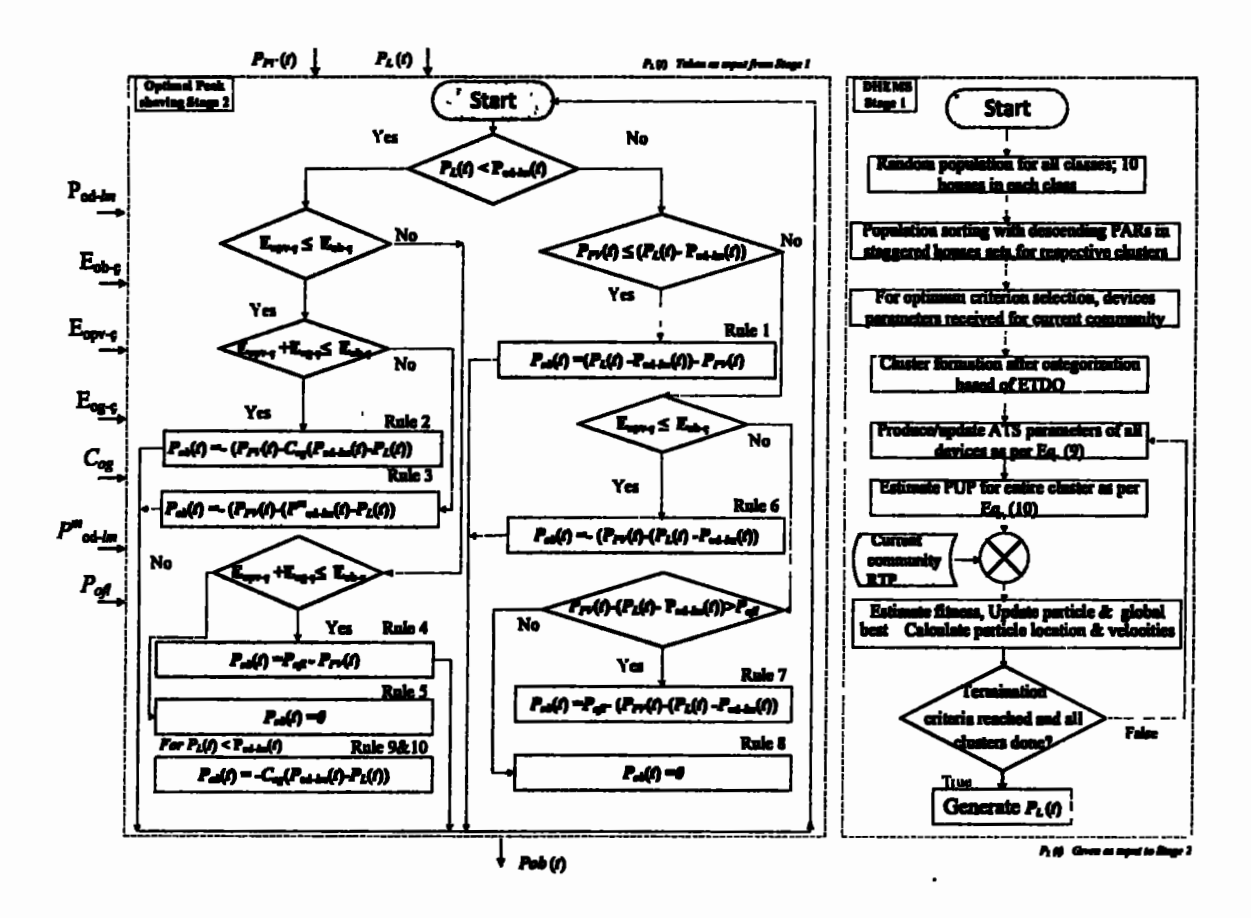


Fig. 7- 4 Proposed two stage HEMS optimal peak shaving control flow diagram

7.4. Simulation Results

This chapter proposes a dynamic HEMS-based optimal peak shaving control strategy. A small community consisting of 40 houses, with 10 houses in each class is considered. To demonstrate the application of the proposed technique for any grid-connected PV system using BES, the technique has been tested on the studied system for various PV power load profiles. Four cases are presented with a combination of more and less PV for both winter and summers load profiles. For less PV, the percentage of penetration is further reduced with none considered from the lower and middle class. The PV penetration percentages for upper-middle and higher classes are also reduced to 3% each. Various modes and rules can be observed in different cases. The

proposed HEMS pre-processing stage improves on PPS which is presented separately for each case.

The qualitative and quantitative assessment in comparison to a reference scheme is also presented in tabular form.

Table 7- 2 Optimal inputs of management algorithm with application to four cases [57]

Input Parameter	Case 1 Dynamic- HEMS	Case1 Without- HEMS	Case 2 Dynamic- HEMS	Case 2 Without- HEMS	Case 3 Dynamic- HEMS	Case 3 Without- HEMS	Case 4 Dynamic- HEMS	Case 4 Without- HEMS
P _{od-lm} (kW)	19.9321	22.6328	23.5445	24.5415	20.3317	25.0750	23.7314	26.5314
E _{ob-ç} (kWh)	156.3791	56.3359	127.4254	122.5867	127.0357	58.9488	107.5714	100.1374
E _{opv−ç} (kWh)	87.8121	59.2679	48.5651	49.1151	94.6973	59.0110	37.7882	35.2805
$E_{og-\varsigma}$ (kWh)	60.5756	NA	86.9795	76.4579	37.4251	NA	75.7643	101.2372
Cog	0.4	NA	0.1602	0.1102	0.3	NA	0.1269	0.1789
P_{od-lm}^{m} (kW)	NA	NA	NA	NA	NA	NA	NA	NA
P _{ofl} (kW)	2.2432	2.2614	NA	NA	2.4009	2.3919	NA	NA

The ideal inputs necessary for performing the control algorithm for these cases are in the second stage and are listed in Table 7.2. The best fitness value is acquired for multiple runs of the PSO algorithm for the case of winter load profile with more PV availability. The minimum value among these best fitness values (considering all runs), i.e., 19.33 kWh, is the optimal peak energy drawn from the utility grid. For these cases, the acquired results using the proposed technique are discussed as follows.

For these cases, the acquired results using the proposed technique are discussed as follows.

Case 1: Dynamic-HEMS Scheme; Load Profile for Winter with High Availability of PV Energy

In this scenario, the load demand profile for winter that has a higher availability of PV energy during a day is taken into account, as shown in Fig. 7-5 (a). The estimations corresponding to P_{od-lm} , E_{ob-c} , E_{opv-c} , E_{og-c} , C_{og} and P_{ofl} are 19.9321 kW, 156.3791 kWh, 87.8121 kWh, 60.5756 kWh, 0.4 and, 2.2432, respectively. The PV energy available to charge the BES exceeds the energy required for charging the BES ($E_{pv-c} > E_{b-c}$).

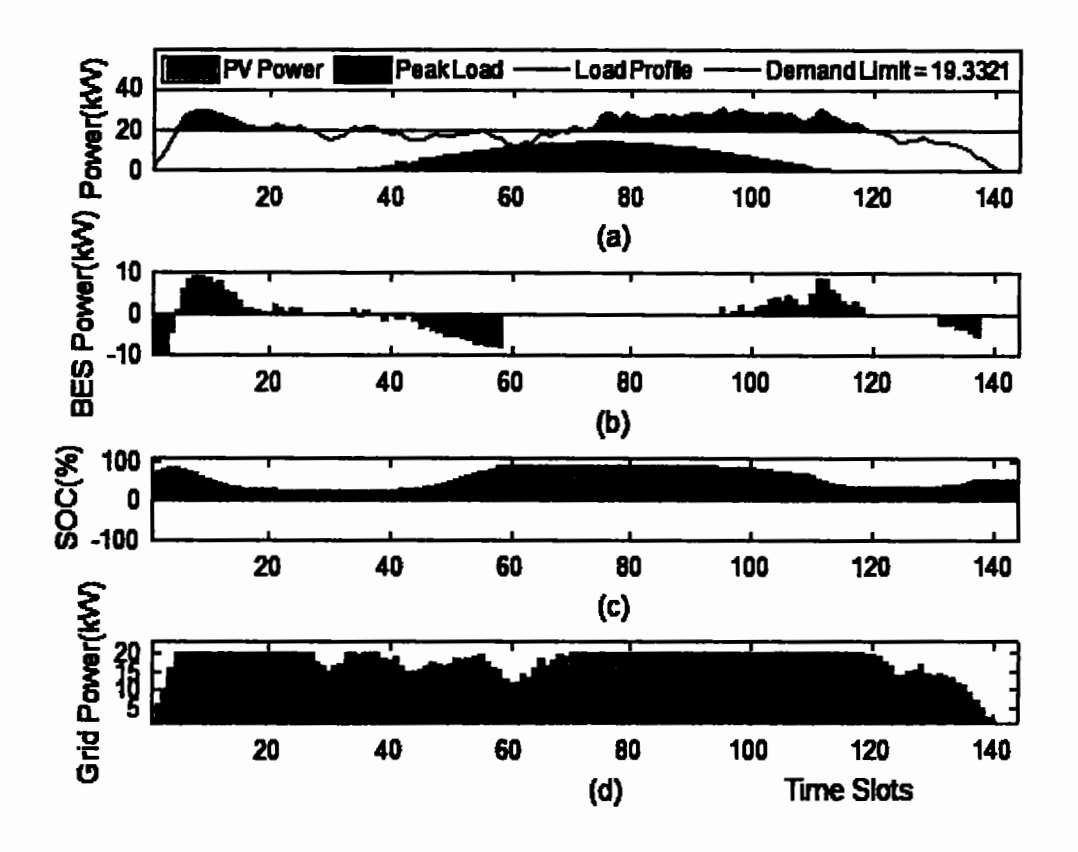


Fig. 7- 5 Dynamic-HEMS Case-1. (a) Profiles for PV power supply and load consumption. (b) Schedules of BES charge/discharge. (c) BES state of charge. (d) Utility grid power

Therefore, $E_{og-\varsigma}$, C_{og} , and P_{od-lm}^m are not applicable (NA) in this case. But the grid power is only used at the beginning for charging BES with off-peak power to handle any arising peak

before PV appears. Also, at the end of the day, the grid power is used to restore BES SoC to 50% for day-to-day management. Hence, the values of E_{og-c} , C_{og} are also shown in Table 7.2. As per Fig. 7-5 for the determined P_{od-lm} , the DCM is during t = 5-25, 34, 36 and 95-118 TS where there is peak and PV is not sufficient to support, CM1 is during t = 39, 41-58 TS. There is no CM2 since BES has sufficient charge during the TSs of high PV. CM3 is during t = 1-5 and t = 131-140 TS. The grid charges BES with off-peak power during t = 1-4 and 131-138 TS. The resultant BES optimal charging/discharging schedules for these modes are illustrated in Fig. 7-5(b). The SoC for BES scheduling is depicted in Fig. 7-5(c). Fig. 7-5 (c) illustrates that $SoC_i = SoC_f = 50\%$, which is desirable to ensure flexibility in day-to-day management. Fig. 7-5(d) reflects the utility grid demand. The illustration suggests that the utility grid demand is capped for $P_{od-lm} = 19.9321$ kW. The feed-in power is restricted to 2.2432 kW.

Case 2: Dynamic-HEMS Scheme; Load Profile for Winter with Low Availability of PV Energy

In this situation, as shown in Fig. 7-6 (a), the load demand profile for winter is considered wherein the availability of PV energy across a day is less. The estimated values corresponding to P_{od-lm} , E_{ob-c} , E_{opv-c} , E_{og-c} , and C_{og} are 23.5445 kW, 127.4254 kWh, 48.5651 kWh, 86.9795 kWh, and 0.1602. The amount of available PV energy for charging the BES is less than the amount of energy needed to charge the BES. Furthermore, the total energy available from PV and the utility grid exceeds the energy needed to charge the BES i.e., $(E_{pv-c} \le E_{b-c}, \&\&E_{g-c} + E_{pv-c} > E_{b-c})$. As a result, the E_{og-c} , C_{og} , and P_{od-lm}^m are not applicable (NA) in the studied scenario, as shown in Table 7.2. According to Fig. 7-6 for the estimated E_{ob-c} , the DCM occurs during t = 6-14, 76-77,79, 80, 84-87,89-114 TS, and CM1 is during t = 16-65, 116, 118-139 TS. CM2 is during t = 78,

81-83 and 88 TS. The battery's optimal charge/discharge schedules for the different modes are depicted in Fig. 7-6 (b). Fig. 7-6 (c) depicts the SoC for the generated BES schedules. Fig. 7-6 (c) illustrates that $soC_i = soC_f = 50\%$, which is appropriate to ensure flexibility in the day-to-day management. Fig. 7-6 (d) depicts the resultant electrical grid demand. According to the illustration, the utility grid demand is capped by P_{od-lm} at 23.5445 kW as indicated in Fig. 7-6 (d). And feedin power is not available.

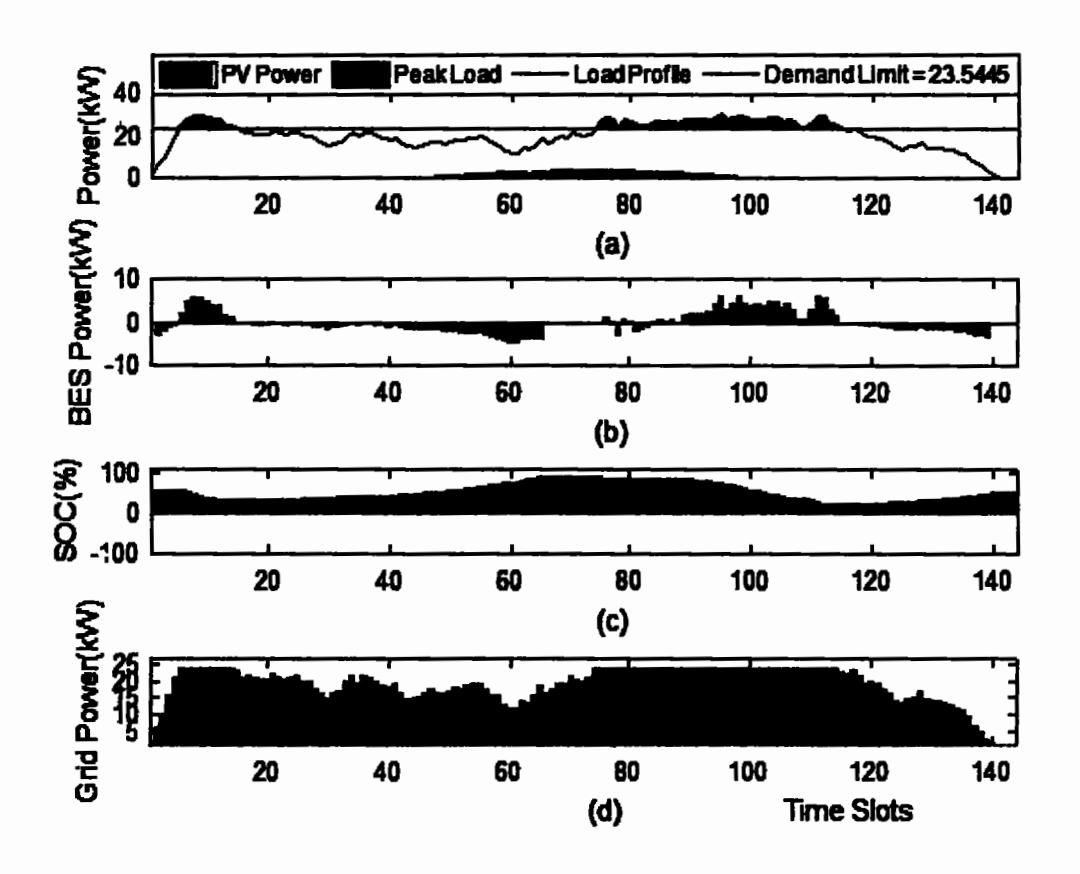


Fig. 7- 6 Dynamic-HEMS Case-2. (a) Profiles for PV power supply and load consumption. (b) Schedules of BES charge/discharge. (c) BES state of charge. (d) Utility grid power

Case 3: Dynamic-HEMS Scheme; Load Profile for Summer with High Availability of PV Energy

In this situation, as shown in Fig. 7-7 (a), the load demand profile for summer is considered wherein the availability of PV energy across a day is higher.

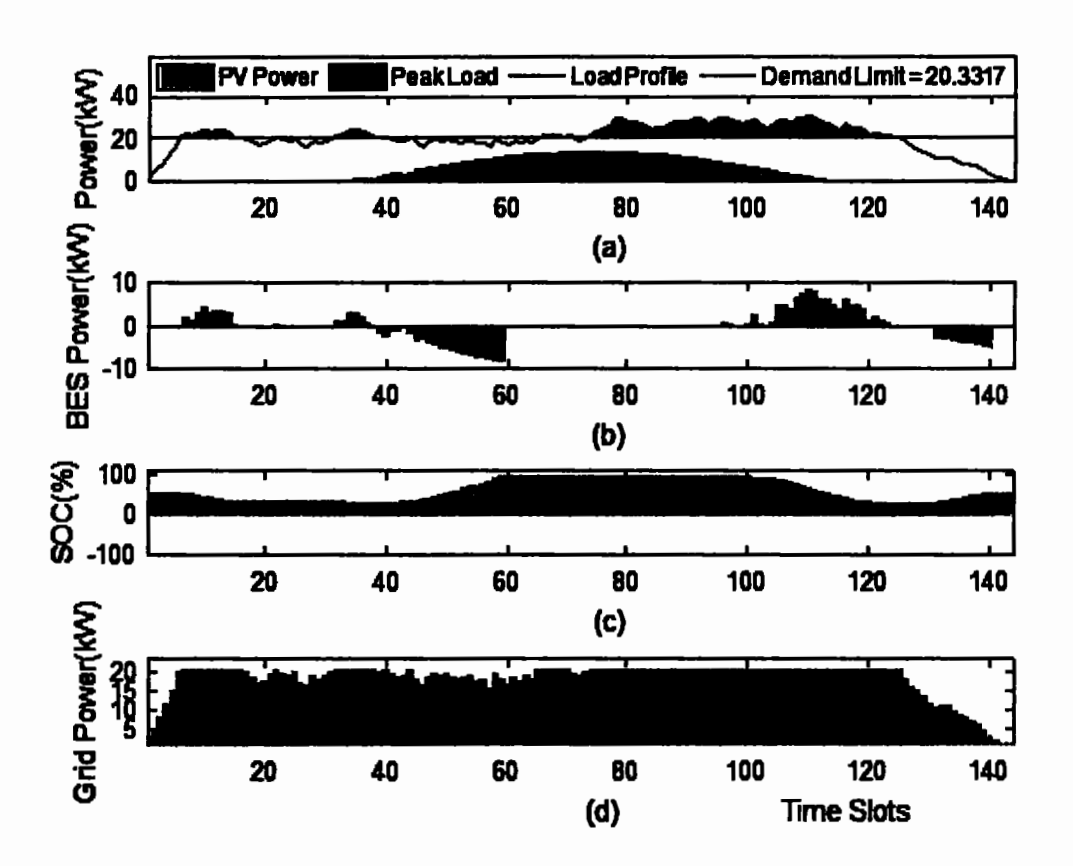


Fig. 7-7 Dynamic-HEMS Case-3. (a) Profiles for PV power supply and load consumption. (b) Schedules of BES charge/discharge. (c) BES state of charge. (d) Utility grid power
The estimated values corresponding to Pod-lm, Eob-c, Eopv-c, Eog-c, Cog and Pofl are 20.3317
kW, 127.0357 kWh, 94.6973 kWh, 37.4251 kWh, 0.3 and 2.4009. The PV energy available to charge the BES exceeds the energy required for charging the BES (Epv-c> Eb-c). Therefore, Eog-c,
Cog, and Pod-lm are not applicable (NA) in this case. But the grid power is only used in the beginning for charging BES with off-peak power to handle any arising peak before PV appears.

Also, at the end of the day, the grid power is used to restore BES SoC to 50% for daily management. Hence, $E_{og-\varsigma}$ ang C_{og} are also shown in Table 7.2. According to Fig. 7-7 for the estimated P_{od-lm} , the DCM occurs during t = 7-15, 32-37, 96, 100-102,104-124 TS where there is peak and PV is not sufficient to support, CM1 is during t = 39-42 and 44-59 TS. There is no CM2 since BES has sufficient charge during the TSs of high PV. CM3 is during t = 131-140. The battery's optimal charge/discharge schedules for the different modes are depicted in Fig. 7-7 (b). Fig. 7-7 (c) depicts the SoC for the generated battery schedules. Fig. 7-7 (c) illustrates that $SoC_i = SoC_f = 50\%$, which is appropriate to ensure flexibility in the day-to-day management. Fig. 7-7 (d) depicts the resultant electrical grid demand. According to the illustration, the utility grid demand is capped by P_{od-lm} at 20.3317 kW as indicated in Fig. 7-7(d). Also, the feed-in power is restricted to P_{ofl} at 2.4009 kW.

Case 4: Dynamic-HEMS Scheme; Load Profile for Summer with Low Availability of PV Energy

In this situation, the load demand profile for summers with decreased availability of PV energy is taken into account, as shown in Fig. 7-8(a). The values are 23.7314 kWh, 107.5714 kWh, 37.7882 kWh, 75.7643 kWh corresponding to P_{od-lm} , E_{ob-c} , E_{opv-c} , E_{og-c} , and C_{og} are and 0.1269, respectively. The amount of PV energy available to charge the battery is less than the amount of energy necessary to charge the battery. Furthermore, the total energy available from PV and the utility grid exceeds the energy required to charge the battery $(E_{pv-c} \le E_{b-c}, \&\&E_{g-c} + E_{pv-c} > E_{b-c})$. As a result, as shown in Table 7.2, P_{od-lm}^m and P_{oft} are not relevant in this scenario. According to Fig. 7-8 for the estimated P_{od-lm} , the DCM occurs during t = 10, 78-81, 87-119 TS, and CM1 is during t = 2-8, 10, 15-34, 37-62, 82-85, 99, 120-144. TS. The battery's ideal

charge/discharge schedules for various modes are presented in Fig. 7-8 (b). Fig. 7-8 depicts the SoC for such battery schedules (c). Fig. 7-8 (c) illustrates that $SoC_l = SoC_f = 50\%$, that is desirable for day-to-day management flexibility. Fig. 7-8 depicts the resulting electric grid demand (d). This means that the utility grid demand is confined to P_{od-lm} or 23.7314 kW. The feed-in power is not available.

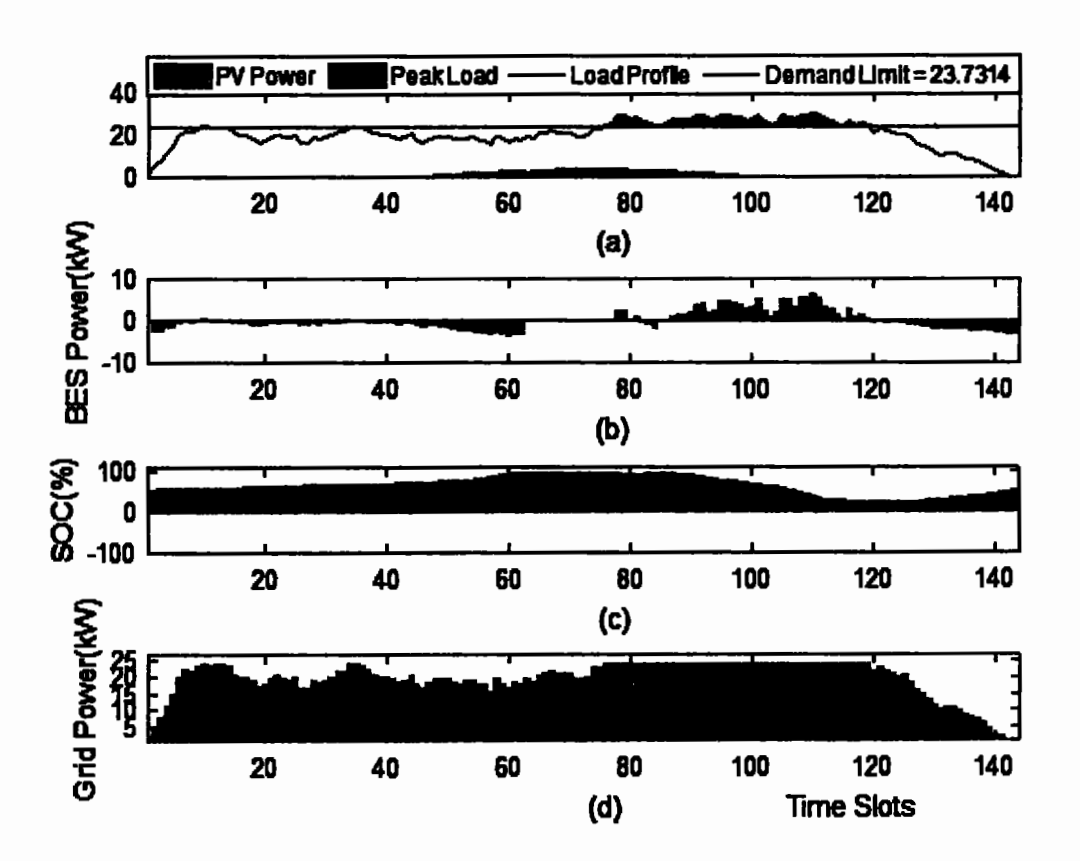


Fig. 7-8 Dynamic-HEMS Case-4. (a) Profiles for PV power supply and load consumption. (b) Schedules of BES charge/discharge. (c) BES state of charge. (d) Utility grid power

The results for the non-dynamic HEMS for all four cases is presented as follows

Case 1: Non-Dynamic-HEMS Scheme; Load Profile for Winter with High Availability of PV Energy

In this scenario, the load demand profile for winter that has a higher availability of PV power during a day is taken into account as illustrated in Fig. 7-9(a). The estimations corresponding to P_{od-lm} , E_{ob-c} , E_{opv-c} , and P_{ofl} are 22.6328 kW, 56.3359 kWh, 59.2679 kWh, 2.2614 kW. The amount of available PV energy for charging the BES exceeds the energy required for charging the BES ($E_{opv-c} > E_{ob-c}$). Therefore, the E_{og-c} , C_{og} , and P_{od-lm}^m are not applicable (NA) for this case, as mentioned in Table 7.2.

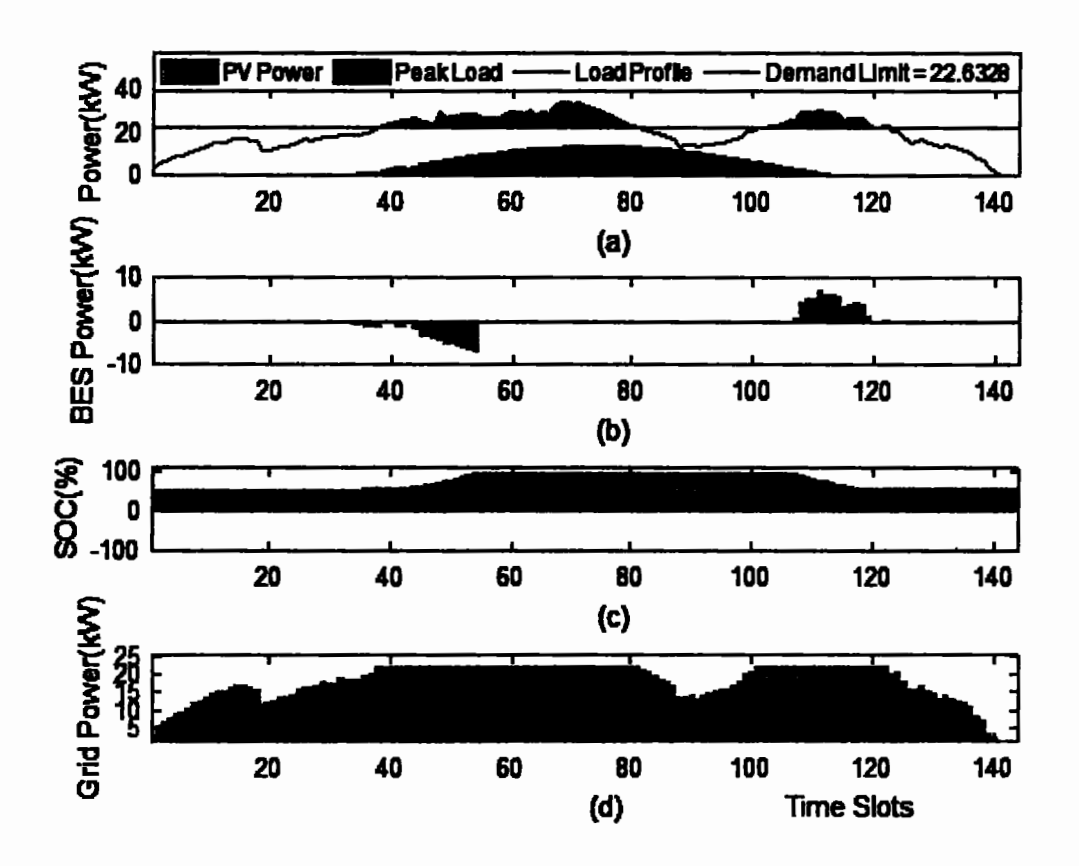


Fig. 7- 9 Without-HEMS Case-1. (a) Profiles for PV power supply and load consumption. (b) Schedules of BES charge/discharge. (c) BES state of charge. (d) Utility grid power

According to Fig. 7-9 for the estimated P_{od-lm} , the DCM is during t = 107-119 and 122 TS, CM1 occurs during t = 31-38 and 41-54 TS. Fig. 7-9 (b) shows the BES's optimal charge/discharge schedules for the different modes. Fig. 7-9 (c) depicts the SoC for the resulting BES schedules. Fig. 7-9 (c) illustrates that $SoC_l = SoC_f = 50\%$, which is desirable to ensure flexibility in day-to-day management. Fig. 7-9 (d) depicts the corresponding utility grid demand. The illustration suggests that the utility grid demand is capped for $P_{od-lm} = 22.6328$ kW. The feed-in power is restricted to 2.2614 kW.

Case 2: Non-Dynamic-HEMS Scheme; Load Profile for Winter with Low Availability of PV Energy

This situation, as shown in Fig. 7-10(a), considers the load demand profile for winter which has a low availability of PV energy through the duration of a day. The values corresponding to P_{od-lm} , E_{ob-c} , E_{opv-c} , E_{og-c} , and C_{og} are 24.5415 kW, 122.5867 kWh, 49.1151 kWh, 76.4579 kWh and 0.1102. The amount of available PV energy available for charging the BES is less than the amount of energy needed to charge the BES. Furthermore, the total energy available from PV and the utility grid exceeds the energy needed to charge the BES ($E_{pv-c} \le E_{b-c}$, && $E_{g-c} + E_{pv-c} > E_{b-c}$). As a result, in this scenario, P_{od-lm}^m and P_{ofl} are not applicable (NA), as shown in Table 7.2. According to Fig. 7-10 for the estimated E_{ob-c} , the DCM occurs during t = 42.46, 57-76, 106-118 TS, and CM1 is during t = 2.39, 47, 77-105, 120-138 TS. There is no CM2 in this case. The battery's optimal charge/discharge schedules for the mentioned modes are depicted in Fig. 7-10 (b). The battery appears to be charged by both the utility grid and PV source. Fig. 7-10 (c) depicts the SoC for the estimated battery schedules. Fig. 7-10 (c) illustrates that $SoC_l = SoC_f = 50\%$, which is appropriate for flexibility in daily management. This means that the utility grid demand is limited

to P_{od-lm} =24.5415 kW as indicated in Fig. 7-10 (d) and the feed-in power is not available for the grid.

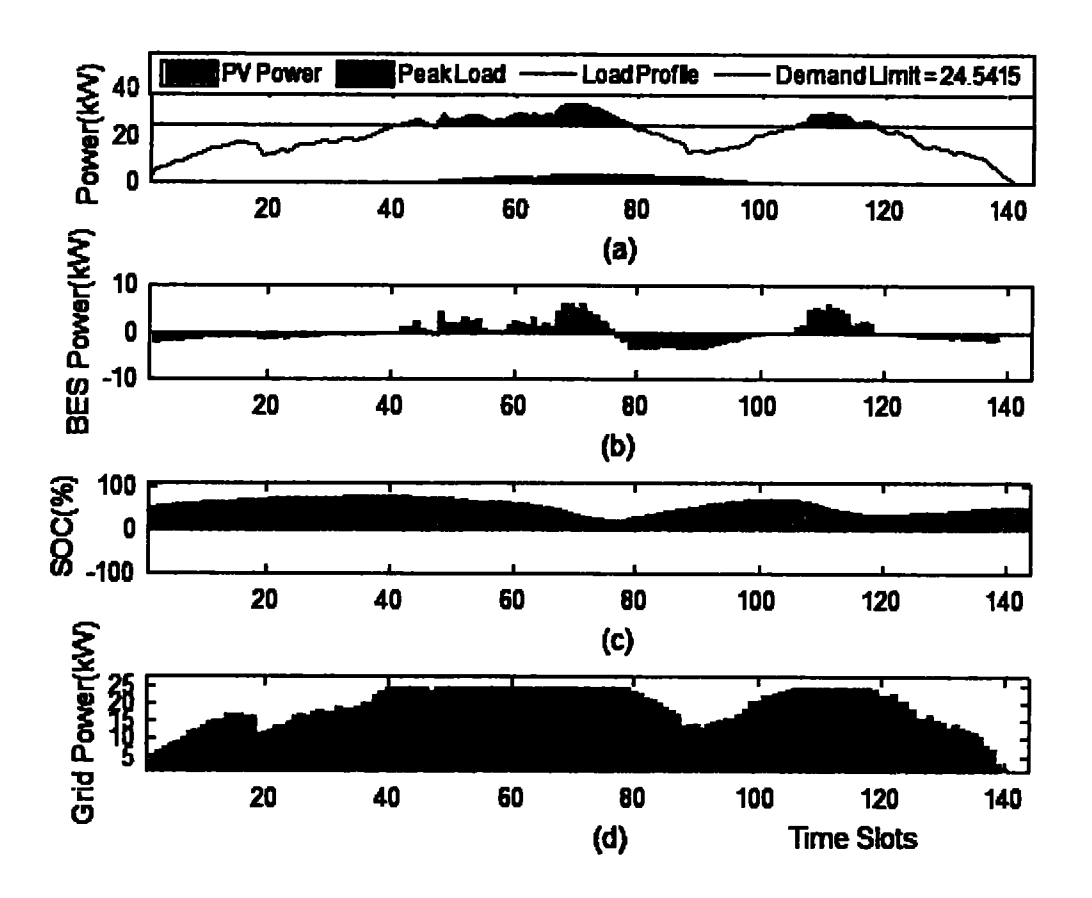


Fig. 7- 10 Without-HEMS Case-2. (a) Profiles for PV power supply and load consumption. (b) Schedules of BES charge/discharge. (c) BES state of charge. (d) Utility grid power

Case 3: Non-Dynamic-HEMS Scheme; Load Profile for Summer with High Availability of PV Energy

In this situation, as shown in Fig. 7-11 (a), the load demand profile for Summer is considered wherein the availability of PV energy across a day is higher. The estimated values corresponding to P_{od-lm} , E_{ob-c} , E_{opv-c} , E_{og-c} , and P_{ofl} are 25.0750 kW, 58.9488 kWh, 59.0110 kWh, 37.4251 kWh, and 2.3919, respectively. The PV energy available to charge the BES exceeds

the energy required for charging the BES $(E_{opv-\varsigma} > E_{ob-\varsigma})$. Therefore, $E_{og-\varsigma}$, C_{og} , and P_{od-lm}^m are not applicable (NA) in this case. But the grid power is only used in the beginning for charging BES with off peak power to handle any arising peak before PV appears. Also, at the end of the day, the grid power is used to restore BES SoC to 50% for daily management. As a result, the $E_{og-\varsigma}$, C_{og} , and P_{od-lm}^m are not applicable (NA) in the studied scenario, as shown in Table 7.2. As shown in Fig. 7-11, for the estimated P_{od-lm} , the DCM occurs during t = 10-13, 10-37, 96, 98,100-117 TS where there is peak and PV is not sufficient to support, CM1 is during t = 38-42 and 44-56 TS. There is no mode 2 charging since BES has sufficient charge during the TSs of high PV.

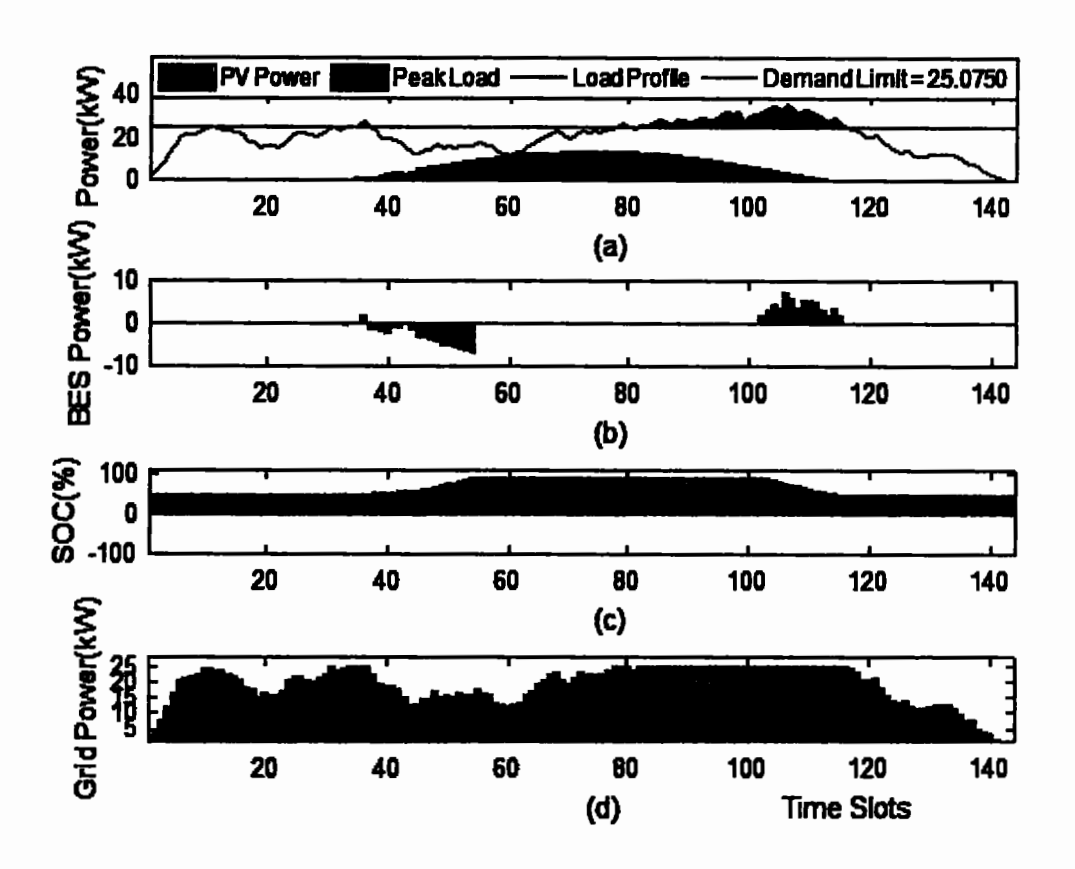


Fig. 7- 11 Without-HEMS Case-3. (a) Profiles for PV power supply and load consumption. (b) Schedules of BES charge/discharge. (c) BES state of charge. (d) Utility grid power

The grid charges BES with off-peak power during t=131-139. The battery's optimal charge/discharge schedules for the different modes are depicted in Fig. 7-11 (b). SoC for the generated battery schedules is depicted in Fig. 7-11 (c). Fig. 7-11 (c) illustrates that $SoC_l = SoC_f = 50\%$, which is appropriate to ensure flexibility in the day-to-day management. Fig. 7-11 (d) depicts the resultant electrical grid demand. According to the illustration, the utility grid demand is capped by $P_{od-lm} = 25.0750$ kW. Also, the feed-in power is restricted to P_{ofl} at 2.3919 kW.

Case 4: Non-Dynamic-HEMS Scheme; Load Profile for Summer with Low Availability of PV Energy

In this situation, the load demand profile for summers with decreased availability of PV energy is considered, as illustrated in Fig. 7-12(a). The values are 26.5314 kWh, 100.1374 kWh, 35.2805 kWh, 101.2372 kWh and 0.1789 corresponding to P_{od-lm} , E_{ob-c} , E_{opv-c} , E_{og-c} , and C_{og} respectively. The amount of available PV energy for charging the battery is less than the amount of energy necessary to charge the battery. Furthermore, the total energy available from PV and the utility grid exceeds the energy required to charge the battery ($E_{pv-c} \le E_{b-c}$, && $E_{g-c} + E_{pv-c} > E_{b-c}$). As a result, as shown in Table 7.2, P_{od-lm}^m and P_{ofl} are not relevant in this scenario. According to Fig. 7-12 for the estimated P_{od-lm} , the DCM occurs during t = 36, 91-115 TS, and CM1 occurs during t = 2-35, 37-48 TS. DCM occurs during t = 90 only due to less PV. The battery's ideal charge/discharge schedules for various modes are presented in Fig. 7-12. (b). SoC for the battery schedules are depicted in Fig. 7-12 (c). Fig. 7-12(c) illustrates that $SoC_l = SoC_f = 50\%$, that is desirable for day-to-day management flexibility. Fig. 7-12 depicts the resulting electric grid demand (d). This means that the utility grid demand is confined to $P_{od-lm} = 26.5314$ kW as indicated in Fig. 7-12(d). And the feed-in power is not available.

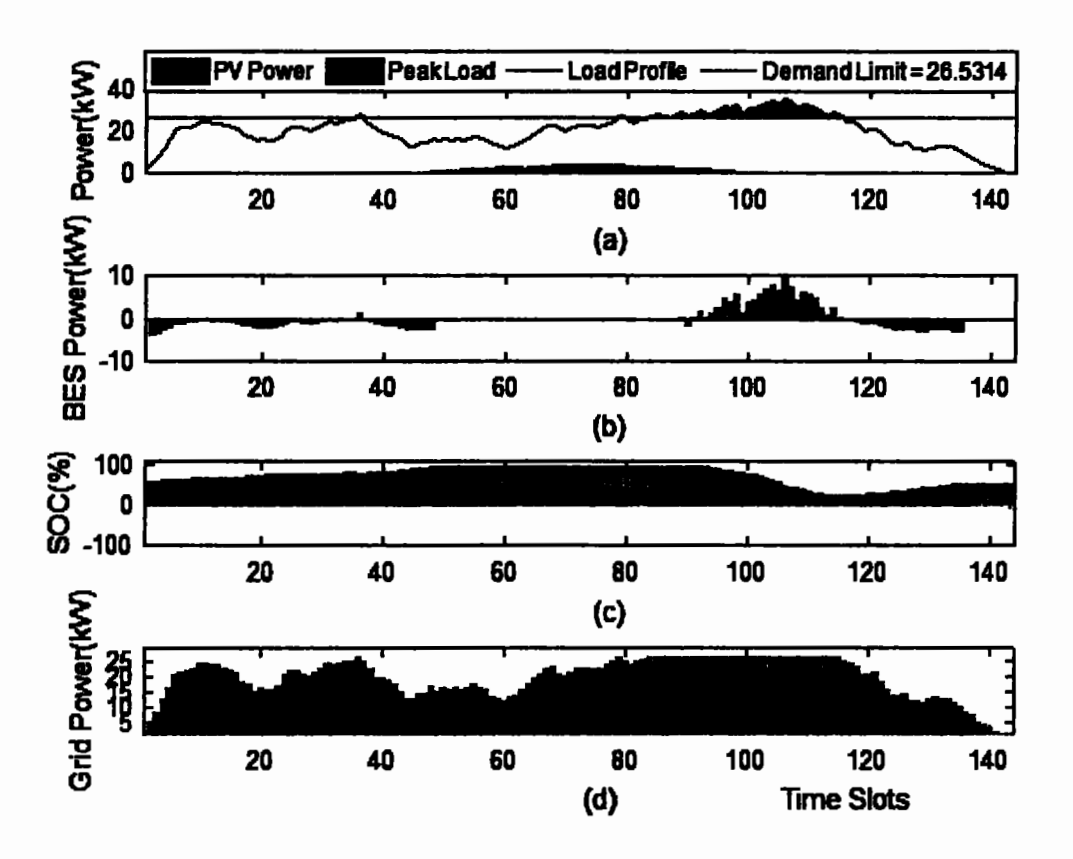


Fig. 7- 12 Without-HEMS Case-4. (a) Profiles for PV power supply and load consumption. (b)

Schedules of BES charge/discharge. (c) BES state of charge. (d) Utility grid power

A discussion of the comparative analysis for the proposed scheme is presented as follows.

7.4.1. Quantitative Comparison

As the dynamic clustered community-based idea in home energy management system is novel, the system as well as the ratings chosen in the suggested literature are not directly comparable to any existing system. But as the study is inspired by the system chosen in [57] by Rampelli et. al., the proposed system is compared quantitatively to it. Table 7-3 shows the quantitative comparison between PUGP and PPS. The method suggested by Rampelli et. al [57] is applied to the MG

community structure to see the comparison with our proposed method. Table 7.3 depicts the improvements in each case, where the non-dynamic method's PUGP is limited to 26.5314 kW, 22.6328 kW, 24.5415 kW, and 25.0750 kW for cases 1-4, respectively. For Cases 1-4, PUGP is restricted to 19.9321 kW, 23.5445 kW, 20.3317 kW, and 23.7314 kW, respectively, in the suggested method. This means that the proposed approach has a lower peak utility grid consumption than [57] in all cases. The improvement in PPS of proposed method is because of the incorporation of DHEMS based stage 1 that leads to reduction of load profile PAR, initially. Moreover, the modification of additional CHM3 in the proposed scheme also utilizes available distributed energy resources effectively. Although, the reference case is not exactly comparable with our proposed strategy due to the consideration of different data sets. But we have performed the simulations to compare the results to see if there are any improvements. The majority of the cases e.g., Case 2, Case 3 and Case 4 shows an improvement of 6.65%, 14.76% and 5.27% in PPS as compared to reference approach. Case 1 shows an overall PPS of 43.55% which is good enough for a community bases HEMS. But it is 12.11% less than the reference technique. The reason for this lag is the timing of the peak load appearance. For the reference case study, the peak load appears in the PV available hours, therefore it is easier to directly shave off the peak with PV. Whereas, in the proposed scenario, the load peaks for all the cases are away from the PV availability time slots. The ratio of PV power taken for proposed method is also lesser as compared to the reference technique. This is because only a little percentage of PV penetration is considered as per the real scenario in Pakistan. Despite of the differences, the improvements in the proposed scheme validates its applicability for community-based MG networks. Higher percentage of PV and BES sizing can improve the scenario further.

Table 7-3 Quantitative Comparison of Suggested Technique with the Previous Work

	PUGP (kW)				PPS (%)			
Schemes	Case 1	Case 2	Case 3	Case 4	Case 1	Case 2	Case 3	Case 4
Reference	1.72	2.437	2.853	2.852	55.66	37.18	28.67	28.7
Without Dynamic- HEMS	22.6328	24.5415	25.0750	26.5314	33.29%	27.59%	30.23%	26.18%
With Dynamic-HEMS	19.1321	23.5445	20.3317	23.7714	43.55%	30.53%	43.43%	33.97%

7.4.2. Qualitative Comparison

Table 7.4 shows a qualitative comparison of the proposed method with previous work. The demand and feed-in restrictions, as well as the dynamic pre-processing step, are not taken into account in the available literature. However, the proposed solution takes into account both demand and feed-in constraints, as well as a dynamic clustering-based pre-processing HEMS scheme, while maintaining the system's flexibility on a day-to-day basis.

Table 7- 4 Qualitative comparison of suggested technique with the previous work

Parameter	References					
	[58-60]	[61]	[62]	[63]	[64]	
Dynamic Optimization	Not considered	Not considered	Not considered	Not considered	Not considered	Dynamic
Demand Limit	Fixed	Fixed	Not considered	Dynamic	Dynamic	Dynamic
Feed in limit	Not considered	Not considered	Dynamic	Not considered	Dynamic	Dynamic
Day-to-day management	Not considered	Flexible	Not considered	Not considered	Flexible	Flexible

Furthermore, demand and feed-in restrictions are assumed to be dynamic. It means that the demand and feed-in restrictions change depending on the PV power and load demand forecasts for the day.

7.5. Summary

This chapter suggests a dynamic clustered community-based HEMS. It also helps determine the optimized dynamic feed-in and demand limits for a community MG with integration of distributed energy sources such as PV source using a battery. The chapter presents an optimal rule-based peak shaving management method. The algorithm limits the utility grid power within the estimated feed-in and demand limitations. The suggested control algorithm is put to test for a variety of PV power and demand profile scenarios. The collected data show that the feed-in powers and utility grid demand are constrained to the day's feed-in and demand limitations in all scenarios. Furthermore, for flexible and daily management, the SoC at the end of the day is kept to be the same as the beginning of the day. The suggested control algorithm is compared to previous work both qualitatively and numerically. This suggests that the suggested control algorithm outperforms prior work in terms of percentage peak shaving.

Chapter 8

Conclusion and Future Directions

8.1. Summary of simulation results

This study presents a novel dynamic device clustering scheme in a community home energy management system for improved stability and resiliency of MGs. The study presents an arrangement of DR implementation that enables resource sharing in MGs. The proposed system designed a novel two-phase HEMS optimization strategy, which can be summarized as follows:

1. Phase 1: Load Scheduling

This phase dealt with the application of a dynamic clustered community home energy management system (DHEMS) scheme to the residential community. It focused on residential power scheduling targeting electricity cost reduction for consumers and load profile PAR curtailment for a relatively large consumer population with non-homogeneous loads. Demonstrated results validate the improvements in PAR and electricity cost for the proposed technique. The results have been compared with Aziz et. al. There is an improvement of 21% in PAR. The electricity cost is also improved by 4% with a supplementary benefit of smooth power consumption pattern. 19% improvement is achieved in variance to mean ratio.

2. Phase 2: Peak Shaving

The second phase proposed a dynamic rule-based peak shaving management method for the photovoltaic (PV) systems and battery energy storage (BES) systems that are connected to the grid. In this phase, the research has been extended to the incorporation of renewable energy

resources such as PV and BES systems. Dynamic HEMS based optimal peak shaving algorithm is implemented for effective utilization of available power to generate balance in demand and supply.

An improvement of nearly 15% is achieved for peak shaving in different cases.

The detailed description of the proposed strategy is presented in various chapters of the dissertation. Chapter 3 presents the concept of home area network in energy management systems. Chapter 4 presents the proposed dynamic clustered community home energy management system (DCHEMS).

Chapter 5 presents the idea of coordinated distributed energy resource management in an MG. The presented peak load shaving coordination scheme highlights the shortcomings of the management system. The requirement of dynamic feed-in and demand limits for utility grid power is emphasized with the help of simulation results. It is also concluded that for reliable and stable management of EMS, SoC of BES should be monitored and regulated for day-to-day management.

Chapter 6 presents an optimized rule-based demand peak shaving control algorithm using dynamic feed-in and demand limitations. The operating modes of BES along with a set of defined rules for each mode are presented. The method of estimation of optimal inputs for the rule-based demand peak shaving control is discussed in detail. Results of case studies are discussed in detail. The issue of using monotonous load profiles that limits testing of a few defined charging/discharging rules is highlighted.

Chapter 7 presents the proposed dynamic HEMS-based optimal peak shaving control in an MG system. Different load profiles for winters and summers are incorporated along with distinct user preferences entertained against the controllable devices. The significance of improvement of

percentage peak shaving by involving a pre-processing stage to the rule-based peak shaving algorithm is also highlighted with the help of results. As mentioned previously, thorough comparison with other techniques is not feasible due to incompatible simulation parameters. However, results are compared with Rampelli et. al. [57]. There is an improvement of almost 14% PPS in different cases which validates the applicability of the proposed scheme for community-based MGs.

8.2. Future Directions

Based on the limitations identified in this dissertation, the presented study can be extended into some more directions in the future, which are described as follows.

- 1. A balance in electricity generation and consumption can be targeted by applying home energy management systems while incorporating multi-objective version of newly introduced metaheuristic computation techniques. These include techniques of grey wolf and crow search algorithm (GWCSA), bald eagle search optimization algorithm (BESOA) and etc. The application of metaheuristic versions of automatization techniques can lead to better optimal solutions of load scheduling for residential consumers. Further improvements in daily electricity cost reduction, peak to average ratio reduction and increase in consumer comfort can be achieved.
- 2. HEMS can be studied with smart homes and smart appliances in the context of COVID-19 pandemic. Smart home management system with renewable energy distributed resources can play an important role for reliability and stability enhancement of microgrids by managing

the immensely increased residential consumer load during the pandemic. Various case studies presented in the proposed strategy can be reviewed in the COVID-19 framework for various classes of consumers.

- 3. The demand and feed in limits determined by our proposed dynamic-HEMS-based peak shaving algorithm is dynamic for various days but fixed for a single day. It can be made further dynamic by calculating the demand limit for each hour or quarterly over a day. This can enhance the reliability of the power grid in case of unexpected peak loads e.g., due to breaking news or unannounced president speech broadcasted on television, etc.
- 4. Currently, community based large scale implementation of HEMS is an active area of research nowadays. Consequently, we implanted the load scheduling algorithm that we named as DCCHEMS for a large population of 1000 houses and a duration of 90 days. But the Dynamic-HEMS based peak shaving algorithm that we proposed is performed for a smaller community of 40 houses for 24 hours. Like DCHEMS, it can also be tested for a bigger population of 1000 houses for 90 days.
- 5. Microgrid can consist of DC, AC, or hybrid loads as well as battery storage systems. The proposed idea of HEMS optimization can be applied on a university campus load type. Such campus based microgrids can have loads based on distributed generation, energy storage as well as electric vehicles. Electric vehicles can be utilized for the vehicle to grid and grid to vehicle power transfer for better optimization of power utilization.

References

- [1] Energy Information Administration: International Energy Outlook 2019 (IEO2019).
- [2] J. Valinejad, M. Marzband, M. Korkali, Y. Xu and A. S. Al-Sumaiti, "Coalition Formation of Microgrids with Distributed Energy Resources and Energy Storage in Energy Market," in Journal of Modern Power Systems and Clean Energy, vol. 8, no. 5, pp. 906-918, September 2020.
- [3] F. S. Al-Ismail, "DC microgrid planning, operation, and control: A comprehensive review," *IEEE Access*, vol. 9, pp. 36154–36172, 2021.
- [4] Q. Fu, A. Hamidi, A. Nasiri, V. Bhavaraju, S. B. Krstic, and P. Theisen, "The role of energy storage in a microgrid concept: Examining the opportunities and promise of microgrids." IEEE Electrif. Mag., vol. 1, no. 2, pp. 21–29, 2013.
- [5] S. Chowdhury and P. Crossley, Microgrids and active distribution networks. The Institution of Engineering and Technology, 2009.
- [6] R. Lasseter, A. Akhil, C. Marnay, J. Stephens, J. Dagle, R. Guttromson, A. Meliopoulous, R. Yinger, and J. Eto, "The certs microgrid concept," White paper for Transmission Reliability Program, Office of Power Technologies, US Department of Energy, vol. 2, no. 3, p. 30, 2002.
- [7] F. Moazeni, J. Khazaei, and A. Asrari, "Step towards energy-water smart microgrids; buildings thermal energy and water demand management embedded in economic dispatch," *IEEE Trans. Smart Grid*, vol. 12, no. 5, pp. 3680–3691, Sep. 2021.
- [8] J. Leitao, P. Gil, B. Ribeiro, and A. Cardoso, "A survey on home energy management," *IEEE Access*, vol. 8, pp. 5699–5722, 2020.
- [9] B. Mahapatra and A. Nayyar, "Home energy management system (HEMS): Concept, architecture, infrastructure, challenges and energy management schemes," *Energy Syst.*, vol. 4, pp. 1–27, Nov. 2019.
- [10] A. Sangswang and M. Konghirun, "Optimal strategies in home energy management system integrating solar power, energy storage, and vehicleto-grid for grid support and energy efficiency," *IEEE Trans. Ind. Appl.*, vol. 56, no. 5, pp. 5716-5728, Sep. 2020.
- [11] A. Abbasi et al., "A Novel Dynamic Appliance Clustering Scheme in a Community Home Energy Management System for Improved Stability and Resiliency of Microgrids," in *IEEE Access*, vol. 9, pp. 142276-142288, 2021.

- [12] J. Liu, H. Chen, W. Zhang, B. Yurkovich and G. Rizzoni, "Energy Management Problems Under Uncertainties for Grid-Connected Microgrids: A Chance Constrained Programming Approach," in *IEEE Transactions on Smart Grid*, vol. 8, no. 6, pp. 2585-2596, Nov. 2017.
- [13] S. Puradbhat, S. Doolla and V. Bhavaraju, "A Framework for Considering Capital Cost Limit in Sizing Microgrid Distributed Energy Resources---Application to Industrial Microgrids," in *IEEE Transactions on Industry Applications*, vol. 57, no. 6, pp. 6688-6699, Nov.-Dec. 2021.
- [14] J. Driesen and F. Katiraei, "Design for distributed energy resources," IEEE Power Energy Mag., vol. 6, no. 3, 2008.
- [15] W. Wei, F. Liu, S. Mei, and Y. Hou, "Robust energy and reserve dispatch under variable renewable generation," IEEE Trans. Smart Grid, vol. 6, no. 1, pp. 369-380, 2015.
- [16] N. Miller, D. Manz, J. Roedel, P. Marken, and E. Kronbeck, "Utility scale battery energy storage systems," in 2010 IEEE PES Gen. Meeting. IEEE, pp. 1-7, 2010.
- [17] H. Alharbi and K. Bhattacharya, "Stochastic optimal planning of battery energy storage systems for isolated microgrids," *IEEE Trans. Sustain. Energy*, vol. 9, no. 1, pp. 211–227, Jan. 2018.
- [18] J. von Appen and M. Braun, "Sizing and improved grid integration of residential PV systems with heat pumps and battery storage systems," *IEEE Trans. Energy Convers.*, vol. 34, no. 1, pp. 562-571, Mar. 2019.
- [19] X. Yan, C. Gu, X. Zhang, and F. Li, "Robust optimization-based energy storage operation for system congestion management," *IEEE Syst. J.*, vol. 14, no. 2, pp. 2694–2702, Jun. 2020.
- [22] S. L. Arun and M. P. Selvan, "Intelligent residential energy management system for dynamic demand response in smart buildings," *IEEE Syst. J.*, vol. 12, no. 2, pp. 1329– 1340, Jun. 2018.
- [21] K. A. Joshi, N. M. Pindoriya, and A. K. Srivastava, "A two-stage fuzzy multi objective optimization for phase-sensitive day-ahead dispatch of battery energy storage system," IEEE Syst. J., vol. 12, no. 4, pp. 3649-3660, Dec. 2018.
- [22] M. Fekri Moghadam, M. Metcalfe, W. G. Dunford, and E. Vaahedi, "Demand side storage to increase hydroelectric generation efficiency," *IEEE Trans. Sustain. Energy*, vol. 6, no. 2, pp. 313–324, Apr. 2015.
- [23] M. G. Damavandi, J. R. Martí, and V. Krishnamurthy, "A methodology for optimal distributed storage planning in smart distribution grids," *IEEE Trans. Sustain. Energy*, vol. 9, no. 2, pp. 729-740, Apr. 2018.

- [24] M. A. Aziz, I. M. Qureshi, T. A. Cheema, and A. N. Malik, "Time based device clustering for domestic power scheduling," *Int. J. Adv. Appl. Sci.*, vol. 4, no. 1, pp. 1–9, Dec. 2016.
- [25] Gellings, Clark W. "The concept of demand-side management for electric utilities." Proceedings of the *IEEE 73*, no. 10, 1468-1470, 1985.
- [26] International Energy Outlook 2019. Available online: https://www.eia.gov/outlooks/ieo/[accessed on 10 January 2020]
- [27] Nadel, Steven. "Utility demand-side management experience and potential-a critical review. "Annual Review of Energy and the Environment 17, no. 1, 507-535, 1992.
- [28] U. Zafar, S. Bayhan, and A. Sanfilippo, "Home energy management system concepts, configurations, and technologies for the smart grid," *IEEE Access*, vol. 8, pp. 119271–119286, 2020.
- [29] M. Hu, J.-W. Xiao, S.-C. Cui, and Y.-W. Wang, "Distributed real-time demand response for energy management scheduling in smart grid," *Int. J. Elect. Power Energy Syst.*, vol. 99, pp. 233–245, Jul. 2018.
- [30] Y. F. Du, L. Jiang, Y. Li, and Q. Wu, "A robust optimization approach for demand side scheduling considering uncertainty of manually operated appliances," *IEEE Trans. Smart Grid*, vol. 9, no. 2, pp. 743-755, Mar. 2018.
- [31] A. Imran, G. Hafeez, I. Khan, M. Usman, Z. Shafiq, A. B. Qazi, A. Khalid, and K.-D. Thoben, "Heuristic-based programable controller for efficient energy management under renewable energy sources and energy storage system in smart grid," *IEEE Access*, vol. 8, pp. 139587–139608, 2020.
- [32] K. Song, Y. Jang, M. Park, H.-S. Lee, and J. Ahn, "Energy efficiency of end-user groups for personalized HVAC control in multi-zone buildings," *Energy*, vol. 206, Art. no. 118116, Sep. 2020.
- [33] D. Danalakshmi, R. Gopi, A. Hariharasudan, I. Otola, and Y. Bilan, "Reactive power optimization and price management in microgrid enabled with blockchain," *Energies*, vol. 13, no. 23, p. 6179, Nov. 2020.
- [34] W. Feng, Z. Wei, G. Sun, Y. Zhou, H. Zang, and S. Chen, "A conditional value-at-risk-based dispatch approach for the energy management of smart buildings with HVAC systems," *Electr. Power Syst. Res.*, vol. 188, Art. no. 106535, Nov. 2020.
- [35] R. Z. Homod, H. Togun, H. J. Abd, and K. S. M. Sahari, "A novel hybrid modelling structure fabricated by using Takagi-Sugeno fuzzy to forecast HVAC systems energy demand in real-time for basra city," Sustain. Cities Soc., vol. 56, Art. no. 102091, May 2020.

- [36] R. Z. Homod, K. S. Gaeid, S. M. Dawood, A. Hatami, and K. S. Sahari, "Evaluation of energy-saving potential for optimal time response of HVAC control system in smart buildings," *Appl. Energy*, vol. 271, Art. no. 115255, Aug. 2020.
- [37] Z. Zhang, Z. Wang, H. Wang, H. Zhang, W. Yang, and R. Cao, "Research on bi-level optimized operation strategy of microgrid cluster based on IABC algorithm," *IEEE Access*, vol. 9, pp. 15520–15529, 2021.
- [38] X. Dong, X. Li, and S. Cheng, "Energy management optimization of microgrid cluster based on multi-agent-system and hierarchical stackelberg game theory," *IEEE Access*, vol. 8, pp. 206183–206197, 2020.
- [39] A. Khalid, N. Javaid, M. Ilahi, T. Saba, A. Rehman, and A. Mateen, "Enhanced time-of-use electricity price rate using game theory," *Electron.*, vol. 8, p. 48, Jan. 2019.
- [40] R. Khalid, N. Javaid, M. H. Rahim, S. Aslam, and A. Sher, "Fuzzy energy management controller and scheduler for smart homes," *Sustain. Comput., Inform. Syst.*, vol. 21, pp. 103–118, Mar. 2019.
- [41] M. Waseem, Z. Lin, S. Liu, I. A. Sajjad, and T. Aziz, "Optimal GWCSO-based home appliances scheduling for demand response considering end-users comfort," *Electr. Power Syst. Res.*, vol. 187, Art. no. 106477, Oct. 2020.
- [42] M. S. Ahmed, A. Mohamed, T. Khatib, H. Shareef, R. Z. Homod, and J. A. Ali, "Real time optimal schedule controller for home energy management system using new binary backtracking search algorithm," *Energy Buildings*, vol. 138, pp. 215–227, Mar. 2017.
- [43] G. Dong and Z. Chen, "Data-driven energy management in a home microgrid based on Bayesian optimal algorithm," *IEEE Trans. Ind. Informat.*, vol. 15, no. 2, pp. 869–877, Feb. 2019.
- [44] N. Javaid, G. Hafeez, S. Iqbal, N. Alrajeh, M. S. Alabed, and M. Guizani, "Energy efficient integration of renewable energy sources in the smart grid for demand side management," *IEEE Access*, vol. 6, pp. 77077–77096, 2018.
- [45] G. Hafeez, N. Islam, A. Ali, S. Ahmad, and M. U. A. K. S. Alimgeer, "A modular framework for optimal load scheduling under price-based demand response scheme in smart grid," *Processes*, vol. 7, no. 8, p. 499, Aug. 2019.
- [46] N. Javaid, M. Naseem, M. B. Rasheed, D. Mahmood, S. A. Khan, N. Alrajeh, and Z. Iqbal, "A new heuristically optimized home energy management controller for smart grid," Sustain. Cities Soc., vol. 34, pp. 211–227, Oct. 2017.
- [47] G. Hafeez, K. S. Alimgeer, Z. Wadud, I. Khan, M. Usman, A. B. Qazi, and F. A. Khan, "An innovative optimization strategy for efficient energy management with day-ahead

- demand response signal and energy consumption forecasting in smart grid using artificial neural network," *IEEE Access*, vol. 8, pp. 84415–84433, 2020.
- [48] X. Jiang and C. Xiao, "Household energy demand management strategy based on operating power by genetic algorithm," *IEEE Access*, vol. 7, pp. 96414–96423, 2019.
- [49] H. Hussain, N. Javaid, and S. Iqbal, "An efficient demand side management system with a new optimized home Energy management controller in smart grid," Energies, vol. 11, no. 1, p. 190, Jan. 2018.
- [50] P. Paudyal and Z. Ni, "Smart home energy optimization with incentives compensation from inconvenience for shifting electric appliances," *Int. J. Elect. Power Energy Syst.*, vol. 109, pp. 652-660, Jul. 2019.
- [51] K. R. Reddy and S. Meikandasivam, "Load flattening and voltage regulation using plug-in electric vehicle's storage capacity with vehicle prioritization using ANFIS," *IEEE Trans.* Sustain. Energy, vol. 11, no. 1, pp. 260–270, Jan. 2020.
- [52] A. K. Barnes, J. C. Balda, and A. Escobar-Mejía, "A semi-Markov model for control of energy storage in utility grids and microgrids with PV generation," *IEEE Trans.* Sustain. Energy, vol. 6, no. 2, pp. 546-556, Apr. 2015.
- [53] F. Hafiz, M. A. Awal, A. R. de Queiroz, and I. Husain, "Real-time stochastic optimization of energy storage management using deep learning-based forecasts for residential PV applications," *IEEE Trans. Ind. Appl.*, vol. 56, no. 3, pp. 2216–2226, May/Jun. 2020.
- [54] L. Lengyel, "Validating rule-based algorithms," J. Appl. Sci., vol. 12, no. 4, pp. 59-75, 2015.
- [55] U. Kumar Jha, N. Soren, and A. Sharma, "An efficient HEMS for demand response considering TOU pricing scheme and incentives," in *Proc. 2nd Int. Conf. Power, Energy Environ.: Towards Smart Technol.*, pp. 1-6, 2018.
- [56] S. Bruno, G. Giannoccaro, and M. La Scala, "A demand response implementation in tertiary buildings through model predictive control," *IEEE Trans.* Ind. Appl., vol. 55, no. 6, pp. 7052–7061, Nov./Dec. 2019.
- [57] R. Manojkumar, C. Kumar, S. Ganguly and J. P. S. Catalão, "Optimal Peak Shaving Control Using Dynamic Demand and Feed-In Limits for Grid-Connected PV Sources with Batteries," in *IEEE Systems Journal*, vol. 15, no. 4, pp. 5560-5570, Dec. 2021.
- [58] J. Leadbetter and L. Swan, "Battery storage system for residential electricity peak demand shaving," *Energy Buildings*, vol. 55, pp. 685-692, 2012.
- [59] K. Mahmud, M. J. Hossain, and G. E. Town, "Peak-load reduction by coordinated response of photovoltaics, battery storage, and electric vehicles," *IEEE Access*, vol. 6, pp. 29353–29365, 2018.

- [60] D. M. Greenwood, N. S. Wade, P. C. Taylor, P. Papadopoulos, and N. Heyward, "A probabilistic method combining electrical energy storage and real-time thermal ratings to defer network reinforcement," *IEEE Trans. Sust. Energy*, vol. 8, no. 1, pp. 374–384, Jan. 2017.
- [61] Y. Riffonneau, S. Bacha, F. Barruel, and S. Ploix, "Optimal power flow management for grid connected PV systems with batteries," *IEEE Trans. Sustain. Energy*, vol. 2, no. 3, pp. 309–320, Jul. 2011.
- [62] G. Angenendt, S. Zurmühlen, R. Mir-Montazeri, D. Magnor, and D. U. Sauer, "Enhancing battery lifetime in PV battery home storage system using forecast based operating strategies," *Energy Procedia*, vol. 99, pp. 80–88, 2016.
- [63] D. T. Vedullapalli, R. Hadidi, and B. Schroeder, "Combined HVAC and battery scheduling for demand response in a building," *IEEE Trans. Ind. Appl.*, vol. 55, no. 6, pp. 7008–7014, Nov./Dec. 2019.
- [64] R. Khezri, A. Mahmoudi and M. H. Haque, "Optimal Capacity of Solar PV and Battery Storage for Australian Grid-Connected Households," in *IEEE Transactions on Industry Applications*, vol. 56, no. 5, pp. 5319-5329, Sept.-Oct. 2020.
- [65] Z. Yi, W. Dong and A. H. Etemadi, "A Unified Control and Power Management Scheme for PV-Battery-Based Hybrid Microgrids for Both Grid-Connected and Islanded Modes," in *IEEE Transactions on Smart Grid*, vol. 9, no. 6, pp. 5975-5985, Nov. 2018.
- [66] Z. Zhao, W. C. Lee, Y. Shin and K. Song, "An Optimal Power Scheduling Method for Demand Response in Home Energy Management System," in IEEE Transactions on Smart Grid, vol. 4, no. 3, pp. 1391-1400, Sept. 2013.
- [67] M. Waseem, Z. Lin, S. Liu, Z. Zhang, T. Aziz, and D. Khan, "Fuzzy compromised solution-based novel home appliances scheduling and demand response with optimal dispatch of distributed energy resources," *Appl. Energy*, vol. 290, Art. no. 116761, May 2021.
- [68] Z. S. Ageed, S. R. M. Zeebaree, M. A. M. Sadeeq, M. B. Abdulrazzaq, B. W. Salim, A. A. Salih, H. M. Yasin, and A. M. Ahmed, "A state of art survey for intelligent energy monitoring systems," *Asian J. Res. Comput. Sci.*, vol. 1804, pp. 46-61, Apr. 2021.
- [69] T. A. A. Victoire, "Week ahead electricity price forecasting using artificial bee colony optimized extreme learning machine with wavelet decomposition," Tehnicki Vjesnik, vol. 28, no. 2, pp. 556–567, Apr. 2021.
- [70] A. Anees, I. Hussain, A. H. AlKhaldi, and M. Aslam, "Linear triangular optimization technique and pricing scheme in residential energy management systems," *Results Phys.*, vol. 9, pp. 858–865, Jun. 2018.

- [71] K. Arya and K. V. Chandrakala, "Day-Ahead Electricity Price Forecasting for Efficient Utility Operation Using Deep Neural Network Approach". *Boca Raton, FL, USA*: CRC Press, 2021.
- [72] B. Hussain, Q. U. Hasan, N. Javaid, M. Guizani, A. Almogren, and A. Alamri, "An innovative heuristic algorithm for IoT-enabled smart Homes for developing countries," *IEEE Access*, vol. 6, pp. 15550–15575, 2018.
- [73] Real-Time Pricing for Residential Customers. Ameren Illinois Power Co. [Online]. Available: https://www2.ameren.com/ retail energy/realtimeprices.aspx
- [74] J. Kennedy and R. Eberhart, "Particle swarm optimization," in *Proc. IEEE Int. Conf. Neural Netw.*, vol. 4, Nov. 1995, pp. 1942–1948.
- [75] Southern California Edison, Energy for What's Ahead. Accessed: Mar. 5, 2021. [Online]. Available: www.sce.com.
- [76] Prepare for Power Shutoffs. Accessed: Mar. 5, 2021. [Online]. Available: https://www.pge.com.
- [77] Matanuska Electric Association. Accessed: Feb. 5, 2020. [Online]. Available: http://www.mea.coop/wp-content/uploads/2014/06/High-BillPacket.pdf
- [78] A. Abbasi, I. M. Qureshi, and H. Abdullah, "An overview of control strategies with emphasis on demand response for stability and reliability enhancement of microgrids," in Proc. Int. Conf. Power Gener. Syst. Renew. Energy Technol. (PGSRET), pp. 1-6, Sep. 2018.
- [79] http://www.pbs.gov.pk/content/housing-units-number-rooms-and-type [Accessed on November 20, 2020].
- [80] Liu, Yu-Jen & Chen, Shang-I & Chang, Yung-Ruei & Lee, Yih-Der. 'Development of a Modelling and Simulation Method for Residential Electricity Consumption Analysis in a Community Microgrid System". Applied Sciences., 2017.
- [81] Jin Sol Hwang, Ismi Rosyiana Fitri, Jung-Su Kim * and Hwachang Song, "Optimal ESS Scheduling for Peak Shaving of Building Energy Using Accuracy-Enhanced Load Forecast" *Energies*, MDPI, 2020.
- [82] S. Chun and A. Kwasinski, "Analysis of classical root-finding methods applied to digital maximum power point tracking for sustainable photovoltaic energy generation," *IEEE Trans. Power Electron.*, vol. 26, no. 12, pp. 3730–3743, Dec. 2011.
- [83] M. Hosseinzadeh and F. R. Salmasi, "Robust optimal power management system for a hybrid AC/DC micro-grid," *IEEE Trans. Sustain. Energy*, vol. 6, no. 3, pp. 675–687, Jul. 2015.

- [84] H. Gong, V. Rallabandi, M. L. McIntyre, E. Hossain, and D. M. Ionel, "Peak reduction and long term load forecasting for large residential communities including smart Homes with energy storage," IEEE Access, vol. 9, pp. 19345–19355, 2021.
- [85] N. Shabbir, L. Kütt, V. Astapov, M. Jawad, A. Allik and O. Husev, "Battery Size Optimization With Customer PV Installations and Domestic Load Profile," in IEEE Access, vol. 10, pp. 13012-13025, 2022

